Supplementary Results

Rapamycin had limited effects on age-dependent functional and histopathological phenotypes in the cardiovascular system. To test for gross structural changes in the aged heart, we performed a basic echocardiographic assessment of the 16 months old and 25 months old cohorts and measured heart dimensions, as well as heart and respiration rates. We also determined heart weights upon pathological assessment.

A few heart dimensional measures showed trends towards an increase in aged mice and a reduction in rapamycin-treated animals (Supplementary Figure 2). Findings were, however, significant for only one parameter: systolic left ventricular internal diameter (LVID) in the 25 months cohort. Subtle reductions in heart dimensional measures in rapamycin-treated animals may be related to a slight overall reduction in heart weight, which was revealed upon pathological assessment (Supplementary Figure 2). Rapamycin also reduced heart weights and had some effects on heart dimensional measures (left ventricular posterior wall during systole) in young C57BL/6J mice (Supplementary Figure 4), demonstrating that rapamycin's heart weight effects were independent of a modulation of aging.

Rapamycin treatment was associated with considerable nephro- and gonadotoxicity. In the kidneys, vehicle-treated aged mice showed the expected progressive tissue alterations occurring during normal aging (1), including glomerulosclerosis, scar formation after chronic infarction and regenerative hyperplasia of tubular epithelial cells (Supplementary Tables 16 and 17; Supplementary Figures 24 and 25). In addition to these age-related pathologies, rapamycin-treated aged animals showed signs of severe toxic tubulus damage (pronounced vacuolization of tubular epithelial cells), indicating that rapamycin treatment was associated with considerable nephrotoxicity.

Histopathological analyses of the male reproductive tract revealed the expected (2) signs of testicular atrophy in aged control mice (Supplementary Table 18; Supplementary Figure 26). Rapamycin-treated mice showed striking reductions of testis weight relative to controls in all age groups (Supplementary Figure 27). Histopathology confirmed that pronounced testicular and epididymal atrophy was present in a large fraction of rapamycin-treated mice, clearly exceeding the severity of atrophic changes in age-matched controls (Supplementary Figures 26 and 28): All rapamycin-treated animals showed a severely reduced meiotic activity in the germinal layer of the seminiferous tubules; the lumina of the seminiferous tubules as well as the tubules of the epididymal ducts contained only few mature or immature spermatids in treated animals, indicating that rapamycin treatment was associated with considerable gonadotoxicity.

Oxidative protein modifications and DNA damage foci in aged mice. We also assessed oxidative protein modifications (carbonylation) in liver homogenates of rapamycin- or vehicle-treated aged mice and young controls. Western blot analyses showed no significant difference in the total amount of carbonylated protein between young controls and 26 months old animals (Supplementary Figure 39), which is consistent with prior data published by others (3).

DNA damage is associated with the recruitment of Ataxia Teleangiectasia Mutated (ATM) and RAD-3 related kinase (ATR) to the site of DNA damage and the local phosphorylation of histone H2A.X at serine 139 (γ-H2A.X) (4). We performed γ-H2A.X immunohistochemical stainings of lung sections to address if aging is associated with increased phosphorylation of H2A.X and, if so, whether rapamycin has effects on γ-H2A.X or not (Supplementary Figure 39). Quantification of

immunostained sections revealed increased levels of γ-H2A.X in 34 months old mice relative to young controls (no age effect in 16 months cohort). Rapamycin had no significant effects on γ-H2A.X signal intensity in lung tissue from 34 months old mice.

We also performed an ELISA-based assessment of an oxidative DNA modification (8-hydroxydeoxyguanosine, 8-OHdG) in 26 months old animals, treated with rapamycin or vehicle control, and the corresponding young controls. In agreement with published data (5), we could not discern significant differences in 8-OHdG concentrations between the age groups used here (Supplementary Figure 39).

Other analyses. Our analyses of aging-associated changes also covered the stomach (Supplementary Figure 29), small intestine (Supplementary Figure 30), large intestine (Supplementary Figure 30), gall bladder (Supplementary Figure 31), pancreas (Supplementary Table 19; Supplementary Figure 32), spleen (Supplementary Figure 33), salivary glands and lymph nodes (Supplementary Figure 34), bones (Supplementary Tables 20 and 21; Supplementary Figure 35), skin (Supplementary Table 22, Supplementary Figure 36), pituitary gland (Supplementary Table 23; Supplementary Figure 37) and the lung (Supplementary Figure 38). These analyses did not reveal statistically discernable effects of aging and were therefore of limited value for addressing the central aim of the current study (i.e., determining if rapamycin slows aging). It will be important to reassess some of these traits using larger sample sizes.

Supplementary References

1. Schmitt R, Jacobi C, Susnik N, Broecker V, Haller H, and Melk A. Ageing mouse kidney--not always the SAME old story. *Nephrol Dial Transplant.* 2009;24(10):3002-5.
2. Schmidt JA, Oatley JM, and Brinster RL. Female mice delay reproductive aging in males. *Biol Reprod.* 2009;80(5):1009-14.
3. Goto S, Nakamura A, Radak Z, Nakamoto H, Takahashi R, Yasuda K, Sakurai Y, and Ishii N. Carbonylated proteins in aging and exercise: immunoblot approaches. *Mech Ageing Dev.* 1999;107(3):245-53.
4. Wang C, Jurk D, Maddick M, Nelson G, Martin-Ruiz C, and von Zglinicki T. DNA damage response and cellular senescence in tissues of aging mice. *Aging Cell.* 2009;8(3):311-23.
5. Kaneko T, Tahara S, and Matsuo M. Retarding effect of dietary restriction on the accumulation of 8-hydroxy-2'-deoxyguanosine in organs of Fischer 344 rats during aging. *Free Radic Biol Med.* 1997;23(1):76-81.

Supplementary Figure Legends

Supplementary Figure 1
Adult hippocampal neurogenesis was substantially reduced in aged mice irrespective of treatment. The figure shows results from a computer-assisted quantification of DCX immunoreactivity in the hippocampal dentate gyrus (young control, *n*=7 mice; 16 months control, *n*=8 mice; 16 months rapamycin, *n*=7 mice). As expected, DCX immunoreactivity was substantially reduced in aged animals; rapamycin treatment had no significant effect on this phenotype (linear model, *P* = 0.0007, 0.3236 for age and treatment, respectively). Representative examples of histological images, as well as probability maps that were generated by automated segmentation of histological images are shown (scale bar: 100 μm). Group data are shown as whisker plots with minimum, 25% percentile, median, 75% percentile and maximum.

Supplementary Figure 2
Basic echocardiographic assessment of rapamycin- and vehicle-treated aged mice. The figure shows results from a basic echocardiography performed on conscious mice (young control for 16 mo cohort: *n*=10 mice; 16 months control: *n*=4 mice; 16 months rapamycin: *n*=10 mice; young control for 25 mo cohort: *n*=10 mice; 25 months control: *n*=11 mice; 25 months rapamycin: *n*=14 mice). (**A**, **B**, **C**, **D**) left ventricular internal diameter during diastole and systole, respectively; (**E**) heart weights obtained during pathological assessment of the 16 and 25 months cohorts, respectively. *P* values and fit coefficients with their 95% confidence intervals are shown. Group data are shown as whisker plots with minimum, 25% percentile, median, 75% percentile and maximum.

Supplementary Figure 3
Aging-associated functional cardiac alterations were not influenced measurably by rapamycin treatment. The figure summarizes data from a comprehensive assessment of cardiac function using echocardiography (young control: *n*=10 mice; 26 months control: *n*=17 mice; 26 months rapamycin: *n*=10 mice). (**I**) Heart dimensions, measured in PSLAX M-Mode; (**II**) Calculation of functional parameters, PSLAX M-Mode; (**III**) measurement of functional parameters, LV trace, PSLAX M-Mode; (**IV**) measurements flow across aortic valve; (**V**) measurements flow across pulmonary valve. Ejection fraction (**II**: **A**) and fractional shortening (**II**: **B**) were reduced in aged mice. There was also a reduction of flow velocities, as well as pressure gradients across the aortic (**IV**: **D**-**G**) and pulmonary valve (**V**: **D**-**G**) in aged mice. Rapamycin treatment had no effect on these aging-associated changes in cardiac function. *P* values and fit coefficients with their 95% confidence intervals are shown. Group data are shown as whisker plots with minimum, 25% percentile, median, 75% percentile and maximum.

Supplementary Figure 4
Basic echocardiographic assessment of young animals treated with rapamycin or vehicle control. The figure shows results from a basic echocardiography performed on young animals treated with rapamycin or vehicle control (young control: *n*=9 mice; young rapamycin: *n*=8 mice). (**A**, **B**) Left ventricular internal diameter during diastole and systole, respectively; (**C**, **D**) dimensions of left ventricular posterior wall during diastole and systole, respectively; (**E**) heart weights obtained during pathological assessment. Group data are shown as whisker plots with minimum, 25% percentile, median, 75% percentile and maximum.

Supplementary Figure 5
Histopathology of myocardium and aorta. The figure shows representative images of heart and aorta sections of the 34 months old cohort, 25 months old cohort and 16 months old cohort.
(**I**, **III**, **V**): Photographs of cross-sections through the myocardium below the valve level (**A**-**C**: HE, 0.4x magnification; **D**-**F**: HE, 10x magnification; **G**-**I**: EvG (Weigert's) stain, 10x magnification). (**I**): 34 months cohort; (**III**): 25 months cohort; (**V**): 16 months cohort; (**A**, **D**, **G**): old rapamycin-treated group; (**B**, **E**, **H**): old control group; (**C**, **F**, **I**): young control group.
Age-related histopathological alterations in the myocardium included fibrotic changes (**I**: **G**, **H**; **III**: **G**, **H; V**: **G**, **H**), ventricular dilation (**I**: **A**; **III**: **A**), ventricular hypertrophy (**V**: **A**), focal hypereosinophilia of cardiomyocytes (**I**: **D**, **E**; **III**: **E**; **V**: **D**), and basophilic mineralization of cardiomyocytes (**III**: **D**), among others. These changes occurred in rapamycin- and vehicle-treated aged mice alike. Young controls showed normal heart morphology (**I**, **III**, **V**: **C**, **F**, **I**).
(**II**, **IV**, **VI**): Panel of aortic root samples (**A**-**C**: 2,5x magnification; **D**-**F**: 20x magnification Movat stain; **G**-**I**: 10x magnification, EvG (Weigert's) stain). (**II**): 34 months cohort; (**IV**): 25 months cohort; (**VI**): 16 months cohort; (**A**, **D**, **G**): old rapamycin-treated group; (**B**, **E**, **H**): old control group; (**C**, **F**, **I**): young control group.
Age-related histopathological alterations of the aortic wall included mucinous degeneration (**II**, **IV**: **A**, **B**, **D**, **E**) and loss/disorganization of elastic fibers, which affected rapamycin- and vehicle-treated aged animals to a similar extent. For comparison, the normal histoarchitecture of a young control animal (**II**, **IV**, **VI**: **C**, **F**, **I**).
For quantitative assessment of myocardial and arterial pathology, see Supplementary Tables 4 and 5.

Supplementary Figure 6
Histopathology of the liver. The figure shows representative images of liver sections of the 34 months old cohort (**I**), 25 months old cohort (**II**) and 16 months old cohort (**III**) (**A**-**C**: 1.25x magnification, HE; **D**-**F**: 10x magnification, HE; **G**-**I**: 10x magnification, Weigert's stain); **A**, **D**, **G**: old rapamycin-treated group; **B**, **E**, **H**: old control group; **C**, **F**, **I**: young control group).
Aging-associated histopathological alterations included polyploidy (**I**, **II**, **III**: **D**, **E**, **G**, **H**), micro- and macrovesicular steatosis (**III**: **D**, **E**, **G**, **H**) and a perivascular fibrosis (**I**: **G**, **H**; **II**: **G**, **H**). These changes occurred in rapamycin-treated animals and age-matched vehicle controls to a similar extent. In addition, the figure shows histiosarcomas with perivascular infiltrates and increased collagen fiber content (**II**: **D**, **E**, **G**, **H**). Young controls showed normal liver morphology (**I**, **II**, **III**: **C**, **F**, **I**).
For quantitative assessment of liver histopathology, see Supplementary Tables 6-8.

Supplementary Figure 7
Histopathology of the thyroid gland. The figure shows representative images of HE-stained thyroid sections of the 34 months old cohort (**I**), 25 months old cohort (**II**) and 16 months old cohort (**III**) (**A**-**C**: 2.5x magnification, **D**-**F**: 20x magnification; **A**, **D**: old rapamycin-treated group; **B**, **E**: old control group; **C**, **F**: young control group).
Both rapamycin- and vehicle-treated aged mice showed degenerative thyroid changes like pallor and/or solidification and mineralization with shrinkage of the colloid next to hyperplasia of follicle cells (**I**-**III**: **A**, **B**, **D**, **E**). **III**: **B**, **E** shows the presence of a papillary follicle cell adenoma. Young controls showed normal follicles with resorption lacunae (**I**-**III**: **C**-**F**).
For quantitative assessment of thyroid histopathology, see Supplementary Table 9 and Figure 7.

Supplementary Figure 8
Histopathology of the adrenal glands. The figure shows representative images of cross-sections through the adrenal glands of the 34 months old cohort (**I**), 25 months old cohort (**II**) and 16 months old cohort (**III**) (a-c: 5x magnification, d-f: 10x magnification, HE stain; g-i: 20x magnification, PAS stain; **A**, **D**, **G**: old rapamycin-treated group; **B**, **E**, **H**: old control group; **C**, **F**, **I**: young control group).
Aging-associated histopathological alterations in rapamycin-treated animals and vehicle controls included basophilic, as well as eosinophilic adenomas (**I**: **A**, **B**, **D**, **E**; **II**: **B**, **E**), subcapsular spindle cell (a-cell) and vesicular cell (b-cell) hyperplasia (**II**, **III**: **A**, **B**, **D**, **E**) and lipofuscin deposits (**II**, **III**: **A**, **B**, **D**, **E**, slightly yellow-brownish deposits in the HE stain; **II**, **III**: **G**, **H** bright purple in the PAS stain). Young control animals showed normal adrenal gland morphology with only rare incidental adenomas (**I**: **C**) and small lipofuscin deposits (**III**: **C**, **F**, **I**), if any.
For quantitative assessment of histopathological changes in the adrenal glands, see Supplementary Table 10 and Supplementary Figure 9.

Supplementary Figure 9
Rapamycin increased lipofuscin deposition in aged adrenal glands. The figure shows lipofuscin deposits in the adrenal glands (young control, *n*=14 mice; 16 months control, *n*=9 mice; 25 months control, *n*=4 mice; 34 months control, *n*=3 mice; 16 months rapamycin, *n*=14 mice; 25 months rapamycin, *n*=8 mice; 34 months rapamycin, *n* = 7 mice). Lipofuscin depositions were automatically identified on PAS-stained adrenal gland sections using image segmentation and analysis software. Shown are examples of histological images and probability maps generated by automated segmentation of histological images (scale bar = 200 μm). Lipofuscin intensity scores were normalized to the surface area analyzed and expressed as percentage of the average of the young control group. *P* values and fit coefficients with their 95% confidence intervals are shown. Group data are shown as whisker plots with minimum, 25% percentile, median, 75% percentile and maximum.

Supplementary Figure 10
Rapamycin partially influenced age-related changes in body weight and body composition. The figure shows results of qNMR analyses performed to assess body composition in rapamycin- and vehicle treated aged mice and young controls. (**A**-**C**): 16 months cohort (young control, *n*=10 mice; 16 months control, *n*=18 mice; 16 months rapamycin, *n*=20 mice); (**D**-**F**): 25 months cohort (young control, *n*=10 mice; 25 months control, *n*=10 mice; 25 months rapamycin, *n*=14 mice); (**G**-**I**): 34 months cohort (young control, *n*=10 mice; 34 months control, *n*=10 mice; 34 months rapamycin, *n*=15 mice). *P* values and fit coefficients with their 95% confidence intervals are shown. (**J**-**L**) Rapamycin effects on body weight (**J**), fat mass (**K**) and lean mass (**L**) in young mice (control, *n*=9 mice; rapamycin, *n*=8 mice). Group data are shown as whisker plots with minimum, 25% percentile, median, 75% percentile and maximum.

Supplementary Figure 11
Rapamycin counteracted a subset of age-related changes in the T lymphocyte compartment in the 16 months cohort. The table shows various leukocyte subpopulations (measured by 10-color polychromatic flow cytometry) in rapamycin-treated and vehicle-treated aged (16 months old) mice and young controls (young control, *n*=10 mice; 16 months control, *n*=17 mice; 16 months rapamycin, *n*=14 mice). (**A**) $CD4^+$ T cells (% of $C45^+$); (**B**) $CD8^+$ T cells (% of $C45^+$); (**C**) T reg cells ($CD4^+CD25^+$, % of $CD4^+$); (**D**) γδ T cells ($CD3^+$ γδ TCR^+, % of $CD45^+$); (**E**) Activated/memory $CD4^+$ T cells ($CD44^{high}CD4^+$, % of $CD4^+$); (**F**) Activated/memory $CD8^+$ T cells ($CD44^{high}CD8^+$, % of $CD8^+$); (**G**) IgD^{high} B cells (% of B cells); (**H**) MHC-II^{high} B cells (% of B cells); (**I**) NK cells (NKp46/NK1.1.$^+CD5^-$, % of $CD45^+$); (**J**)

CD11b^{+} NK cells (% of NK cells); (**K**) Monocytes (Cd11b^{+}Gr1^{-}NKp46/NK1.1.$^{-}$, % of CD45^{+}). *P* values and fit coefficients with their 95% confidence intervals are shown. Group data are displayed as whisker plots with minimum, 25% percentile, median, 75% percentile and maximum.

Supplementary Figure 12
Rapamycin did not restore age-related changes in the proportions of leukocyte populations in the 25 months cohort. The table shows various leukocyte subpopulations (measured by 10-color polychromatic flow cytometry) in rapamycin-treated and vehicle-treated aged (25 months old) mice and young controls (young control, *n*=6 mice; 25 months control, *n*=5 mice; 25 months rapamycin, *n*=8 mice). (**A**) CD4^{+} T cells (% of C45^{+}); (**B**) CD8^{+} T cells (% of C45^{+}); (**C**) T reg cells (CD4^{+}CD25^{+}, % of CD4^{+}); (**D**) γδ T cells (CD3^{+} γδ TCR^{+}, % of CD45^{+}); (**E**) Activated/memory CD4^{+} T cells (CD44^{high}CD4^{+}, % of CD4^{+}); (**F**) Activated/memory CD8^{+} T cells (CD44^{high}CD8^{+}, % of CD8^{+}); (**G**) IgD^{high} B cells (% of B cells); (**H**) MHC-II^{high} B cells (% of B cells); (**I**) NK cells (NKp46/NK1.1.$^{+}$CD5^{-}, % of CD45^{+}); (**J**) CD11b^{+} NK cells (% of NK cells); (**K**) Monocytes (Cd11b^{+}Gr1^{-}NKp46/NK1.1.$^{-}$, % of CD45^{+}). *P* values and fit coefficients with their 95% confidence intervals are shown. Group data are displayed as whisker plots with minimum, 25% percentile, median, 75% percentile and maximum.

Supplementary Figure 13
Rapamycin did not restore age-related changes in the proportions of leukocyte populations in the 34 months cohort. The table shows various leukocyte subpopulations (measured by 10-color polychromatic flow cytometry) in rapamycin-treated and vehicle-treated aged (34 months old) mice and young controls (young control, *n*=10 mice; 34 months control, *n*=9 mice; 34 months rapamycin, *n*=14 mice). (**A**) CD4^{+} T cells (% of C45^{+}); (**B**) CD8^{+} T cells (% of C45^{+}); (**C**) T reg cells (CD4^{+}CD25^{+}, % of CD4^{+}); (**D**) γδ T cells (CD3^{+} γδ TCR^{+}, % of CD45^{+}); (**E**) Activated/memory CD4^{+} T cells (CD44^{high}CD4^{+}, % of CD4^{+}); (**F**) Activated/memory CD8^{+} T cells (CD44^{high}CD8^{+}, % of CD8^{+}); (**G**) IgD^{high} B cells (% of B cells); (**H**) MHC-II^{high} B cells (% of B cells); (**I**) NK cells (NKp46/NK1.1.$^{+}$CD5^{-}, % of CD45^{+}); (**J**) CD11b^{+} NK cells (% of NK cells); (**K**) Monocytes (Cd11b^{+}Gr1^{-}NKp46/NK1.1.$^{-}$, % of CD45^{+}). *P* values and fit coefficients with their 95% confidence intervals are shown. Group data are displayed as whisker plots with minimum, 25% percentile, median, 75% percentile and maximum.

Supplementary Figure 14
Rapamycin effects on age-related changes in plasma immunoglobulin concentrations (16 months cohort). The figure shows plasma immunoglobulin levels in rapamycin-treated and vehicle-treated aged mice and young controls (**A**-**F**: young control, *n*=10 mice; 16 months control, *n*=11 mice; 16 months rapamycin, *n*=18 mice; **G**: young control, *n*=5 mice; 16 months control, *n*=12 mice; 16 months rapamycin, *n*=7 mice). *P* values and fit coefficients with their 95% confidence intervals are shown. Group data are displayed as whisker plots with minimum, 25% percentile, median, 75% percentile and maximum.

Supplementary Figure 15
Rapamycin effects on age-related changes in plasma immunoglobulin concentrations (25 months cohort). The figure shows plasma immunoglobulin levels in rapamycin-treated and vehicle-treated aged mice and young controls (**A**-**F**: young control, *n*=6 mice; 25 months control, *n*=3 mice; 25 months rapamycin, *n*=8 mice; **G**: young control, *n*=3 mice; 25 months control, *n*=4 mice; 25 months rapamycin, *n*=7 mice). *P* values and fit coefficients with their 95% confidence

intervals are shown. Group data are displayed as whisker plots with minimum, 25% percentile, median, 75% percentile and maximum.

Supplementary Figure 16
Rapamycin effects on age-related changes in plasma immunoglobulin concentrations (34 months cohort). The figure shows plasma immunoglobulin levels in rapamycin-treated and vehicle-treated aged mice and young controls (**A**-**F**: young control, *n*=6 mice; 34 months control, *n*=9 mice; 34 months rapamycin, *n*=14 mice; **G**: young control, *n*=7 mice; 34 months control, *n*=8 mice; 34 months rapamycin, *n*=13 mice). *P* values and fit coefficients with their 95% confidence intervals are shown. Group data are displayed as whisker plots with minimum, 25% percentile, median, 75% percentile and maximum.

Supplementary Figure 17
Rapamycin treatment had no apparent effect on most aging-associated changes on clinical chemistry parameters. The table shows clinical chemistry results from the 16 months cohort (young control, *n*=10 mice; 16 months control, *n*=16 mice; 16 months rapamycin, *n*=19 mice). *P* values and fit coefficients with their 95% confidence intervals are shown. Group data are displayed as whisker plots with minimum, 25% percentile, median, 75% percentile and maximum.

Supplementary Figure 18
Rapamycin treatment had no apparent effect on most aging-associated changes on clinical chemistry parameters. The table shows clinical chemistry results from the 25 months cohort (young control, *n*=6 mice; 25 mo control, *n*=5 mice; 25 mo rapamycin, *n*=6 mice). *P* values and fit coefficients with their 95% confidence intervals are shown. Group data are displayed as whisker plots with minimum, 25% percentile, median, 75% percentile and maximum.

Supplementary Figure 19
Rapamycin treatment had no apparent effect on most aging-associated changes on clinical chemistry parameters. The table shows clinical chemistry results from the 34 months cohort (young control, *n* = 10 mice; 34 months control, *n* = 9 mice; 34 months rapamycin, *n* = 15 mice). *P* values and fit coefficients with their 95% confidence intervals are shown. Group data are displayed as whisker plots with minimum, 25% percentile, median, 75% percentile and maximum. UIBC: unsaturated iron binding capacity.

Supplementary Figure 20
Rapamycin had an adverse effect on glucose tolerance. The figure shows blood glucose levels before and after glucose bolus injection (glucose tolerance test) in rapamycin- or vehicle-treated 16 months old mice and young controls (young control, *n*=10 mice; 16 months control, *n*=16 mice; 16 months rapamycin, *n*=20 mice). Aged mice showed an increased area under the curve (AUC) (t-test, 16 mo control vs. young control, $P<0.05$), consistent with age-related impairments in glucose tolerance. Rapamycin treatment resulted in higher AUC values in treated mice compared to vehicle-treated age-matched controls (t-test, $P<0.05$), indicating that rapamycin had an adverse effect on glucose tolerance in treated animals.

Supplementary Figure 21
Rapamycin increased red blood cell counts in the 16 months cohort. The figure shows the full set of hematology results of 16 months old vehicle- or rapamycin-treated mice and corresponding young controls (young control, *n*=10 mice; 16 months control, *n*=16 mice; 16 months rapamycin, *n*=19 mice). (**A**) White blood cell count (WBC); (**B**) platelet count; (**C**) red blood cell count (RBC); (**D**) hemoglobin concentrations; (**E**)

hematocrit; (**F**) mean corpuscular volume (MCV); (**G**) mean corpuscular hemoglobin (MCH); (**H**) mean corpuscular hemoglobin concentration (MCHC); (**I**) red blood cell distribution width (RDW). *P* values and fit coefficients with their 95% confidence intervals are shown. Group data are displayed as whisker plots with minimum, 25% percentile, median, 75% percentile and maximum.

Supplementary Figure 22
Rapamycin had no significant effects on hematology findings in the 25 months cohort. The figure shows the full set of hematology results of 25 months old vehicle- or rapamycin-treated mice and corresponding young controls (young control, *n*=6 mice; 25 months control, *n*=5 mice; 25 months rapamycin, *n*=6 mice). (**A**) White blood cell count (WBC); (**B**) platelet count; (**C**) red blood cell count (RBC); (**D**) hemoglobin concentrations; (**E**) hematocrit; (**F**) mean corpuscular volume (MCV); (**G**) mean corpuscular hemoglobin (MCH); (**H**) mean corpuscular hemoglobin concentration (MCHC); (**I**) red blood cell distribution width (RDW). *P* values and fit coefficients with their 95% confidence intervals are shown. Group data are displayed as whisker plots with minimum, 25% percentile, median, 75% percentile and maximum.

Supplementary Figure 23
Rapamycin had no significant effects on hematology findings in the 34 months cohort. The figure shows the full set of hematology results of 34 months old vehicle- or rapamycin-treated mice and corresponding young controls (young control, *n*=10 mice; 34 months control, *n*=8 mice; 34 months rapamycin, *n*=13 mice). (**A**) White blood cell count (WBC); (**B**) platelet count; (**C**) red blood cell count (RBC); (**D**) hemoglobin concentrations; (**E**) hematocrit; (**F**) mean corpuscular volume (MCV); (**G**) mean corpuscular hemoglobin (MCH); (**H**) mean corpuscular hemoglobin concentration (MCHC); (**I**) red blood cell distribution width (RDW). *P* values and fit coefficients with their 95% confidence intervals are shown. Group data are displayed as whisker plots with minimum, 25% percentile, median, 75% percentile and maximum.

Supplementary Figure 24
Kidney histopathology. Photographs of kidneys from rapamycin and control mice (**I**: 34 months cohort, **II**: 25 months cohort; **III**: 16 months cohort; **A**, **D**, **G**: old rapamycin-treated group; **B**, **E**, **H**: old control group; **C**, **F**, **I**: young control group; **A**-**C**: 1.25x magnification, HE; **D**-**F**: 20x magnification, HE; **G**-**I**: 20x magnification, PAS stain).
Progressive age-related nephropathy was seen in, both, treated animals and vehicle controls to a similar extent and included scar and focal cyst formation (**I**: **A**, **D**), regenerative hyperplasia of tubular epithelial cells, formation of protein casts (**I**: **D**, **E**) and focal glomerulosclerosis (**I**: **G**, **H**). Aging was further associated with an increase in epithelia (kidney) associated lymphatic tissue (KALT, **I**: **B**). In addition to the aging-associated changes mentioned above, rapamycin-treated animals showed clear signs of toxic-induced tubular epithelial vacuolization (**II**, **III**: **D**), indicating that treatment was associated with considerable nephrotoxicity. Young controls did not show any pathological changes (**I**-**III**: **C**, **F**, **I**).
For quantitative assessment of kidney histopathology, see Supplementary Tables 16 and 17, as well as Supplementary Figure 25.

Supplementary Figure 25
Rapamycin had no effect on age-related fibrotic kidney changes. The age-related accumulation of connective tissue in the kidneys was quantified using automated segmentation and image analysis of EvG-stained histological kidney sections (young controls, *n*=12 mice; 16 mo controls, *n*=8 mice; 25 mo controls, *n*=3 mice; 34 mo controls, *n*=4 mice; 16 mo rapamycin, *n*=15 mice; 25 mo rapamycin, *n*=7 mice; 34 mo rapamycin, *n*=9 mice). Aging was associated with an accumulation

of fibrotic tissue within the renal parenchyma, while rapamycin treatment did not alter this measure (*P*=0.0019, 0.9617 for age and treatment, respectively). Shown are examples of histological images and probability maps generated via automated segmentation of histological images. 'Connective tissue' intensity scores were normalized to the surface area analyzed and expressed as percentage of the average of the young control group. *P* values and fit coefficients with their 95% confidence intervals are shown. Group data are displayed as whisker plots with minimum, 25% percentile, median, 75% percentile and maximum.

Supplementary Figure 26
Histopathology of testis and epididymis. The figure shows representative images of HE-stained cross-sections through testis and epididymis of the 34 months cohort (**I**), 25 months cohort (**II**) and 16 months cohort (**III**) (**A**-**C**: 0.4x magnification, **D**-**I**: 20x magnification. **A**, **D**, **G**: old rapamycin-treated group; **B**, **E**, **H**: old control group; **C**, **F**, **I**: young control group).
Rapamycin-treated animals showed severe testicular atrophy with remarkable decrease in total testis size (**I**-**III**: **A**) and reduction of germinal cells, focal presence of multinucleated giant cells (**I**: **D**), proliferation of interstitial cells (**II**, **III**: **D**) and virtually no mature sperm in the epididymis (**I**-**III**: **G**). A slight age-related atrophy was seen in the old control animals with less decrease in testis size (**I**-**III**: **B**), germinal cells and spermatids present in the testicular ducts (**I**-**III**: **E**) and slightly reduced mature sperm in the epididymis (**I**-**III**: **H**). For comparison, the normal testis, epididymis and sperm of a young control animal (**I**-**III**: **C**, **F**, **I**).
For quantitative assessment of testicular/epididymal pathology, see Supplementary Table 18 and Supplementary Figures 27 and 28.

Supplementary Figure 27
Rapamycin treatment was associated with substantial testis atrophy. The figure shows body and organ weights of rapamycin- and vehicle-treated aged mice and young control animals (young control, *n*=18 mice; 16 months control, *n*=10 mice; 25 months control, *n*=5 mice; 34 months control, *n*=5 mice; 16 months rapamycin, *n*=15 mice; 25 months rapamycin, *n*=7 mice; 34 months rapamycin, *n*=10 mice). (**A**) Body weights, (**B**) testis weights. *P* values and fit coefficients with their 95% confidence intervals are shown. Group data are displayed as whisker plots with minimum, 25% percentile, median, 75% percentile and maximum.

Supplementary Figure 28
Rapamycin compromised spermatogenesis. The figure shows the percentage of seminiferous tubule surface area covered by spermatogenic epithelium in rapamycin- or vehicle-treated aged mice and young controls (young control, *n*=16 mice; 16 months control, *n*=10 mice; 24 months control, *n*=4 mice; 34 months control, *n*=5 mice; 16 months rapamycin, *n*=12 mice; 24 months rapamycin, *n*=6 mice; 34 months rapamycin, *n*=8 mice). *P* values and fit coefficients with their 95% confidence intervals are shown. Whisker plot shows 10% percentile, 25% percentile, median, 75% percentile and 90% percentile. Representative examples of histological images, as well as probability maps that were generated by automated segmentation of histological images are displayed.

Supplementary Figure 29
Histopathology of the stomach. The figure shows representative images of cross-sections through the forestomach-glandular stomach junction (HE, 5x magnification). Despite differences in keratinization (**A**, **B**) no obvious differences regarding ulcers, epithelia atrophy or adenoma formation were detectable. (**I**)**:** 34 months cohort, (**II**): 25 months cohort, (**III**): 16 months cohort. (**A, D**, **G**): old rapamycin-treated group; (**B**, **E**, **H**): old control group; (**C**, **F**, **I**): young control group.

Supplementary Figure 30
Histopathology of the intestine. The figure shows representative images of HE-stained cross-sections (10x magnification) through the duodenal (**I**) and ileal (**II**) parts of the small intestine, as well as the large intestine (**III**). (**A**, **B**, **C**): 34 months old cohort; (**D**, **E**, **F**): 25 months old cohort; (**G**, **H**, **I**): 16 months old cohort. (**A**, **D**, **G**): old rapamycin-treated group; (**B**, **E**, **H**): old control group; (**C**, **F**, **I**): young control group. Histopathological assessment of the intestinal tract showed no obvious effects of aging or rapamycin treatment; specifically, there was no inflammation or mucosal atrophy and no difference regarding mucosa-associated lymphatic tissue (MALT), goblet cells and thickness of the muscular layer.

Supplementary Figure 31
Histopathology of the gallbladder. The figure shows representative images of HE-stained gall bladder sections (10x magnification) of the 34 months old cohort (**A**, **B**, **C**); 25 months old cohort (**D**, **E**, **F**); and 16 months old cohort (**G**, **H**, **I**). (**a**, **d**, **g**): old rapamycin-treated group; (**B**, **E**, **H**): old control group; (**C**, **F**, **I**): young control group. No differences regarding villi formation of the epithelia or thickening of the submucosal soft tissue or muscular layer were detectable between rapamycin-treated animals and age-matched controls. Younger animals (**C**, **F**, **G**, **H**, **I**) showed a slightly higher prismatic epithelium (indicative of higher secretory activity) than relatively older mice.

Supplementary Figure 32
Histopathology of the pancreas. The figure shows representative images of HE-stained pancreas sections (**A-C**: 1.25x magnification, **D-I**: 20x magnification) of the 34 months old cohort (**I**), 25 months old cohort (**II**) and 16 months old cohort (**III**). (**A**, **D**, **G**): old rapamycin-treated group; (**B**, **E**, **H**): old control group; (**C**, **F**, **I**): young control group.
Aging-related pathological alterations in the pancreas included exocrine pancreatitis (**I**: **E** shows a pancreatic lobule presenting an interstitial exocrine pancreatitis), scarring, as well as ductal metaplasia (**I**: **H**) that can occur as a consequence of chronic inflammatory changes and replace exocrine tissue, eosinophilic and basophilic foci (**I**: **D**), fat vacuoles within the pancreatic parenchyma (**II**: **H**, **III**: **D**). Chronic rapamycin treatment did not appear to have effects on these age-related changes within our dataset.
For quantitative assessment of pancreas histopathology, see Supplementary Table 19.

Supplementary Figure 33
Histopathology of the spleen. The figure shows representative images of cross-sections through the spleen of the 34 months cohort (**A**, **B**, **C**), 25 months cohort (**D**, **E**, **F**) and 16 months cohort (**G**, **H**, **I**). (**A**, **D**, **G**): old rapamycin-treated group; (**B**, **E**, **H**): old control group; (**C**, **F**, **I**): young control group (10x magnification, HE stain).
No obvious group differences were detectable regarding the size or activation status of the germinal centers, the proportion between red and white pulp, and the presence and extent of extramedullary hematopoiesis.

Supplementary Figure 34
Histopathology of salivary glands and lymph nodes. Photographs of salivary glands (sublingual, submandibular and parotid gland) and the associated lymph node samples (**A**-**I**: 2.5x magnification, HE): No obvious inflammation, cysts, tumours or fatty degenerative changes in the salivary glands were visible, while the lymphnodes presented a slight edematous loosening independent of age or treatment (**A**-**E**, **G**-**H**).

Supplementary Figure 35
Bone histopathology. The figure shows representative images of bone sections of the 34 months old cohort (**I**), 25 months old cohort (**II**) and 16 months old cohort (**III**) (**A**-**C**: 2.5x magnification, HE; **D**-**F**: 10x magnification, HE; **G**-**I**: 2.5x magnification, EvG (Weigert's)-stain; **A**, **D**, **G**: old rapamycin-treated group; **B**, **E**, **H**: old control group; **C**, **F**, **I**: young control group).
Both, rapamycin- and vehicle-treated aged mice showed a slight rarefaction of bone trabeculae (**I**-**III**: **A**, **B**, **G**, **H**), no obvious thinning of the cortical bone substance or an erosion, fibrosis and inflammation of the hyaline cartilage (**I**-**III**: **D**, **E**). Normal bone histoarchitecture was present in young control animals (**I**-**III**: **C**, **F**, **I**).
For quantitative assessment of bone histopathology, see Supplementary Table 21.

Supplementary Figure 36
Skin histopathology. The figure shows representative images of skin sections from the left flank of mice of the 34 months old cohort (**I**), 25 months old cohort (**II**) and 16 months old cohort (**III**) (HE; **A**-**C**, 5x; **D**-**F** 20x magnification; **A**, **D**: old rapamycin-treated group; **B**, **E**: old control group; **C**, **F**: young control group).
No obvious differences in skin atrophy, as indicated by reduced thickness of the subcutaneous fat layer, reduced dermal and epidermal layers, reduced elastic fiber content (EvG (Weigert's) stain, not shown), increased waviness and condensation of the collagen fibers in the corium layer, were present between the rapamycin- and vehicle-treated aged cohorts.
For quantitative assessment of skin atrophy, see Supplementary Table 22.

Supplementary Figure 37
Histopathology of the pituitary gland. The figure shows representative images of HE-stained pituitary gland sections of the 34 months old cohort (**A**, **B**, **C**); 25 months old cohort (**D**, **E**, **F**); and 16 months old cohort (**G**, **H**, **I**) (5x magnification; **A**, **D**, **G**: old rapamycin-treated group; **B**, **E**, **H**: old control group; **C**, **F**, **I**: young control group).
The images illustrate the normal architecture of the anterior, intermediate and neural part of the pituitary gland. No differences regarding the presence of hyperplastic clones or regressive cystic changes were detectable between the different treatment groups.
For quantitative assessment of histopathological changes in the pituitary glands (hyperplastic clones, cystic changes), see Supplementary Table 23.

Supplementary Figure 38
Histopathology of the lung. The figure shows representative images of HE-stained lung sections of the 34 months old cohort (**I**, **II**), 25 months old cohort (**I**, **III**) and 16 months old cohort (**I**, **IV**) (10x magnification).
Lungs were not completely expanded with formalin, therefore collapsed, blood filled alveoli are present next to inflated ones (**I**-**IV**). No increase in collagen fiber content (EvG (Weigert's) stain, not shown) of the alveolar septa or a decrease of the thickness of the alveolar septa was detected. Note broncheoli-associated lymphatic tissue (BALT) (**III**: **E**; **IV**: **D**, **E**).

Supplementary Figure 39
Oxidative protein modifications and DNA damage response in rapamycin- or vehicle-treated aged mice. The figure shows results from an automated quantification of γ-H2A.X-stained lung sections (**A**; young control, *n*=5 mice; 16 mo control, *n*=3 mice; 16 mo rapamycin, *n*=13 mice; 34 mo control, *n*=5 mice; 34 mo rapamycin, *n*=6 mice), an immunoblot analysis of carbonylated proteins in liver lysates (**B**; young control, *n*=7 mice; 26 mo control, *n*=7 mice; 26 mo rapamycin, *n*=7 mice) and an ELISA based assessment of 8-hydroxydeoxyguanosine (**C**; young control, *n*=7 mice; 26 mo control, *n*=7 mice; 26 mo rapamycin, *n*=7 mice). (**A**) Shown

are examples of histological images; probability maps for nuclei either γ-H2A.X positive or negative were generated via automated segmentation of histological images. Intensity scores of γ-H2A.X positive nuclei were normalized to γ-H2A.X negative nuclei and are expressed as percentage of the average of the young control group. (**B**) Shown are results from an immunoblot analysis performed to detect carbonylated proteins in liver homogenates. Negative control reactions did not show any signal (data not shown). Signal intensity was quantified per vertical lane and normalized to the corresponding loading control (actin). Lanes 1-4: young control; lanes 5-8: 26 mo rapamycin; lanes 9-12: 26 mo control. Data are expressed as percentage of the average of the young control group. (**C**) This panel shows results from an ELISA-based assessment of oxidative DNA damage (8-OHdG). Group data are displayed as whisker plots with minimum, 25% percentile, median, 75% percentile and maximum. All graphs show *P* values and fit coefficients with their 95% confidence intervals.

Supplementary Figure 40
Cancers and precancerous lesions detected during pathological assessment. The figure shows representative examples of incidental tumor findings in our aged mouse cohorts. (**I**) Photographs of incidental tumors in two 16 months old control animals (**A**: 1.25x magnification; **B**, **C**: 2.5x magnification; **D**-**F**: 10x magnification, **G**-**I**: 20x magnification; HE stain): A large hepatocellular carcinoma (HCC) comprising nearly the entire liver lobe (**A**), infiltrating the vicinity (**D**) and displaying numerous cells in mitosis (**G**). A diffuse infiltration of the liver (**B**) of spindle cells and histiocytes (**E**, **H**), characteristic for histiosarcoma, accompanied by perivascular spreading of metastases in a lung lobe (**C**, **F**, **I**). (**II**) Photographs of incidental tumors in a 25 months old control animal (**A**, **D**), a 16 months old control animal (**B**, **E**) and a 34 months old rapamycin-treated animal (**C**, **F**) (**A**: 1.25x magnification; **B**, **C**: 2.5x magnification; **D**-**G**: 20x magnification, HE stain): a bronchoalveolar adenocarcinoma (**A**) with local invasion (**D**), perivascular lymphoma infiltrates in the kidney (**B**, **E**) and a massive follicular adenocarcinoma in the thyroid (**C**, **F**). (**G**) Ductal metaplasia (a precancerous lesion) in the pancreas of a 34 months old control animal.

Supplementary Tables

Supplementary Table 1: Blood and tissue rapamycin concentrations

	Rapamycin blood/tissue concentration in treated animals
Whole blood (*n* = 3 mice)	4.57 +/- 0.65 ng/ml
Brain (*n* = 2 mice)	14.5 +/- 3.5 ng/g
Heart (*n* = 2 mice)	33.28 +/- 9.72 ng/g
Muscle (*n* = 2 mice)	26 +/- 2 ng/g
Kidney (*n* = 2 mice)	50 +/- 13 ng/g
Liver (*n* = 2 mice)	24 +/- 1 ng/g
Visceral fat (*n* = 2 mice)	13 +/- 2 ng/g

Supplementary Table 2: Summary of aging phenotypes worsened by rapamycin/phenotypes influenced by rapamycin only

Tests	Aging phenotypes	Rapamycin effects
Kidney (Supplementary Figures 24 and 25; Supplementary Tables 16 and 17)		
Histopathology	*Vacuolization of tubular epithelia cells*	*Toxic tubulus damage with pronounced vacuolization of tubular epithelial cells (rapamycin-induced nephrotoxicity)*
Male reproductive tract (Supplementary Figure 26; Supplementary Table 18)		
Pathology	*Testicular atrophy*	*Worsening of age effects, ablation of spermatogenesis (rapamycin-induced gonadotoxicity)*
Muscle (Figure 4)		
Histopathological assessment of quadriceps femoris muscle	*Cross-sectional muscle fiber area⇓*	*Cross-sectional muscle fiber area⇓*
Immune system (Supplementary Figures 11-13)		
FACS-based analysis of immune cell populations	*No significant effect on CD8+ T lymphocytes* *CD4+ T lymphocytes⇓*	*CD8+ T lymphocytes⇑* *CD4+ T lymphocytes⇓*
Clinical chemistry (Supplementary Figures 17-20; Supplementary Tables 13-15)		
Clinical chemistry	*No significant effect on plasma cholesterol* *Impaired glucose tolerance* *Plasma alkaline phosphatase⇑* *No significant effect on plasma corticosterone*	*Hypercholesterolemia* *Worsening of age effect* *Plasma alkaline phosphatase⇑* *Plasma corticosterone⇓*
Endocrine organs (Supplementary Figure 9)		
Histopathology, adrenal glands	*Lipofuscin deposits*	*Lipofuscin deposits⇑*
Cardiovascular system (Supplementary Figure 3)		
Echocardiography	*No significant effect on cardiac output*	*Cardiac output⇓*

Supplementary Table 3: SHIRPA assessment of neurological aging phenotypes

Group	Tremor present	Gait lacking fluidity	No startle response
Young control (*n* = 30 mice)	13.3%	0%	0%
16 months control (*n* = 18 mice)	0%	0%	5.9%
25 months control (*n* = 11 mice)	27.3%	36.4%	100%
34 months control (*n* = 10 mice)	100%	80%	100%
16 months rapamycin (*n* = 20 mice)	10%	0%	5%
25 months rapamycin (*n* = 15 mice)	53.3%	53.3%	100%
34 months rapamycin (*n* = 15 mice)	100%	93.3%	100%

Supplementary Table 4: Aging-associated myocardial pathology

Group	Myocardial pathology		
	1	**2**	**3**
Young control (*n* = 17 mice)	—	—	—
16 months control (*n* = 10 mice)	40%	—	—
25 months control (*n* = 5 mice)	—	80%	—
34 months control (*n* = 5 mice)	—	100%	—
16 months rapamycin (*n* = 15 mice)	33.3%	—	—
25 months rapamycin (*n* = 8 mice)		75%	12.5%
34 months rapamycin (*n* = 10 mice)	—	—	100%

Supplementary Table 5: Aging-associated aortic degeneration

Group	Aortic degeneration		
	1	2	3
Young control (*n* = 17 mice)	—	—	—
16 months control (*n* = 10 mice)	—	—	—
25 months control (*n* = 5 mice)	20%	—	—
34 months control (*n* = 5 mice)	100%	—	—
16 months rapamycin (*n* = 15 mice)	—	—	—
25 months rapamycin (*n* = 8 mice)	12.5%	—	—
34 months rapamycin (*n* = 10 mice)	30%	—	60%

Supplementary Table 6: Aging-associated liver changes

Group	Steatosis			Periportal fibrosis		
	1	2	3	1	2	3
Young control (*n* = 17 mice)	17.6%	17.6%	—	—	—	—
16 months control (*n* = 10 mice)	50%	20%	—	—	—	—
25 months control (*n* = 5 mice)	20%	—	—	20%	—	—
34 months control (*n* = 5 mice)	20%	20%	—	60%	—	—
16 months rapamycin (*n* = 15 mice)	40%	13.3%	13.3%	13.3%	—	—
25 months rapamycin (*n* = 8 mice)	50%	—	—	12.5%	—	—
34 months rapamycin (*n* = 10 mice)	30%	—	—	40%	—	—

Supplementary Table 7: Aging-associated liver changes

Group	Histiocytic sarcoma	Hepatocellular carcinoma	Foci	Polyploidy		
				1	2	3
Young control (*n* = 17 mice)	—	—	—	23.5%	—	—
16 months control (*n* = 10 mice)	10%	10%	—	40%	20%	—
25 months control (*n* = 5 mice)	20%	—	—	40%	40%	—
34 months control (*n* = 5 mice)	—	—	—	60%	40%	—
16 months rapamycin (*n* = 15 mice)	—	—	6.7%	66.7%	25%	—
25 months rapamycin (*n* = 8 mice)	25%	—	12.5%	25%	25%	—
34 months rapamycin (*n* = 10 mice)	10%	10%	—	40%	60%	—

Supplementary Table 8: Aging-associated liver changes

Group	Hepatitis			Microgranuloma
	1	2	3	
Young control (*n* = 17 mice)	—	—	—	23.5%
16 months control (*n* = 10 mice)	10%	—	—	50%
25 months control (*n* = 5 mice)	—	—	—	60%
34 months control (*n* = 5 mice)	20%	—	—	80%
16 months rapamycin (*n* = 15 mice)	—	—	—	20%
25 months rapamycin (*n* = 8 mice)	25%	12.5%	—	37.5%
34 months rapamycin (*n* = 10 mice)	50%	10%	—	80%

Supplementary Table 9: Age-related thyroid pathology

Group	Thyroid adenoma/follicular cell hyperplasia
Young control (*n* = 17 mice)	—
16 months control (*n* = 10 mice)	40%
25 months control (*n* = 5 mice)	20%
36 months control (*n* = 5 mice)	80%
16 months rapamycin (*n* = 15 mice)	33.3%
25 months rapamycin (*n* = 8 mice)	37.5%
34 months rapamycin (*n* = 10 mice)	50%

Supplementary Table 10: Age-related pathology in the adrenal glands

Group	Adrenal adenoma	Adrenal nodular hyperplasia
Young control (*n* = 17 mice)	11.8%	23.5%
16 months control (*n* = 10 mice)	10%	70%
25 months control (*n* = 5 mice)	40%	60%
36 months control (*n* = 5 mice)	40%	40%
16 months rapamycin (*n* = 15 mice)	6.7%	53.3%
25 months rapamycin (*n* = 8 mice)	50%	62.5%
34 months rapamycin (*n* = 10 mice)	10%	60%

Supplementary Table 11: Age-related metabolic changes (effect of age)

Parameter	**Young control (*n* = 10 mice)**	**16 months control (*n* = 15 mice)**	**Linear model, age (*P* value)**	**Linear model, body mass (*P* value)**	**Young control (*n* = 10 mice)**	**25 months control (*n* = 10 mice)**	**Linear model, age (*P* value)**	**Linear model, body mass (*P* value)**
Avg. mass [g]	32.6 ± 1.4	44.5 ± 6.9	**<0.0001**	N/A	32.2 ± 1.0	38.7 ± 7.1	**0.0104**	N/A
Body temperature [°C]	35.9 ± 0.4	35.6 ± 0.5	0.1326	N/A	36.2 ± 0.7	34.8 ± 0.6	**0.0002**	N/A
Food intake [g]	3.4 ± 0.7	3.0 ± 0.8	0.1942	0.5279	3.4 ± 0.7	2.0 ± 1.3	0.1886	0.0060
Avg. VO2 [ml/(h animal)]	101.1 ± 5.8	112.3 ± 10.5	0.2741	<0.001	103.4 ± 9.2	104.7 ± 113.5	0.0555	0.0006
Min. VO2 [ml/(h animal)]	71.5 ± 3.9	83.5 ± 8.4	0.7388	0.001	72.5 ± 4.7	76.1 ± 11.3	0.1043	0.0001
Max. VO2 [ml/(h animal)]	135.1 ± 9.5	150.2 ± 13.5	0.8253	0.001	143.2 ± 15.7	134.6 ± 16.5	**0.0064**	0.0038
Avg. RER [VCO2/VO2]	0.91 ± 0.03	0.87 ± 0.03	**0.0035**	N/A	0.90 ± 0.02	0.83 ± 0.06	**0.0024**	N/A
Avg. Distance [cm]	641 ± 142	604 ± 219	0.6450	N/A	894 ± 268	806 ± 230	0.4397	N/A
Avg. Rearing [counts]	96 ± 32	118 ± 37	0.1366	N/A	117 ± 36	151 ± 40	0.0604	N/A

Supplementary Table 12: Age-related metabolic changes (effect of rapamycin)

Parameter	**Young control (*n* = 10 mice)**	**16 months control (*n* = 15 mice)**	**16 months control (*n* = 19 mice)**	**Linear model, treatment (*P* value)**	**Linear model, body mass (*P* value)**	**Young control (*n* = 10 mice)**	**25 months control (*n* = 10 mice)**	**25 months rapamycin (*n* = 14 mice)**	**Linear model, treatment (*P* value)**	**Linear model, body mass (*P* value)**
Avg. mass [g]	32.6 ± 1.4	44.5 ± 6.9	44.1 ± 6.6	0.8486	N/A	32.2 ± 1.0	38.7 ± 7.1	34.1 ± 5.0	0.0789	N/A
Body temperature [°C]	35.9 ± 0.4	35.6 ± 0.5	35.5 ± 0.5	0.6248	N/A	36.2 ± 0.7	34.8 ± 0.6	34.0 ± 2.7	0.3642	N/A
Food intake [g]	3.4 ± 0.7	3.0 ± 0.8	3.1 ± 0.7	0.8010	0.8247	3.4 ± 0.7	2.0 ± 1.3	3.3 ± 1.2	0.0981	0.0090
Avg. VO2 [ml/(h animal)]	101.1 ± 5.8	112.3 ± 10.5	113.0 ± 9.6	0.5973	<0.0001	103.4 ± 9.2	104.7 ± 113.5	97.1 ± 13.4	0.9056	<0.0001
Min. VO2 [ml/(h animal)]	71.5 ± 3.9	83.5 ± 8.4	83.4 ± 9.6	0.9137	<0.0001	72.5 ± 4.7	76.1 ± 11.3	66.1 ± 10.9	0.2957	<0.0001
Max. VO2 [ml/(h animal)]	135.1 ± 9.5	150.2 ± 13.5	149.1 ± 11.2	0.8206	<0.0001	143.2 ± 15.7	134.6 ± 16.5	127.1 ± 20.1	0.6703	<0.0001
Avg. RER [VCO2/VO2]	0.91 ± 0.03	0.87 ± 0.03	0.88 ± 0.03	0.6465	N/A	0.9 ± 0.02	0.83 ± 0.06	0.88 ± 0.04	**0.0202**	N/A
Avg. Distance [cm]	641 ± 142	604 ± 219	661 ± 213	0.4506	N/A	894 ± 268	806 ± 230	822 ± 323	0.8929	N/A
Avg. Rearing [counts]	96 ± 32	118 ± 37	145 ± 56	0.1256	N/A	117 ± 36	151 ± 40	127 ± 60	0.2771	N/A

Supplementary Table 13: Steroid metabolism (16 months old cohort)

Parameter	**Young control (*n* = 17 mice)**	**16 months control (*n* = 10 mice)**	**16 months rapamycin (*n* = 19 mice)**	**P value young control vs. 16 months control**	**P value 16 months control vs. 16 months rapamycin**
Corticosterone [nmol/L]	177.2 [136.5, 185.3]	151.2 [93.9, 250.2]	71.6 [51.7, 115.5]	NA	**0.018**
Androstenedione [nmol/L]	1.9 [<0.4, 6.5]	<0.4 [<0.4, 0.4]	<0.4 [<0.4, <0.4]	**0.039**	NA
Testosterone [nmol/L]	40.0 [5.9, 96.7]	3.5 [2.4, 19.1]	3.0 [1.0, 10.5]	NA	NA

Supplementary Table 14: Steroid metabolism (25 months old cohort)

Parameter	**Young control (*n* = 10 mice)**	**25 months control (*n* = 9 mice)**	**25 months rapamycin (*n* = 16 mice)**	**P value young control vs. 25 months control**	**P value 25 months control vs. 25 months rapamycin**
Corticosterone [nmol/L]	159.0 [121.2, 269.9	56.6 [34.5, 243.8]	29.0 [25.5, 46.0]	NA	**0.016**
Androstenedione [nmol/L]	0.5 [<0.4, 1.0]	<0.4 [<0.4, 0.5]	<0.4 [<0.4, <0.4]	NA	NA
Testosterone [nmol/L]	24.5 [16, 68.0]	11.9 [3.9, 38.1]	6.4 [4.0, 7.7]	NA	NA

Supplementary Table 15: Steroid metabolism (34 months old cohort)

Parameter	**Young control (*n* = 10 mice)**	**34 months control (*n* = 9 mice)**	**34 months rapamycin (*n* = 14 mice)**	**P value young control vs. 34 months control**	**P value 34 months control vs. 34 months rapamycin**
Corticosterone [nmol/L]	99.3 [72.4, 158.5]	266.1 [80.4, 337.7]	92.1 [36.9, 124.69]	NA	NA
Androstenedione [nmol/L]	<0.4 [<0.4, 1.1]	<0.4 [<0.4, 0.5]	<0.4 [<0.4, <0.4]	NA	NA
Testosterone [nmol/L]	13.6 [4.6, 70.0]	0.8 [0.4, 1.6]	4.4 [1.3, 17.1]	**<0.001**	NA

Supplementary Table 16: Histopathological assessment of kidney

Group	Glomerulosclerosis			Scars			Hydronephrosis
	1	2	3	1	2	3	
Young control (*n* = 17 mice)	—	—	—	—	—	—	—
16 months control (*n* = 10 mice)	—	—	—	60%	10%	—	20%
25 months control (*n* = 5 mice)	20%	—	—	40%	40%	—	—
36 months control (*n* = 5 mice)	60%	—	—	40%	40%	—	60%
16 months rapamycin (*n* = 15 mice)	—	—	—	33%	20%	—	—
25 months rapamycin (*n* = 8 mice)	50%	—	—	—	88%	—	13%
36 months rapamycin (*n* = 10 mice)	60%	—	—	—	100%	—	40%

Supplementary Table 17: Histopathological assessment of kidney

Group	Vacuolization of tubulus epithelia			Hyperplasia of tubulus epithelia			Protein casts
	1	2	3	1	2	3	
Young control (*n* = 17 mice)	18%	—	—	—	—	—	—
16 months control (*n* = 10 mice)	80%	—	—	90%	10%	—	50%
25 months control (*n* = 5 mice)	80%	—	—	80%	—	—	20%
36 months control (*n* = 5 mice)	20%	—	—	40%	40%	—	20%
16 months rapamycin (*n* = 15 mice)	33%	27%	40%	80%	20%	—	27%
25 months rapamycin (*n* = 8 mice)	25%	38%	38%	—	100%	—	13%
36 months rapamycin (*n* = 10 mice)	50%	—	—	—	100%	—	30%

Supplementary Table 18: Histopathological assessment of the male reproductive tract

Group	Testicular atrophy			Leydig cell hyperplasia	Spermatohydrocele
	1	2	3		
Young control (*n* = 17 mice)	—	—	—	—	6%
16 months control (*n* = 10 mice)	80%	20%	—	30%	10%
25 months control (*n* = 5 mice)	100%	—	—	—	20%
34 months control (*n* = 5 mice)	80%	—	—	20%	20%
16 months rapamycin (*n* = 15 mice)	53%	27%	20%	67%	33%
25 months rapamycin (*n* = 8 mice)	—	50%	50%	63%	25%
34 months rapamycin (*n* = 10 mice)	—	40%	60%	60%	30%

Supplementary Table 19: Histopathological assessment of age-related pancreatic alterations

Group	Exocrine pancreatitis	Ductal metaplasia
Young control (*n* = 17 mice)	—	—
16 months control (*n* = 10 mice)	30%	30%
25 months control (*n* = 5 mice)	40%	—
34 months control (*n* = 5 mice)	—	—
16 months rapamycin (*n* = 15 mice)	33.3%	—
25 months rapamycin (*n* = 8 mice)	—	—
34 months rapamycin (*n* = 10 mice)	20%	10%

Supplementary Table 20: Bone densitometry

Parameter	**Young control (*n* = 10 mice)**	**16 months control (*n* = 15 mice)**	**16 months rapamycin (*n* = 19 mice)**	**T-test vehicle vs. rapamycin (adj. p-value)**
Bone mineral density (BMD) [mg/cm^2]	48 ± 2	56 ± 5	59 ± 7	0.163
Bone mineral content (BMC) [mg]	513 ± 58	678 ± 253	705 ± 317	0.790
Bone content [%]	1.59 ± 0.16	1.59 ± 0.51	1.70 ± 0.69	0.624
Body length [cm]	10.18 ± 0.22	10.61 ± 0.35	10.46 ± 0.27	0.163
Body Weight [g]	32.50 ± 3.93	42.05 ± 5.82	41.33 ± 6.19	0.739
Fat mass [g]	3.65 ± 1.87	13.49 ± 8.45	14.40 ± 8.28	0.761
Lean mass [g]	23.72 ± 1.49	21.32 ± 5.20	19.93 ± 5.63	0.479

Supplementary Table 21: Bone histopathology

Group	Osteoporosis		
	1	2	3
Young control (*n* = 17 mice)	—	—	—
16 months control (*n* = 10 mice)	—	—	—
25 months control (*n* = 5 mice)	—	—	—
34 months control (*n* = 5 mice)	40%	—	—
16 months rapamycin (*n* = 15 mice)	—	—	—
25 months rapamycin (*n* = 8 mice)	—	—	—
34 months rapamycin (*n* = 10 mice)	40%	—	—

Supplementary Table 22: Age-related skin atrophy

Group	Skin atrophy		
	1	2	3
Young control (*n* = 17 mice)	—	—	—
16 months control (*n* = 10 mice)	—	—	—
25 months control (*n* = 5 mice)	—	—	—
34 months control (*n* = 5 mice)	60%	—	—
16 months rapamycin (*n* = 15 mice)	—	—	—
25 months rapamycin (*n* = 8 mice)	—	—	—
34 months rapamycin (*n* = 10 mice)	50%	—	—

Supplementary Table 23: Pathologies of the pituitary gland

Group	Pituitary degenerative cysts	Hyperplastic clones
Young control (*n* = 17 mice)	11.8%	—
16 months control (*n* = 10 mice)	30%	10%
25 months control (*n* = 5 mice)	20%	—
36 months control (*n* = 5 mice)	40%	40%
16 months rapamycin (*n* = 15 mice)	13.3%	13.3%
25 months rapamycin (*n* = 8 mice)	37.5%	12.5%
36 months rapamycin (*n* = 10 mice)	—	10%

Supplementary Table 24: Cancers and precancerous lesions

16 mo control (4 out of 10 animals with cancers and/or precancerous lesions)	1 animal with histiocytic sarcoma and ductal metaplasia 1 animal with hepatocellular carcinoma 1 animal with lymphoma and ductal metaplasia 1 animal with ductal metaplasia
16 mo rapamycin (0 out of 15 animals with cancers and/or precancerous lesions)	

25 mo control (1 out of 5 animals with cancers and/or precancerous lesions)	1 animal with histiocytic sarcoma and adenocarcinoma of the lung
25 mo rapamycin (2 out of 8 animals with cancers and/or precancerous lesions)	1 animal with histiocytic sarcoma 1 animal with histiocytic sarcoma and adenocarcinoma of the lung

34 mo control (1 out of 5 animals with cancers and/or precancerous lesions)	1 animal with ductal metaplasia
34 mo rapamycin (3 out of 10 animals with cancers and/or precancerous lesions)	1 animal with hepatocellular carcinoma and ductal metaplasia 1 animal with histiocytic sarcoma 1 animal with adenocarcinoma of the thyroid

Supplementary Table Legends

Supplementary Table 1
Rapamycin showed extensive tissue distribution. The table shows rapamycin concentrations in the blood and a number of tissues of treated animals. Blood and tissue was harvested for HPLC detection of rapamycin from 22 months old animals that had been on the rapamycin-containing chow (for details, see Material and Methods) for 5 months. The table shows the distribution of blood/tissue concentrations (means +/- SEM) in these mice. As expected, the compound showed wide tissue distribution in treated animals.

Supplementary Table 2
A few aging-associated pathologies were promoted by rapamycin treatment. The table summarizes aging phenotypes that were worsened by rapamycin treatment and shows phenotypes influenced by rapamycin, but not aging.

Supplementary Table 3
Aging was associated with neurological findings, which remained unaltered by rapamycin. The table shows a selection of findings from the SHIRPA assessment. Listed is the percentage of mice in each group that displayed the phenotypes mentioned. Logistic regression analyses revealed significant effects of aging, but not rapamycin, on the presence of tremor (odds ratio per month increase in aging: 1.14, 95% CI [1.07, 1.22], *P*=5.49e-14; odds ratio due to treatment with rapamycin: 0.01, 95% CI [7.17e-05, 0.59], *P*=0.63) and gait abnormalities (odds ratio per month increase in aging: 1.35, 95% CI [1.18, 1.67], *P*=3.82e-20; odds ratio due to treatment with rapamycin is 0.23, 95% CI [3.39e-05, 361.46] *P*=0.19).

Supplementary Table 4
Pronounced myocardial pathology in aged mice was not measurably improved by rapamycin. The table shows the percentage of mice that displayed myocardial pathology (e.g., fresh/old myocardial infarcts, thickening of the heart valves, ventricular dilation, myocardial hypertrophy). The following grading system was used to describe the severity of pathological lesions: 1 – mild pathology; 2 – moderate pathology; 3 – severe pathology.
Logistic regression analyses showed the expected significant effects of aging on the prevalence of myocardial pathology (odds ratio per month increase in aging: 1.64, 95% CI [1.19, 2.25], *P*=0.0026). Rapamycin appeared to have no clear protective effect on myocardial aging-associated pathology and may have even worsened findings in 34 months old mice.

Supplementary Table 5
Arterial degeneration during aging was not measurably affected by rapamycin. The table shows the percentage of mice that displayed aortic degeneration (split-up and disorganization of elastic fibers, replacement of smooth muscle cells by mucinous substance). The following grading system was used to describe the severity of pathological lesions: 1 – mild pathology; 2 – moderate pathology; 3 – severe pathology.
Logistic regression analyses revealed an increased prevalence of aortic degeneration in aged mice (odds ratio per month increase in aging: 1.48, 95% CI [1.09, 2.0], *P*=0.01). We could not detect a significant effect of rapamycin on the prevalence of histopathological alterations in the aorta (odds ratio due to treatment with rapamycin: 0.0007, 95% CI [1.98e-09, 215.6], *P*=0.19).

Supplementary Table 6

Age-related periportal fibrosis was not measurably influenced by rapamycin. Supplementary Table 6 displays the proportion of rapamycin-treated or vehicle-treated aged mice, as well as young controls, that show different histopathological hepatic alterations (steatosis, periportal fibrosis) of various degrees of severity. The following qualitative grading system was used to determine severity of pathological tissue alterations: 1 – mild pathology; 2 – moderate pathology; 3 – severe pathology.

Logistic regression analyses showed a significant aging effect on the prevalence of periportal fibrosis (odds ratio per month increase in aging: 1.3, 95% CI [1.03, 1.66], *P*=0.03). The analyses could not discern a significant effect of rapamycin on this aging-associated liver alteration (odds ratio due to treatment with rapamycin: 150.5, 95% CI [0.05, 413288], *P*=0.18). Statistical analyses did not reveal significant effects of aging and rapamycin on steatosis (odds ratio per month increase in aging: 1.0, 95% CI [0.94, 1.06], *P*=0.98; odds ratio due to treatment with rapamycin: 12.6, 95% CI [1.12, 141.78], *P*=0.07).

Supplementary Table 7

Age-related liver polyploidy was not measurably influenced by rapamycin. Supplementary Table 7 displays the proportion of rapamycin-treated or vehicle-treated aged mice, as well as young controls, that show different histopathological hepatic alterations (cancers, foci, polyploidy) of various degrees of severity. The following qualitative grading system was used to determine severity of pathological tissue alterations: 1 – mild pathology; 2 – moderate pathology; 3 – severe pathology.

Logistic regression analyses showed a significant effect of aging on the prevalence of polyploidy (odds ratio per month increase in aging: 1.12, 95% CI [1.06, 1.20], *P*=2.2e-04), but could not discern a significant treatment effect on this histopathological aging phenotype (odds ratio due to treatment with rapamycin: 7.26, 95% CI [0.70, 75.22], *P*=0.22).

Supplementary Table 8

Age-associated increases in the prevalence of hepatic microgranulomas may be reduced by rapamycin. The table displays the proportion of rapamycin-treated or vehicle-treated aged mice, as well as young controls, that show different histopathological hepatic alterations (hepatitis, microgranuloma) of various degrees of severity. The following qualitative grading system was used to determine severity of pathological tissue alterations: 1 – mild pathology; 2 – moderate pathology; 3 – severe pathology.

Logistic regression analyses showed a clear effect of aging on the prevalence of hepatic microgranulomas (odds ratio per month increase in aging: 1.1, 95% CI [1.02, 1.17], *P*=8.8e-04) and suggested that rapamycin may reduce the frequency of this hepatic lesion (odds ratio due to treatment with rapamycin: 0.08, 95% CI [0.003, 1.34], *P*=0.08). Our analyses showed no significant effects of aging and rapamycin on the prevalence of hepatitis (odds ratio per month increase in aging: 1.1, 95% CI [0.95, 1.26], *P*=0.20; odds ratio due to treatment with rapamycin: 0.19, 95% CI [0.0007, 50.28], *P*=0.27).

Supplementary Table 9

Rapamycin did not measurably affect aging-associated thyroid pathology. The table shows the percentage of mice that displayed thyroid adenomas and/or follicular cell hyperplasia.

Logistic regression analyses showed a clear effect of aging on the prevalence of thyroid adenoma/follicular cell hyperplasia (odds ratio per month increase in aging: 1.15, 95% CI [1.06, 1.29], *P*=3.8e-04). We were unable to discern a significant effect of rapamycin on these age-related thyroid pathologies (odds ratio due to treatment with rapamycin: 9.22, 95% CI [0.43, 266.98], *P*=0.97).

Supplementary Table 10
Age-related adrenal gland pathology. The table shows the proportion of mice with adrenal gland pathology.
According to logistic regression analyses, there were non-significant trends towards an increased prevalence of adrenal nodular hyperplasia and adrenal adenomas in aged mice (age: adrenal nodular hyperplasia, odds ratio per month increase in aging: 1.04, 95% CI [0.98, 1.11], *P*=0.07; adrenal adenoma, odds ratio per month increase in aging: 1.06, 95% CI [0.99, 1.15], *P*=0.15. Rapamycin: adrenal nodular hyperplasia, odds ratio due to treatment with rapamycin: 2.18, 95% CI [0.18, 26.79], *P*=0.65; adrenal adenoma, odds ratio due to treatment with rapamycin: 1.27, 95% CI [0.03, 34.44], *P*=0.46).

Supplementary Table 11
Aging was associated with significant metabolic changes, such as declining maximal oxygen consumption, reduced body temperature and a decreased respiratory exchange ratio. The table shows effects of age and body weight on metabolic parameters. Shown are means +/- SD. Significant age effects are highlighted in bold.

Supplementary Table 12
Rapamycin treatment had no significant effect on age-related changes in maximal oxygen consumption and body temperature, but led to an increase in the respiratory exchange ratio. The table shows effects of rapamycin treatment and body weight on metabolic parameters. Shown are means +/- SD. Significant treatment effects are highlighted in bold.

Supplementary Table 13
Rapamycin had no measurable effects on age-related changes in plasma steroid concentrations. The table shows plasma steroid levels. Data shown are: median [25%, 75%]. Significant age/rapamycin effects are highlighted in bold.

Supplementary Table 14
Rapamycin reduced plasma corticosterone concentrations. The table shows plasma steroid levels. Data shown are: median [25%, 75%]. Significant age/rapamycin effects are highlighted in bold.

Supplementary Table 15
Rapamycin had no measurable effects on age-related changes in plasma steroid concentrations. The table shows plasma steroid levels. Data shown are: median [25%, 75%]. Significant age/rapamycin effects are highlighted in bold.

Supplementary Table 16
Rapamycin treatment did not prevent age-related glomerulosclerosis and fibrotic kidney alterations. The table displays the proportion of rapamycin-treated or vehicle-treated aged mice, as well as young controls, that show different histopathological renal alterations (glomerulosclerosis, fibrotic changes, hydronephrosis). The following qualitative grading system was used to determine severity of pathological tissue alterations: 1 – mild pathology; 2 – moderate pathology; 3 – severe pathology.
Logistic regression analyses showed significant effects of aging on all histopathological parameters mentioned above (odds ratio per month increase in age: glomerulosclerosis, 1.30, 95% CI [1.02, 1.66], *P*=0.03; scars, 1.16, 95% CI [1.08, 1.26], *P*=1.29e-04; hydronephrosis, 1.14, 95% CI [1.04, 1.31], *P*=1.77e-04). Rapamycin had no significant effect on glomerulosclerosis and hydronephrosis, but

tended to aggravate fibrotic kidney alterations (odds ratio due to rapamycin: glomerulosclerosis, 13.0, 95% CI [0.004, 47618], *P*=0.63; scars, 0.04, 95% CI [0.0003, 3.83], *P*=0.07; hydronephrosis, 0.02, 95% CI [5.0e-07, 15.2], *P*=0.19).

Supplementary Table 17
Rapamycin treatment was associated with significant nephrotoxicity. The table displays the proportion of rapamycin-treated or vehicle-treated aged mice, as well as young controls, that show different histopathological renal alterations (vacuolization and hyperplasia of tubulus epithelia, protein casts). The following qualitative grading system was used to determine severity of pathological tissue alterations: 1 – mild pathology; 2 – moderate pathology; 3 – severe pathology.
According to logistic regression analyses, rapamycin led to a significant increase in the proportion of animals with toxic vacuolization of tubulus epithelial cells (odds ratio due to rapamycin: 8256, 95% CI [248, 274710], *P*=4.68e-05; odds ratio per month increase in age: 1.04, 95% CI [0.98, 1.11], *P*=0.14). Aging had a significant effect on the hyperplasia of tubulus epithelial cells (odds ratio per month increase in age: 1.24, 95% CI [1.14, 1.37], *P*=1.21e-05). The prevalence of kidney protein casts was not significantly influenced by age or rapamycin (odds ratio per month increase in age: 1.1, 95% CI [0.99, 1.15], *P*=0.14; odds ratio due to rapamycin: 3.1, 95% CI [0.14, 65.7], *P*=0.94).

Supplementary Table 18
Rapamycin treatment promoted age-related testicular atrophy. The table shows the percentage of mice that displayed testicular/epididymal pathology. The following grading system was used: 1 – mild pathology; 2 – moderate pathology; 3 – severe pathology.
Logistic regression analyses showed significant effects of aging and/or rapamycin on testicular atrophy (odds ratio per month increase in age: 1.19, 95% CI [1.09, 1.30], *P*=1.5e-05; odds ratio due to treatment with rapamycin: 118.39, 95% CI [3.35, 4180.66], *P*=0.69) and Leydig cell hyperplasia (odds ratio per month increase in aging is 1.06, 95% CI [0.97, 1.17], P=0.0096; odds ratio due to treatment with rapamycin: 54.89, 95% CI [2.95, 1692.81], *P*=5.22e-05). Effects on the prevalence of spermatohydrocele were non-significant (odds ratio per month increase in age: 1.05, 95% CI [0.96, 1.16], *P*=0.15; odds ratio due to treatment with rapamycin: 10.12, 95% CI [0.49, 282.91], *P*=0.11).

Supplementary Table 19
Age-related pancreas pathology. The table shows the proportion of mice in each group with pancreatic pathology (exocrine pancreatitis, ductal metaplasia).
Logistic regression analyses could not detect significant age- or treatment-related effects on exocrine pancreatitis (odds ratio per month increase in age: 1.05, 95% CI [0.97, 1.15], *P*=0.46; odds ratio due to treatment with rapamycin: 14.36, 95% CI [0.58, 444.0], *P*=0.56) and could not be applied to the analysis of ductal metaplasia data due to low observation frequency.

Supplementary Table 20
Bone density was unaltered in 16 months old mice. The table shows results from bone densitometry measurements using a pDEXA Sabre Bone Densitometer. There was no significant drop in bone mineral density by 16-months of age in mice, suggesting that bone density reductions are simply not yet apparent in this age group. The data are presented as means ± SD.

Supplementary Table 21
Mild osteoporotic changes were present in treated and untreated mice. The table shows percentage of mice that displayed osteoporotic changes. The following

grading system was used: 1 – mild osteoporosis; 2 – moderate osteoporosis; 3 – severe osteoporosis. Mild osteoporosis was present in 40% of 34 months old mice assessed (in both, the vehicle and the rapamycin group).

Supplementary Table 22
Mild skin atrophy was present in treated and untreated animals. The table shows the proportion of mice that displayed histopathological signs of skin atrophy. Severity of skin atrophy was graded as follows: 1 – mild pathology; 2 – moderate pathology; 3 – severe pathology. Aged mice, regardless of treatment, had mild atrophic changes affecting the skin.

Supplementary Table 23
Pathological findings in the pituitary gland were independent of age and treatment. The table shows the proportion of mice in each group with pituitary gland pathology. Both age and rapamycin did not appear to have a major effect on degenerative cysts and hyperplastic clones within the pituitary gland (degenerative cysts: odds ratio per month increase in age, 1.05, 95% CI [0.98, 1.13], *P*=0.67; odds ratio due to treatment with rapamycin, 3.80, 95% CI [0.12, 122.67]; P=0.33). Hyperplastic clones: odds ratio per month increase in age, 1.15, 95% CI [1.02, 1.39] *P*=0.08; odds ratio due to treatment with rapamycin, 40.49, 95% CI [0.31, 31684], P=0.92).

Supplementary Table 24
Cancers and precancerous lesions. The table shows the prevalence of cancers and precancerous lesions found during pathological assessment performed at conclusion of our study.

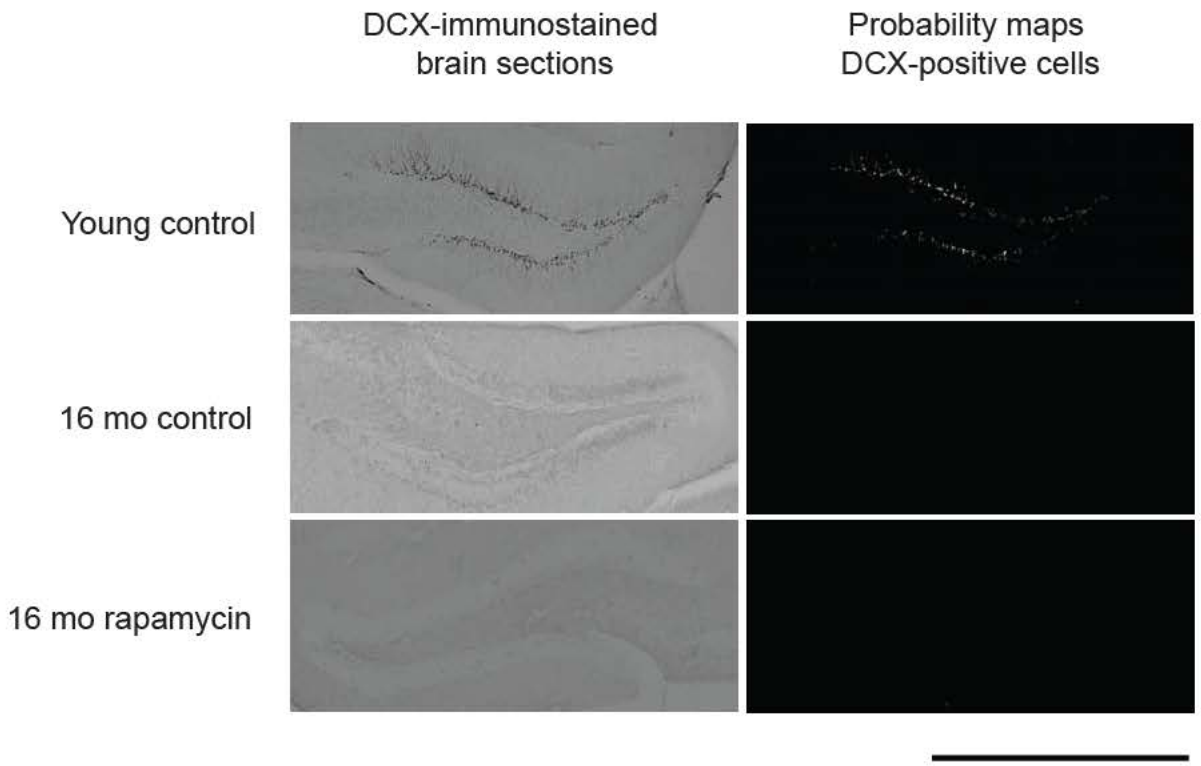

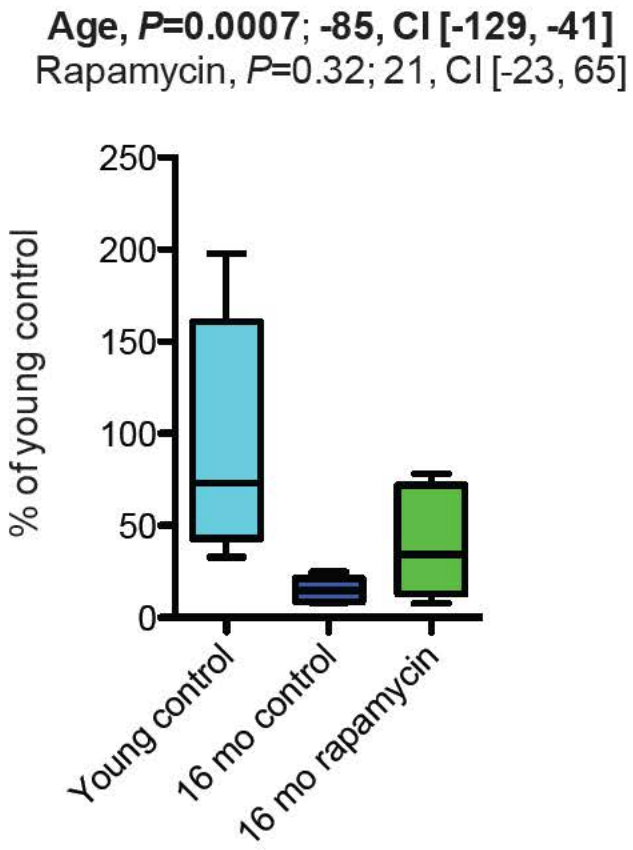

Supplementary Figure 1

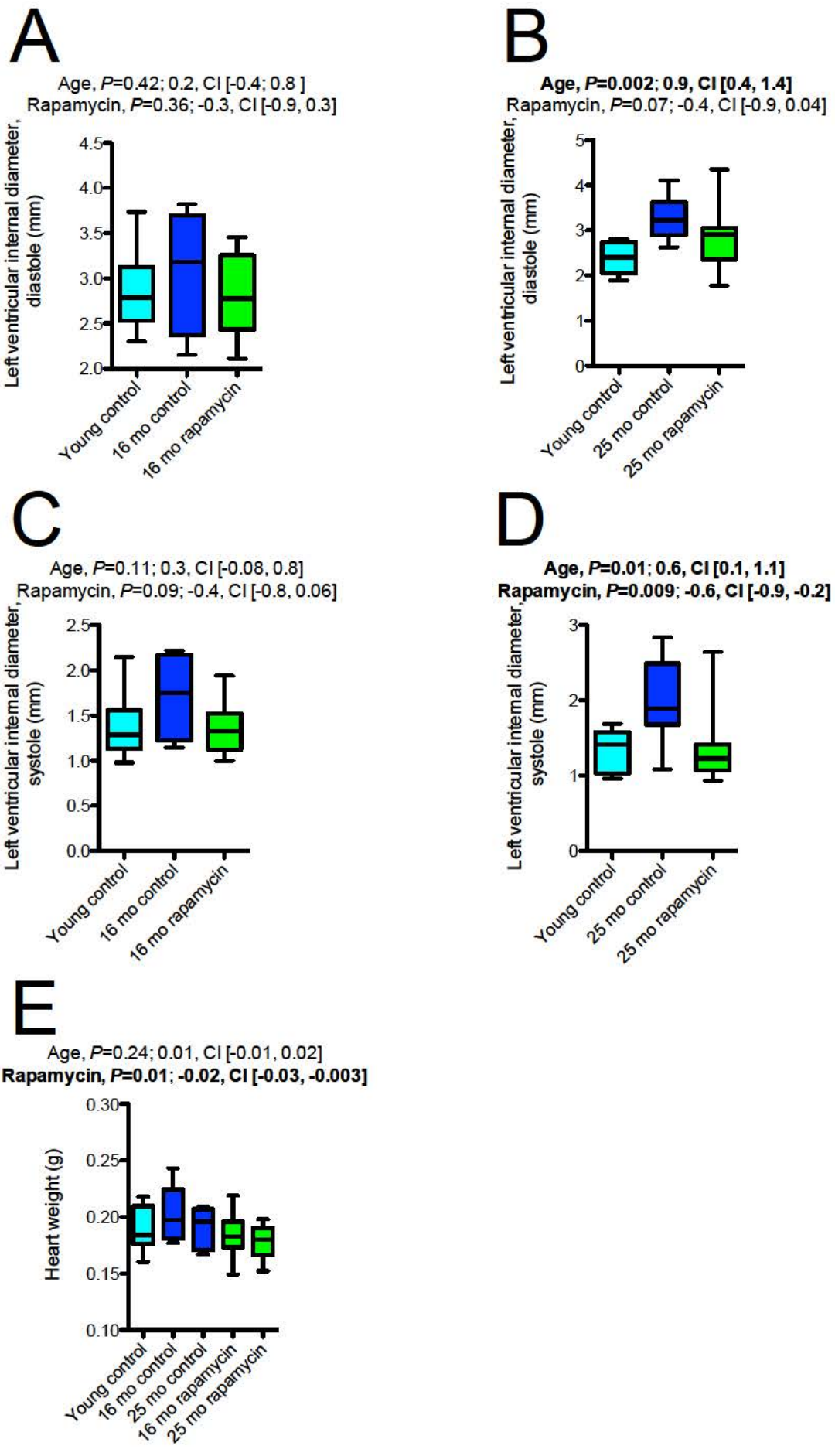

Supplementary Figure 2

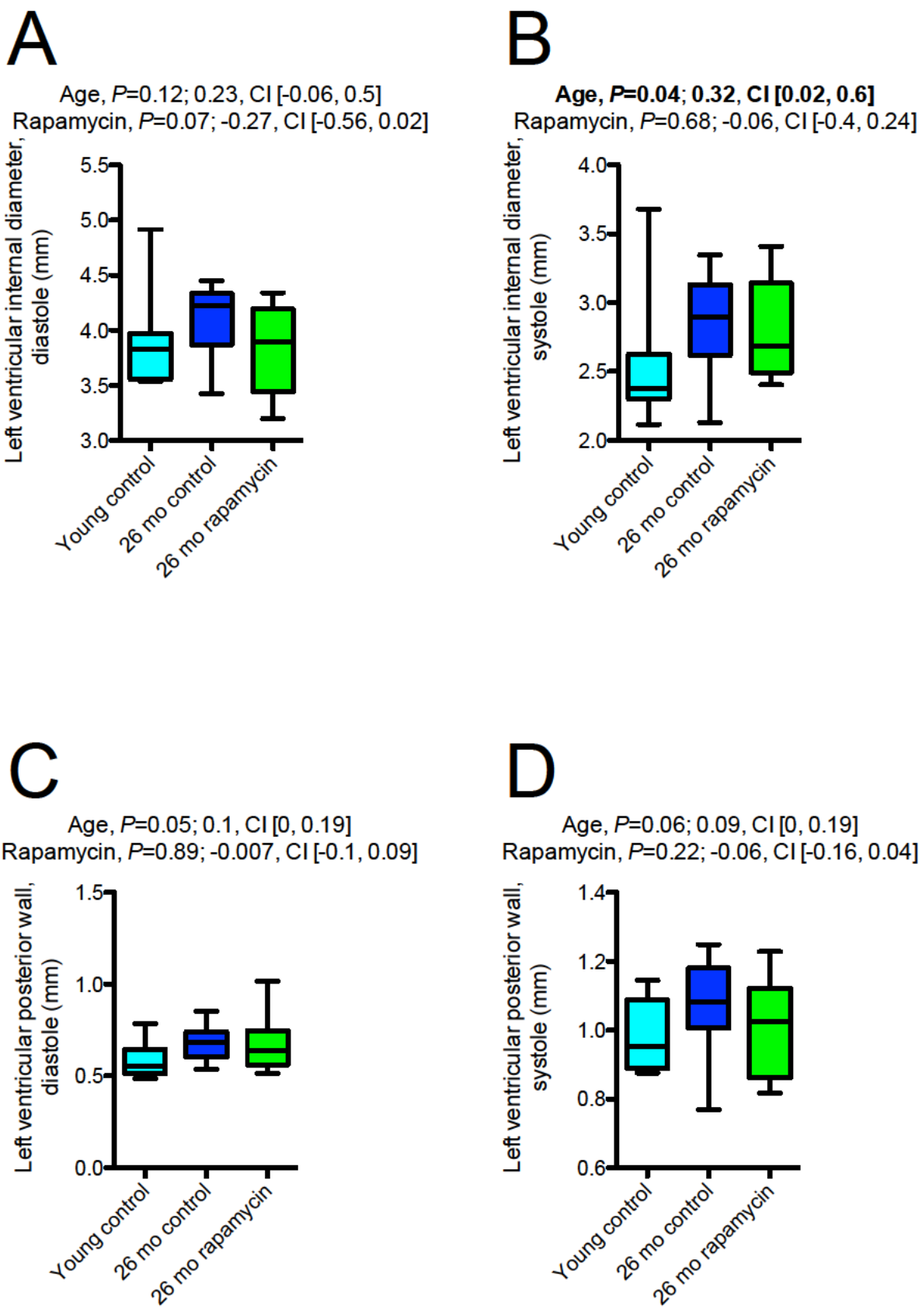

Supplementary Figure 3-I

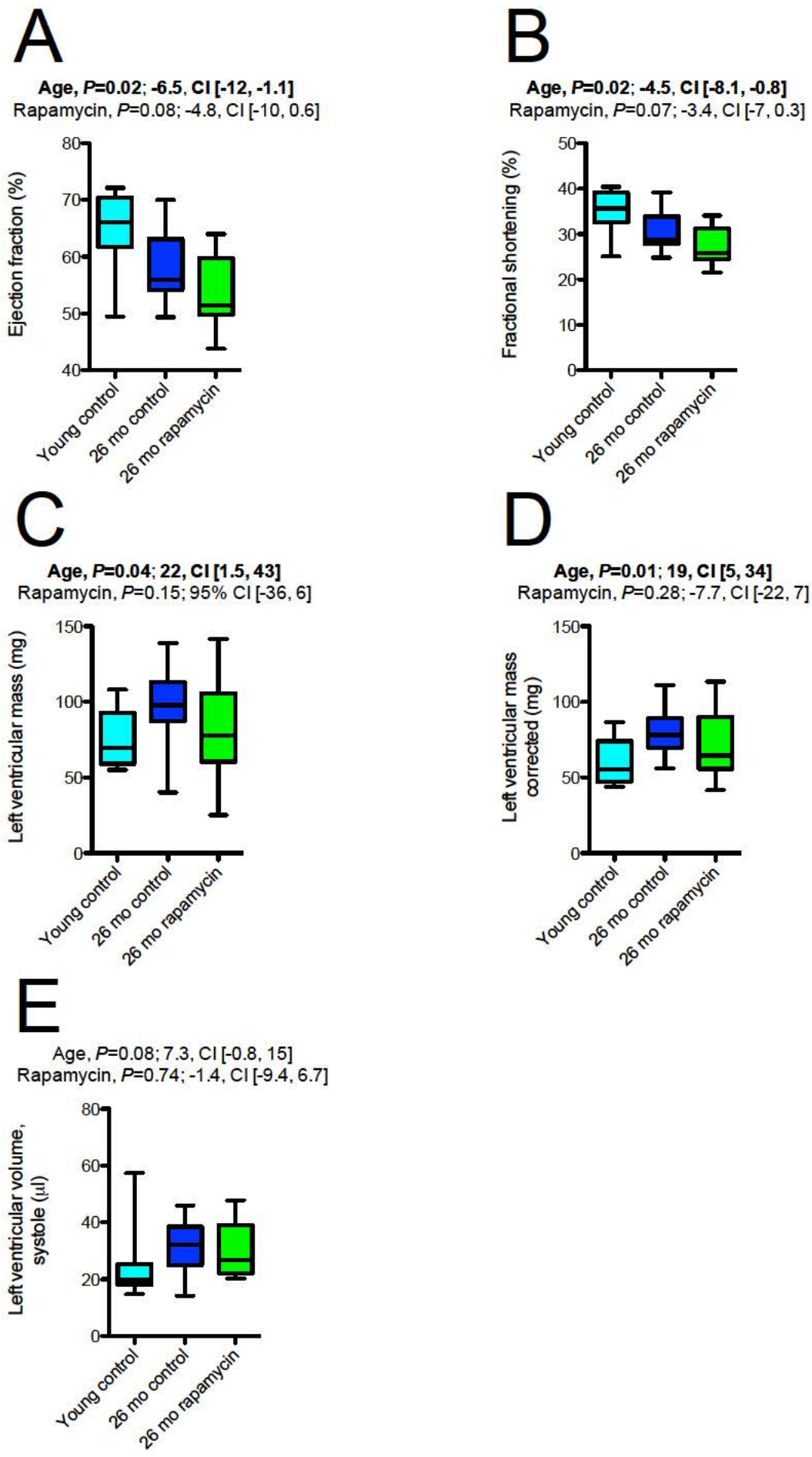

Supplementary Figure 3-II

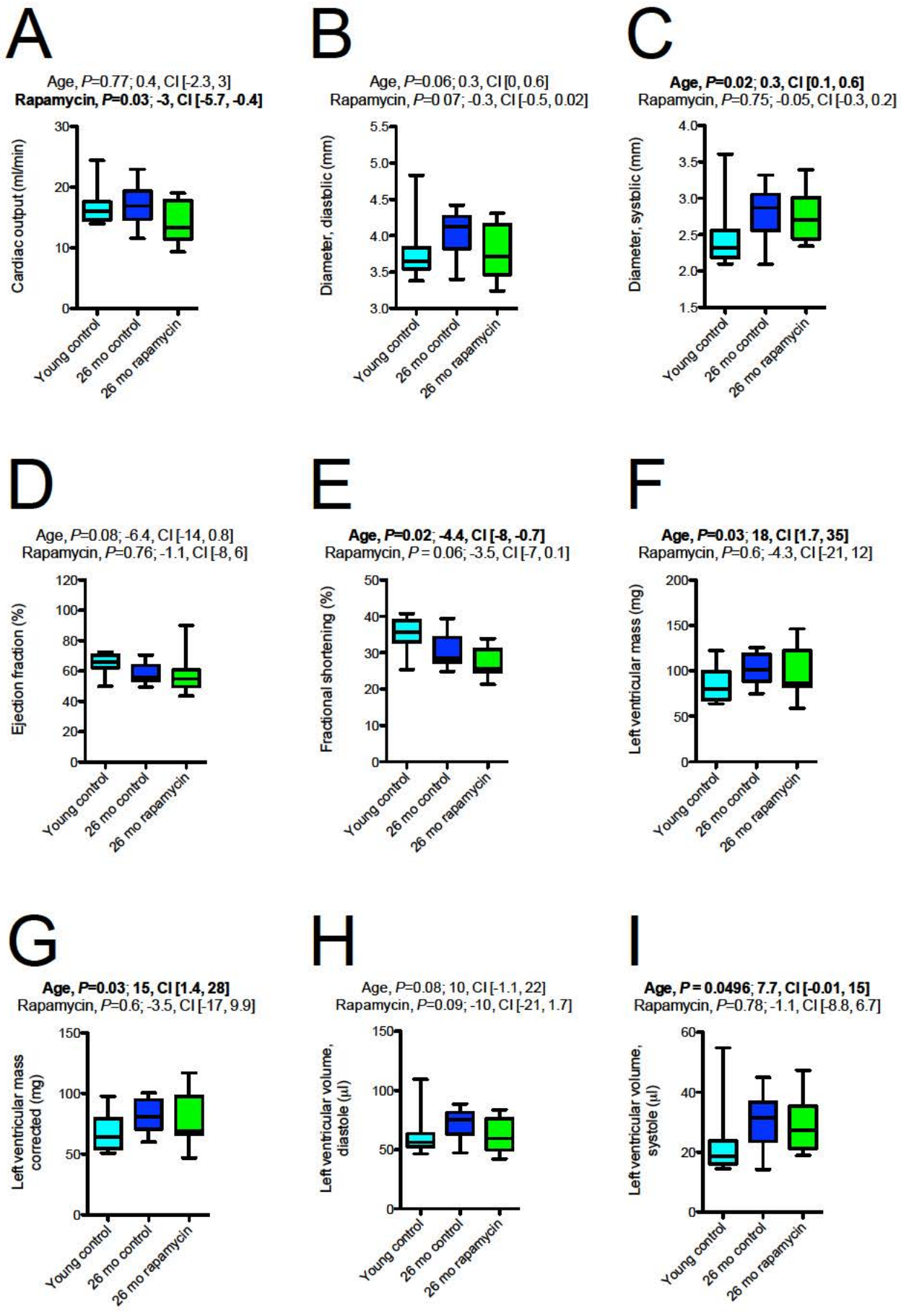

Supplementary Figure 3-III

A

Age, *P*=0.0006; -75, CI [-116, -35]
Rapamycin, *P*=0.84; 4.1, CI [-36, 44]

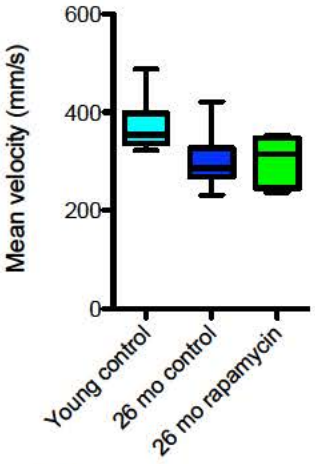

B

Age, *P*=0.02; -110, CI [-200, -20]
Rapamycin, *P*=0.38; -40, CI [-130, 51]

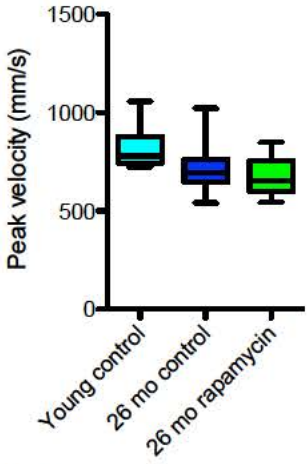

C

Age, *P*=0.0006; -0.21, CI [-0.32, -0.1]
Rapamycin, *P*=0.81; 0.01, CI [-0.1, 0.13]

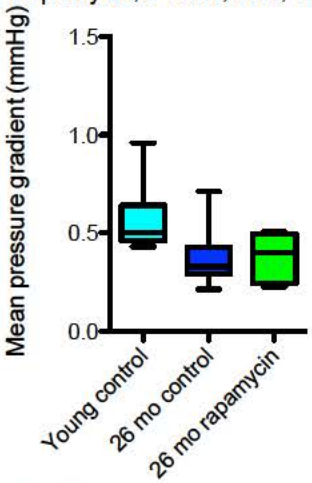

D

Age, *P*=0.02; -0.68, CI [-1.3, -0.1]
Rapamycin, *P*=0.44; -0.23, CI [-0.8, 0.4]

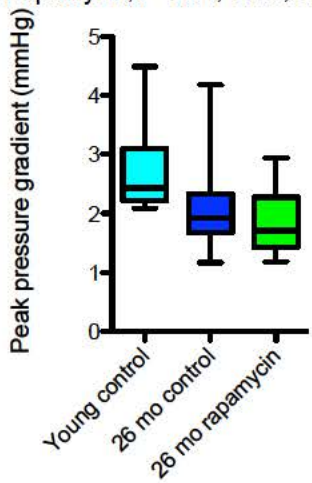

E

Age, *P*=0.001; -6.7, CI [-11, -2.8]
Rapamycin, *P*=0.18; -2.6, CI [-6.5, 1.2]

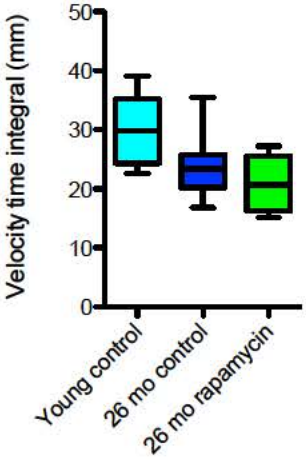

Supplementary Figure 3-IV

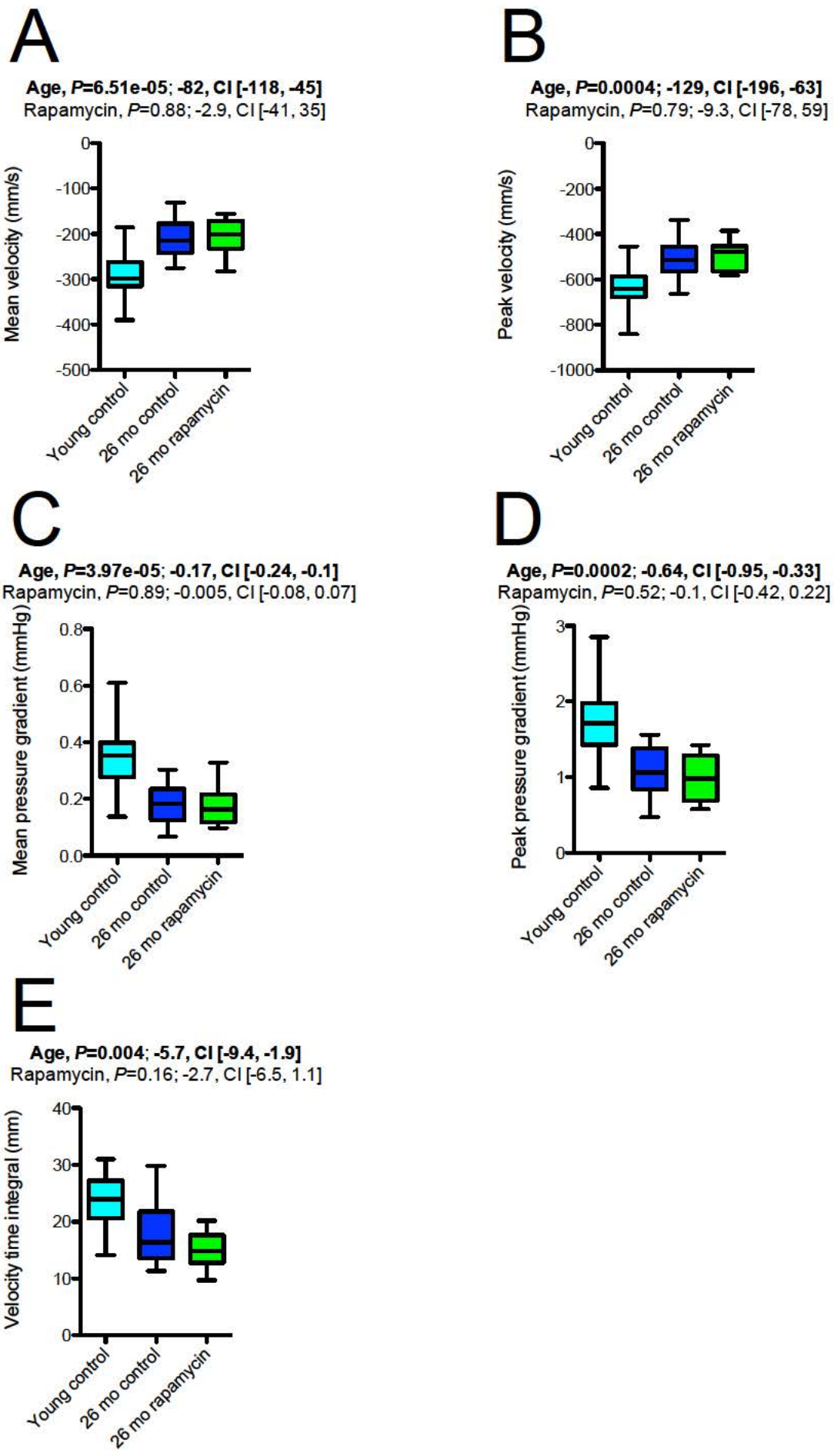

Supplementary Figure 3-V

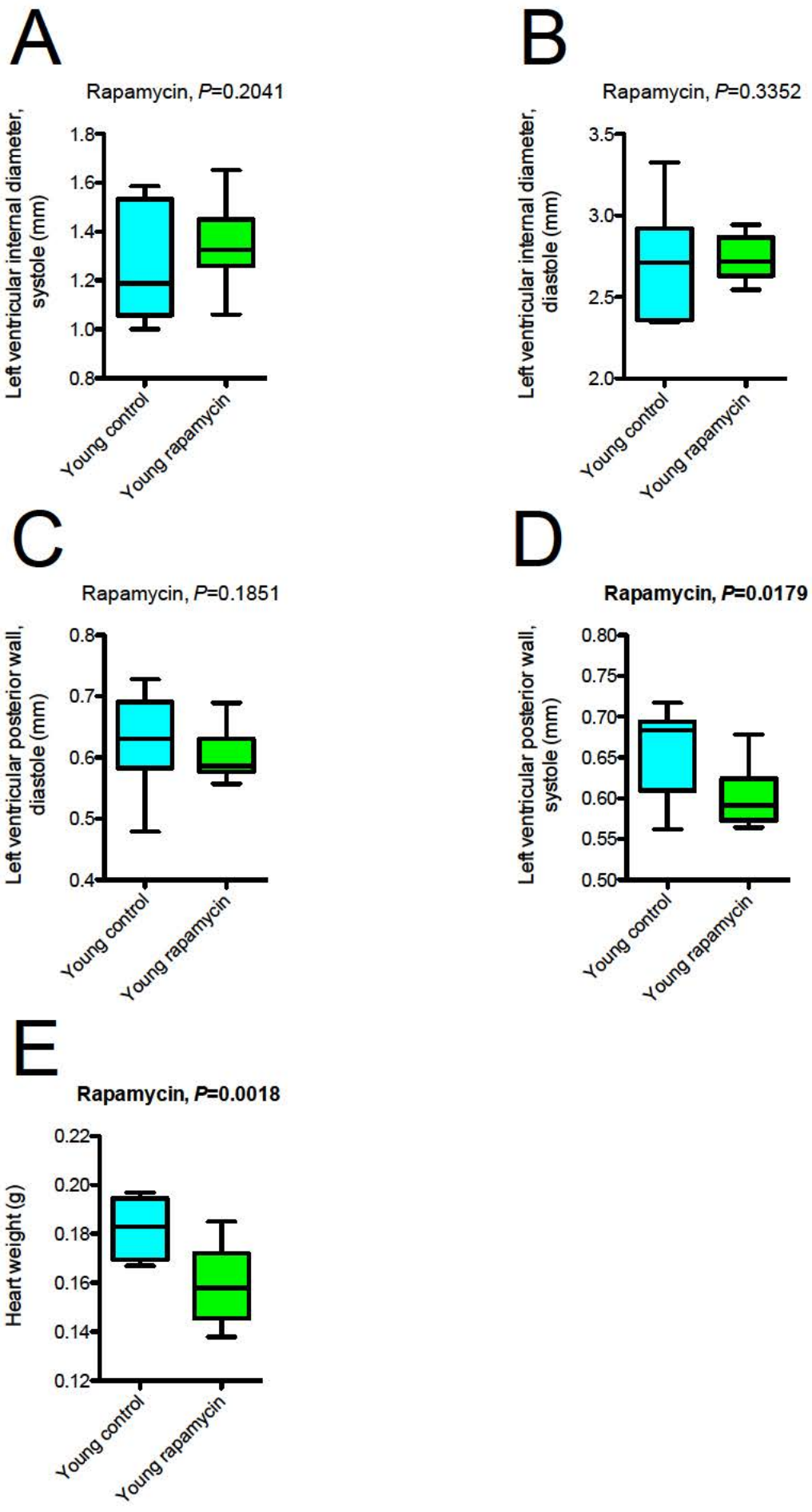

Supplementary Figure 4

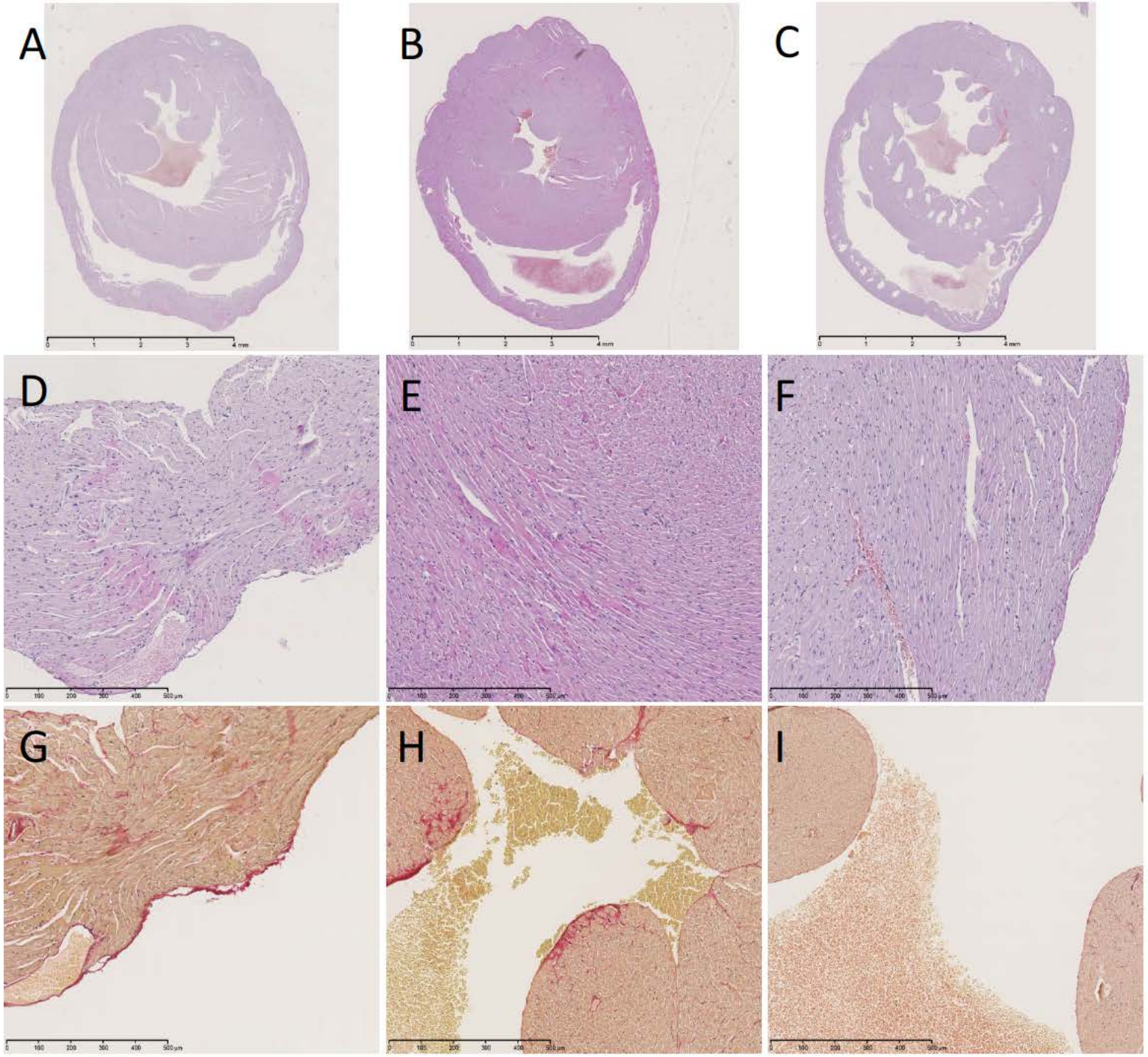

Supplementary Figure 5-I

34 months cohort

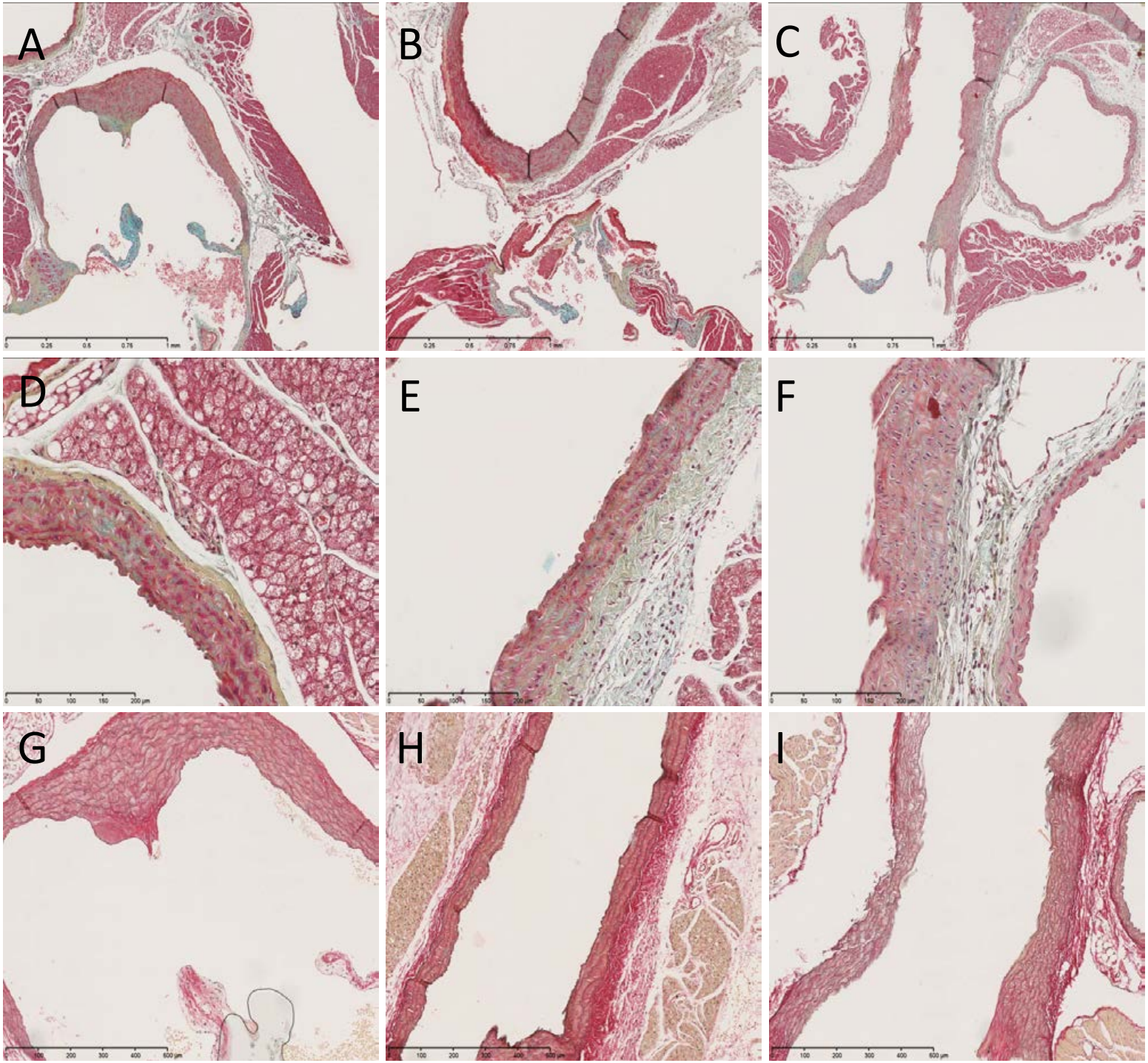

Supplementary Figure 5-II

34 months cohort

Old rapamycin

Old control

Young control

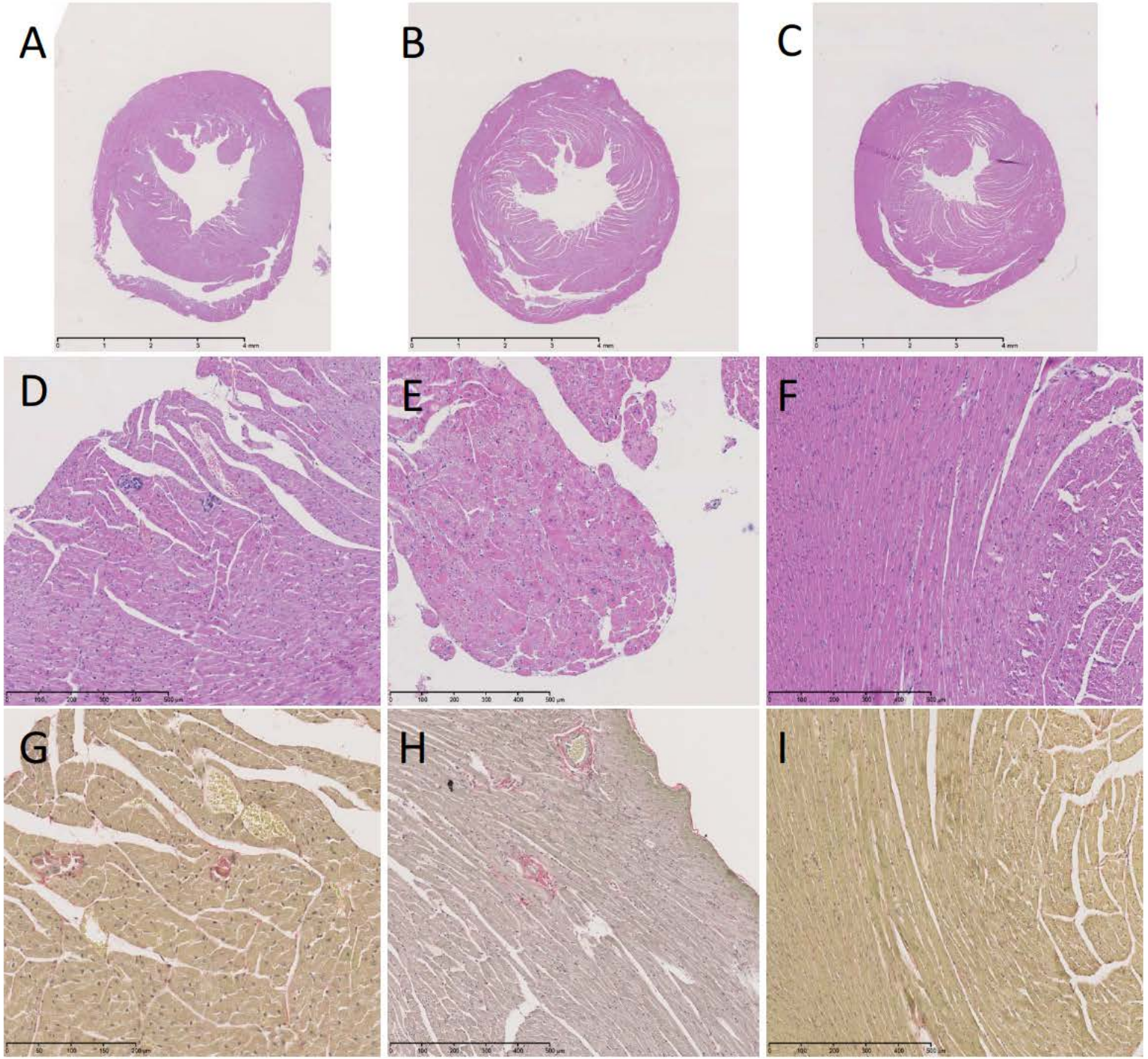

Supplementary Figure 5-III

25 months cohort

Old rapamycin

Old control

Young control

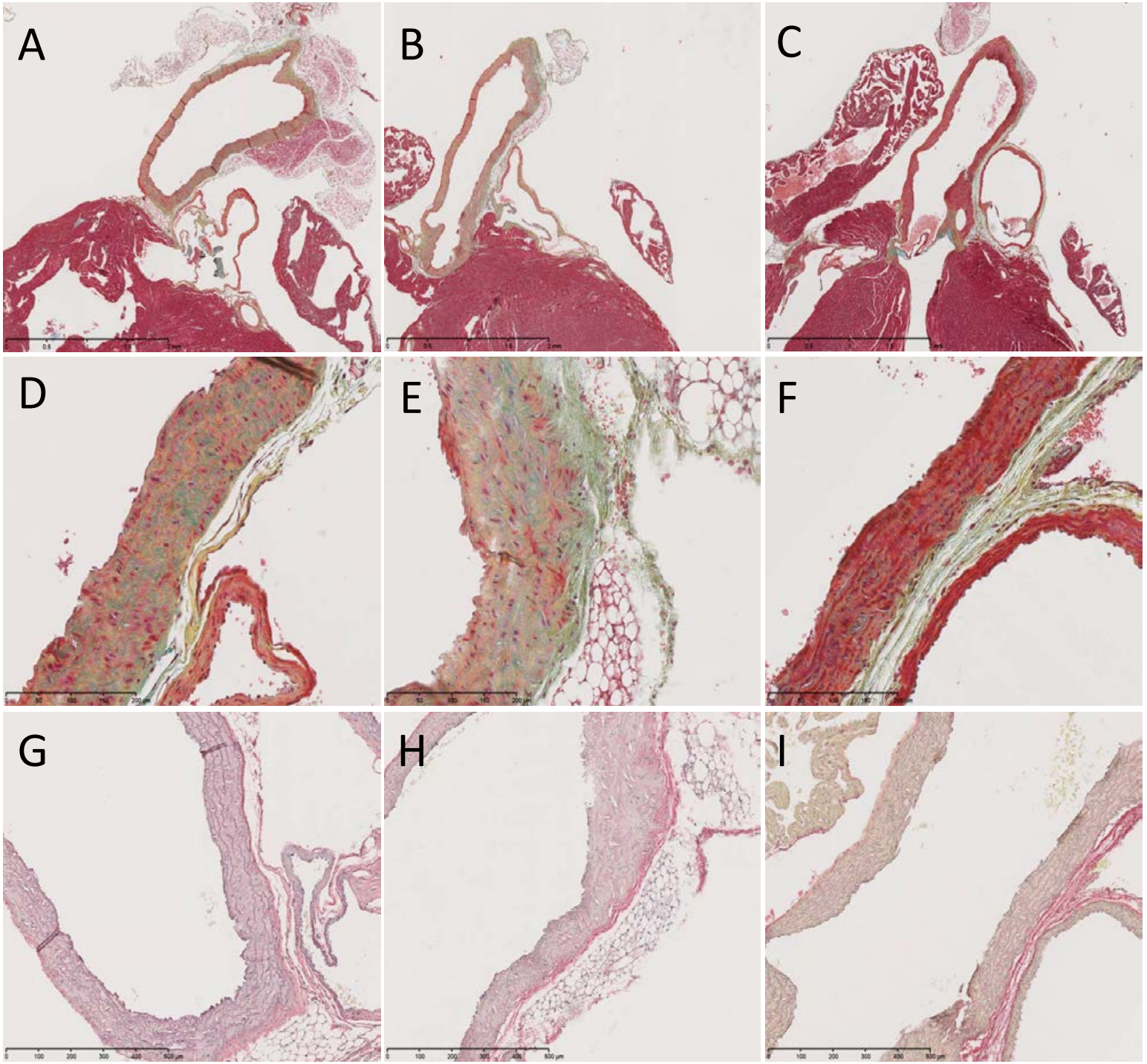

Supplementary Figure 5-IV

25 months cohort

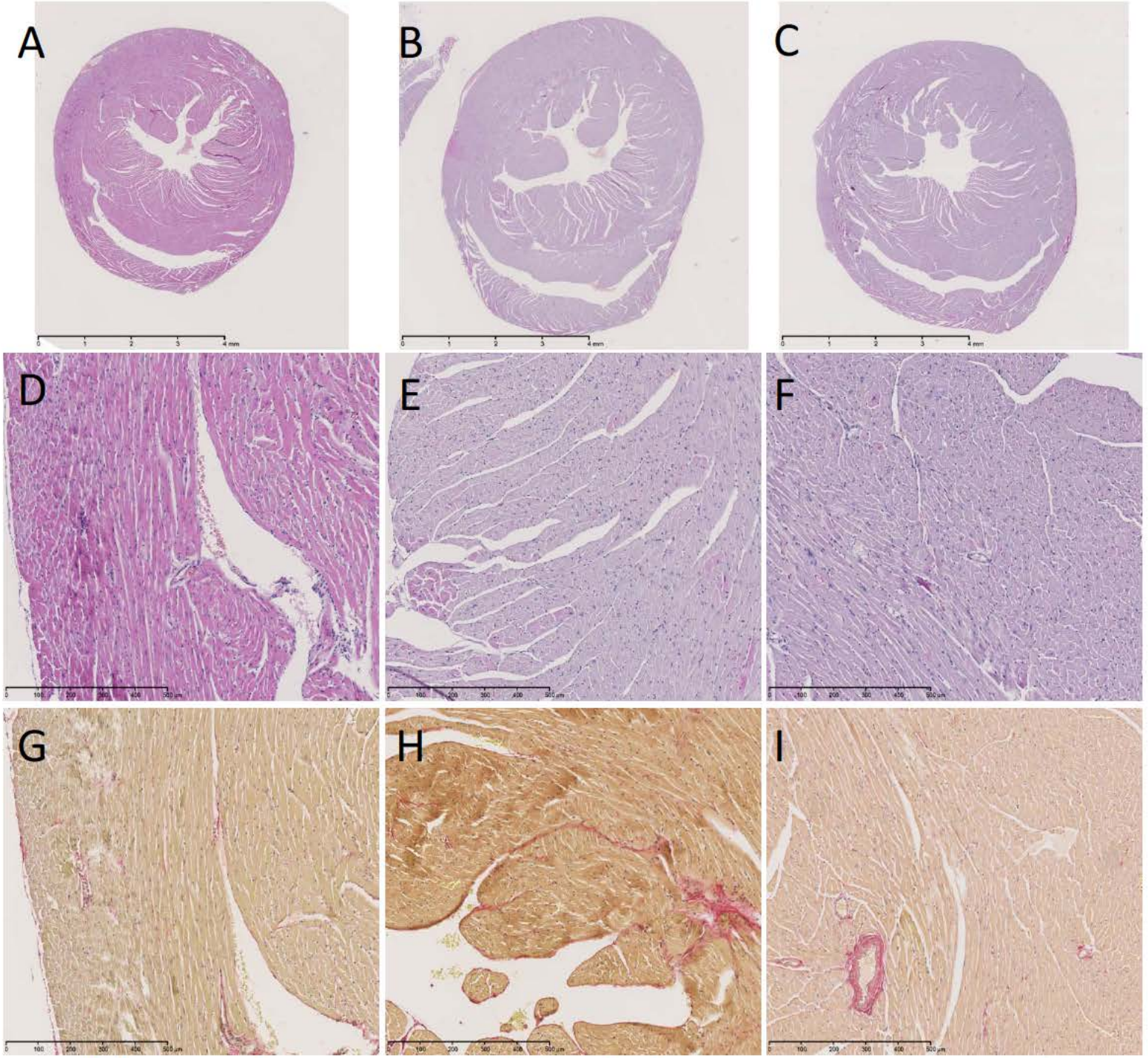

Supplementary Figure 5-V

16 months cohort

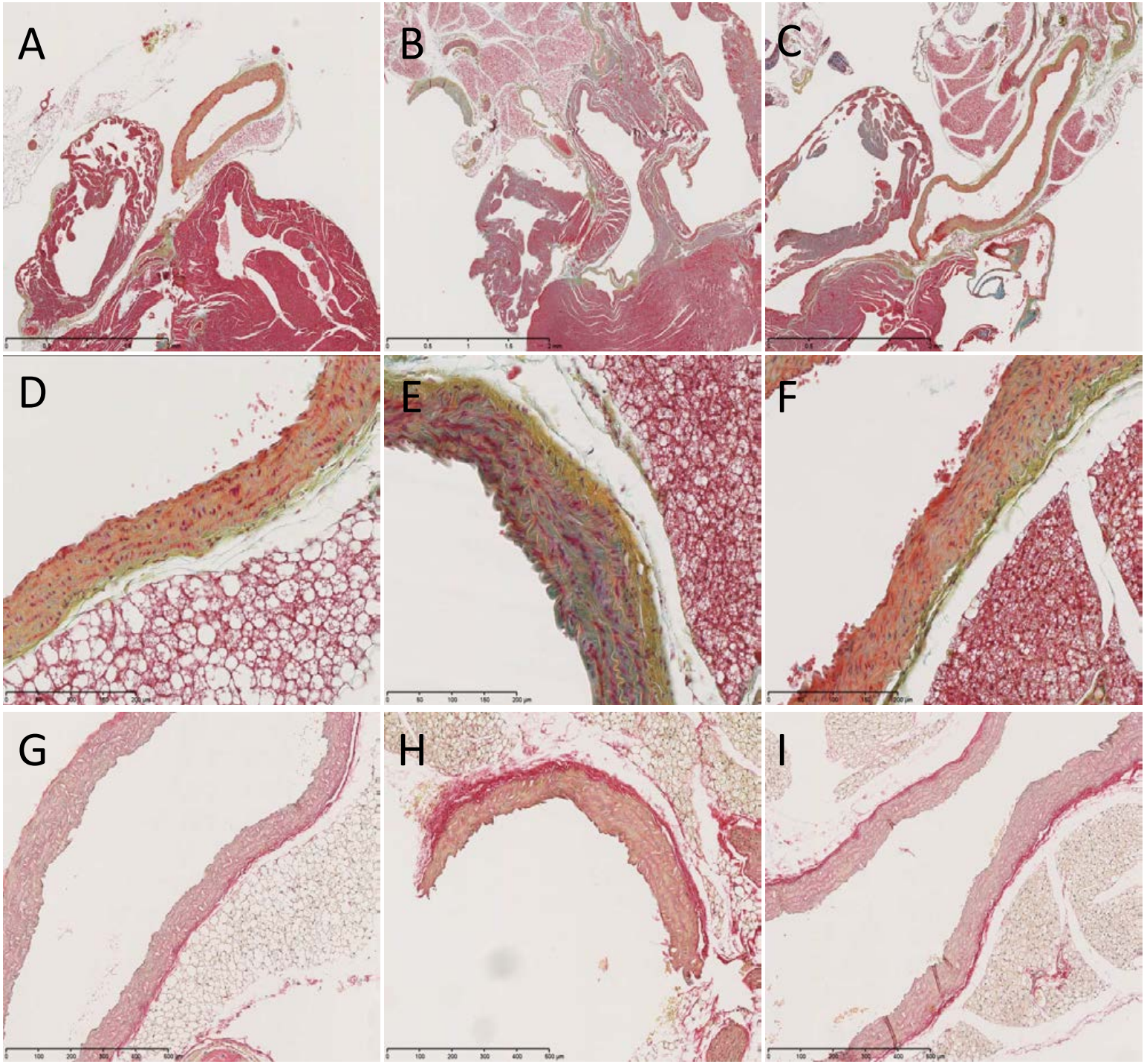

Supplementary Figure 5-VI

16 months cohort

Old rapamycin

Old control

Young control

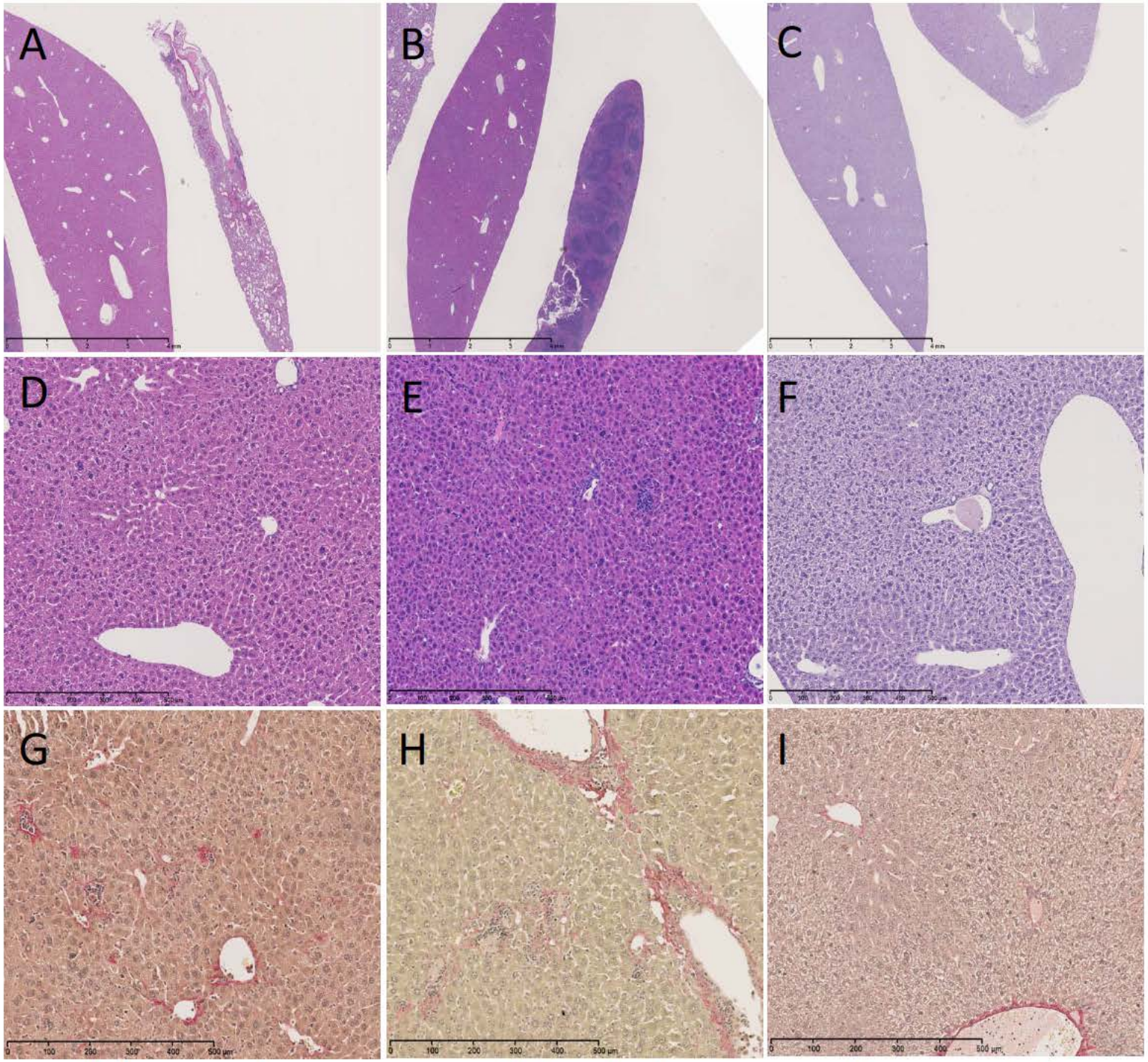

Supplementary Figure 6-I

34 months cohort

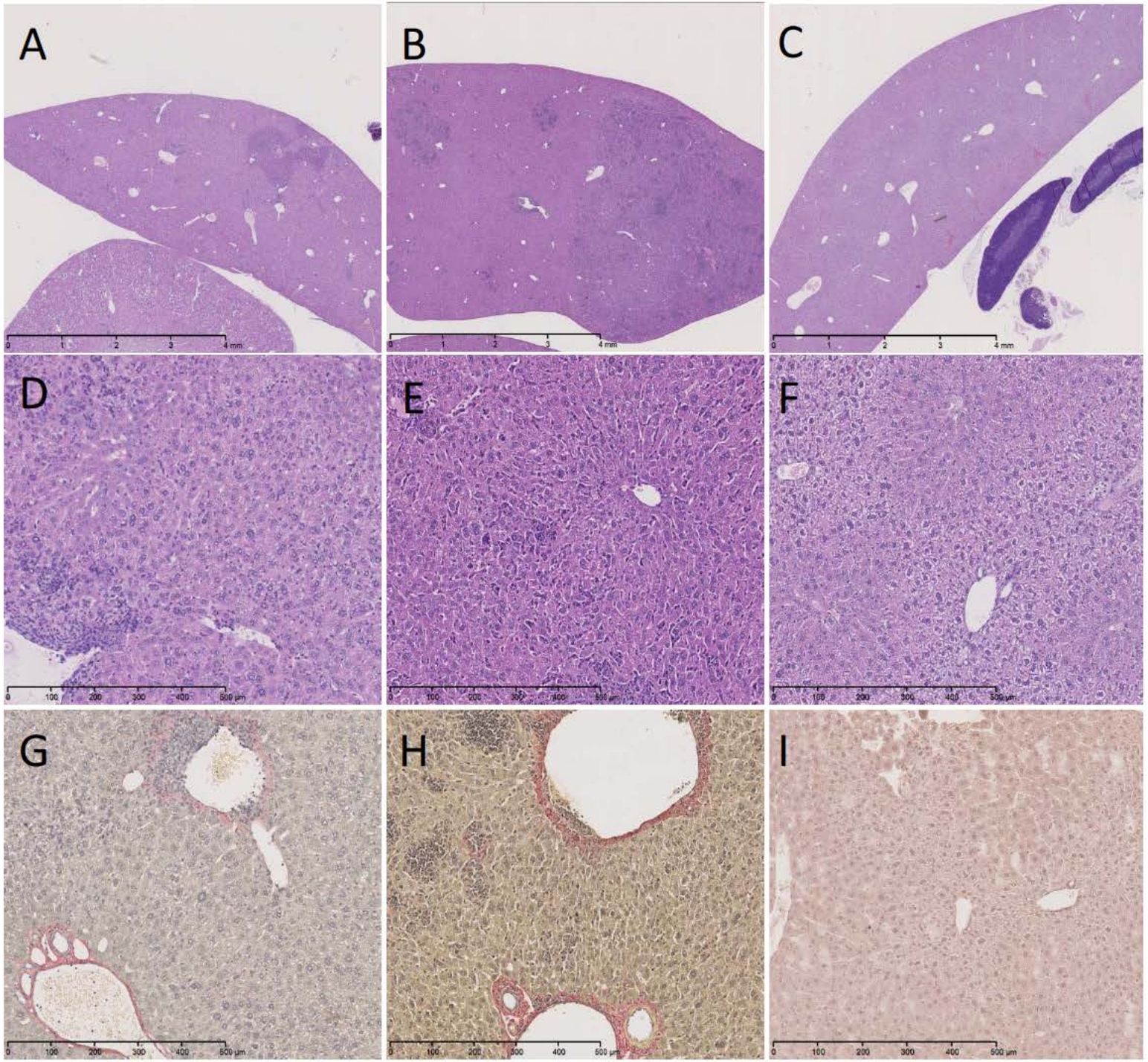

Supplementary Figure 6-II

25 months cohort

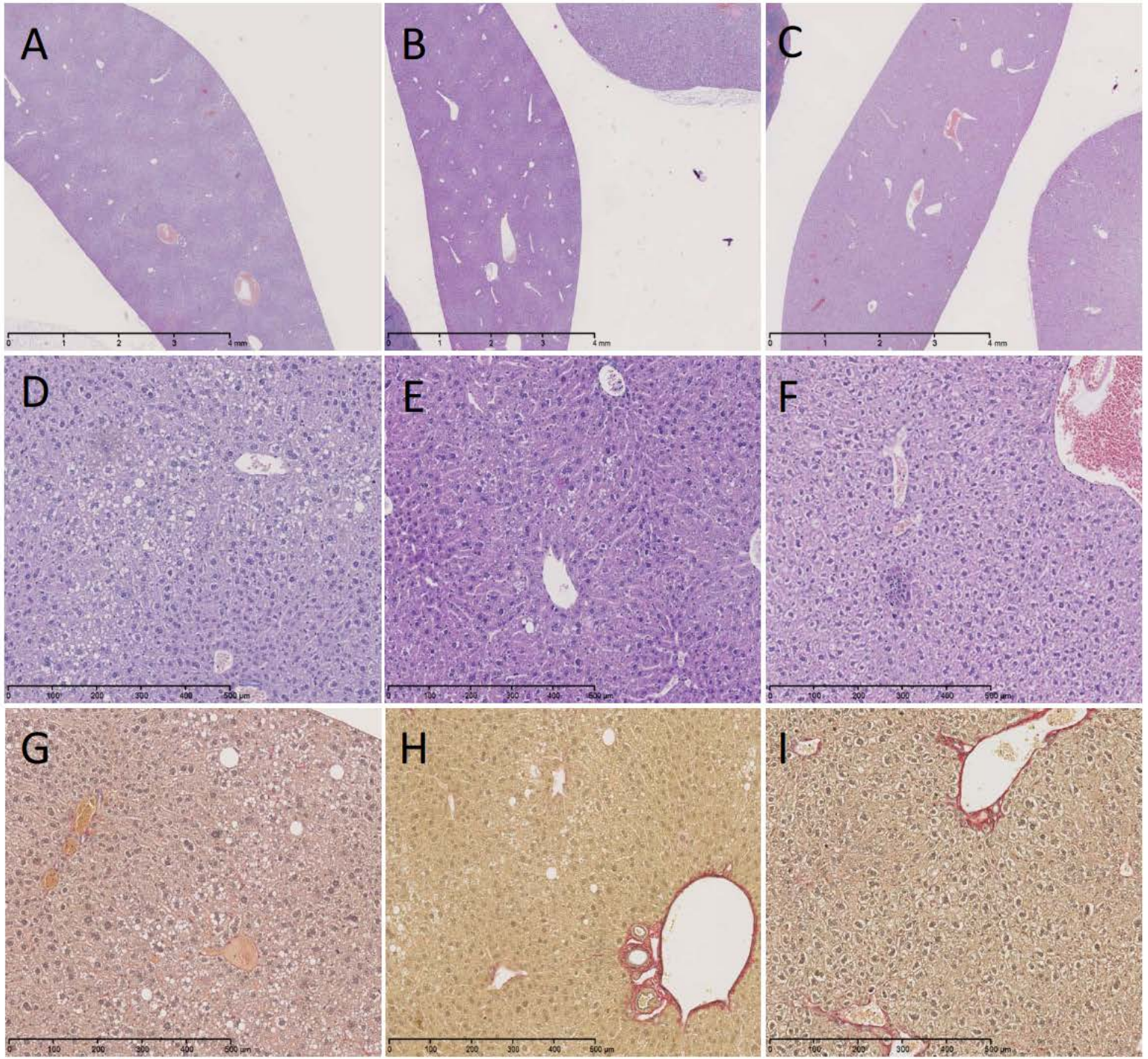

Supplementary Figure 6-III

16 months cohort

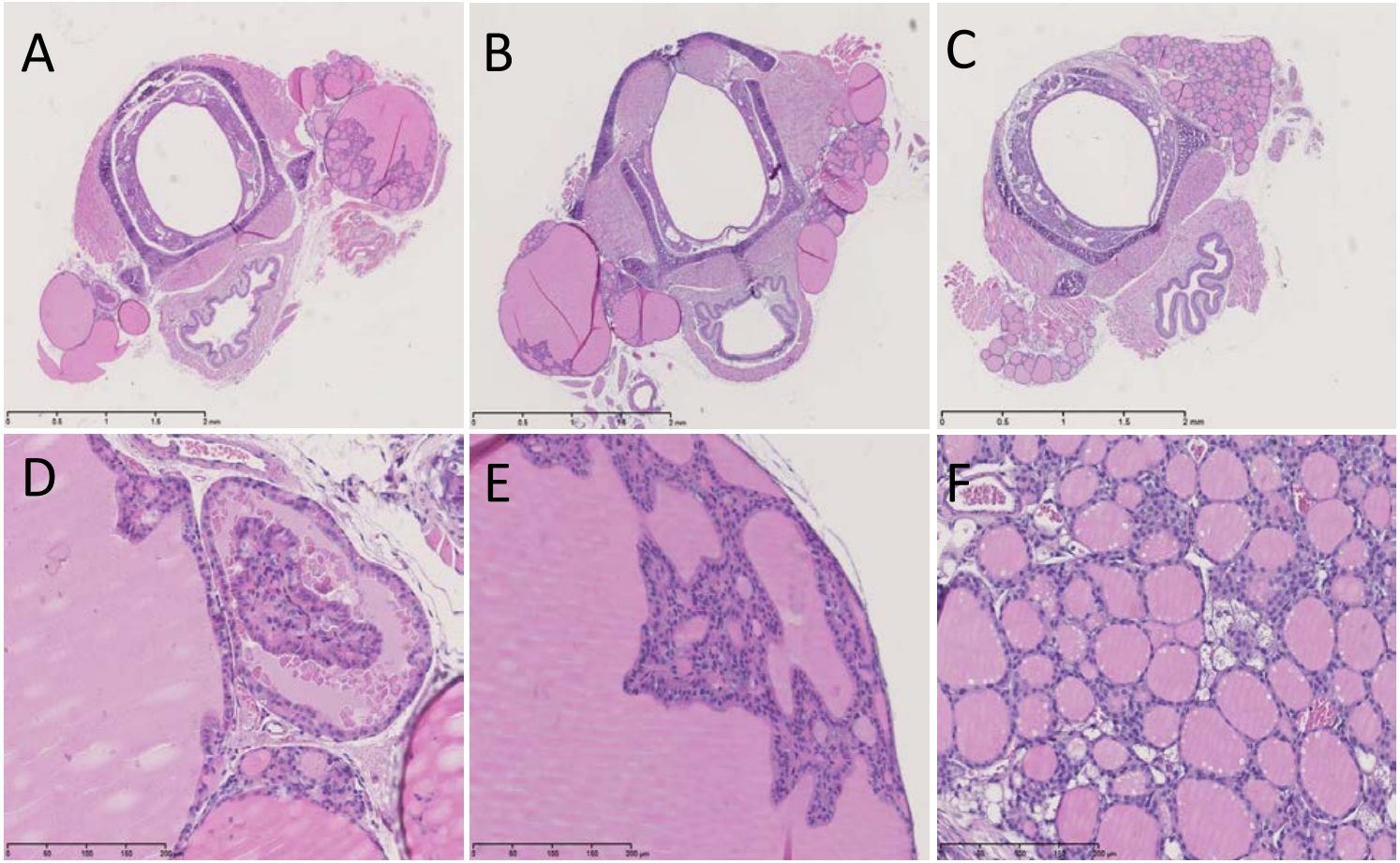

Old rapamycin

Old control

Young control

Supplementary Figure 7

34 months cohort

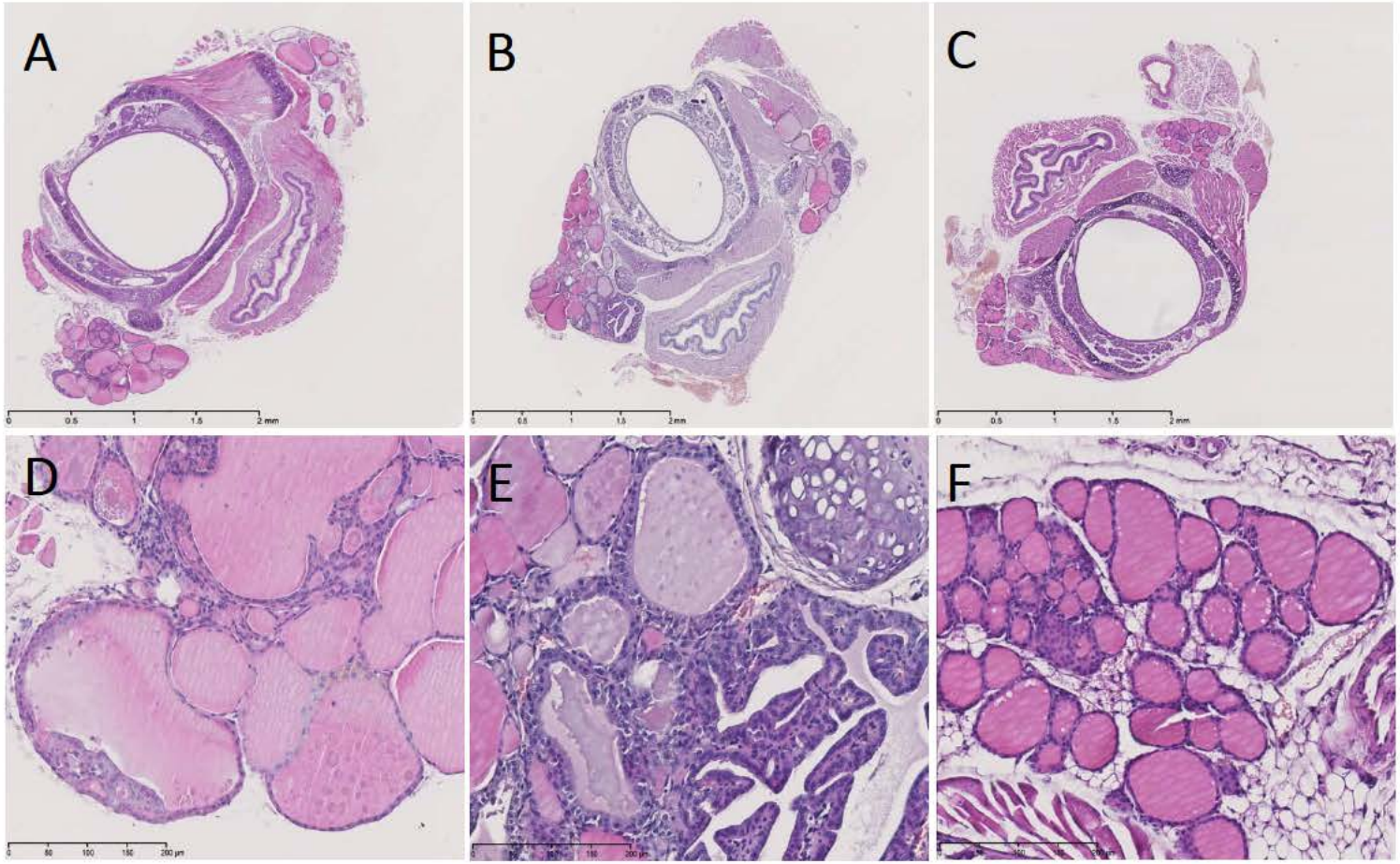

Supplementary Figure 7

25 months cohort

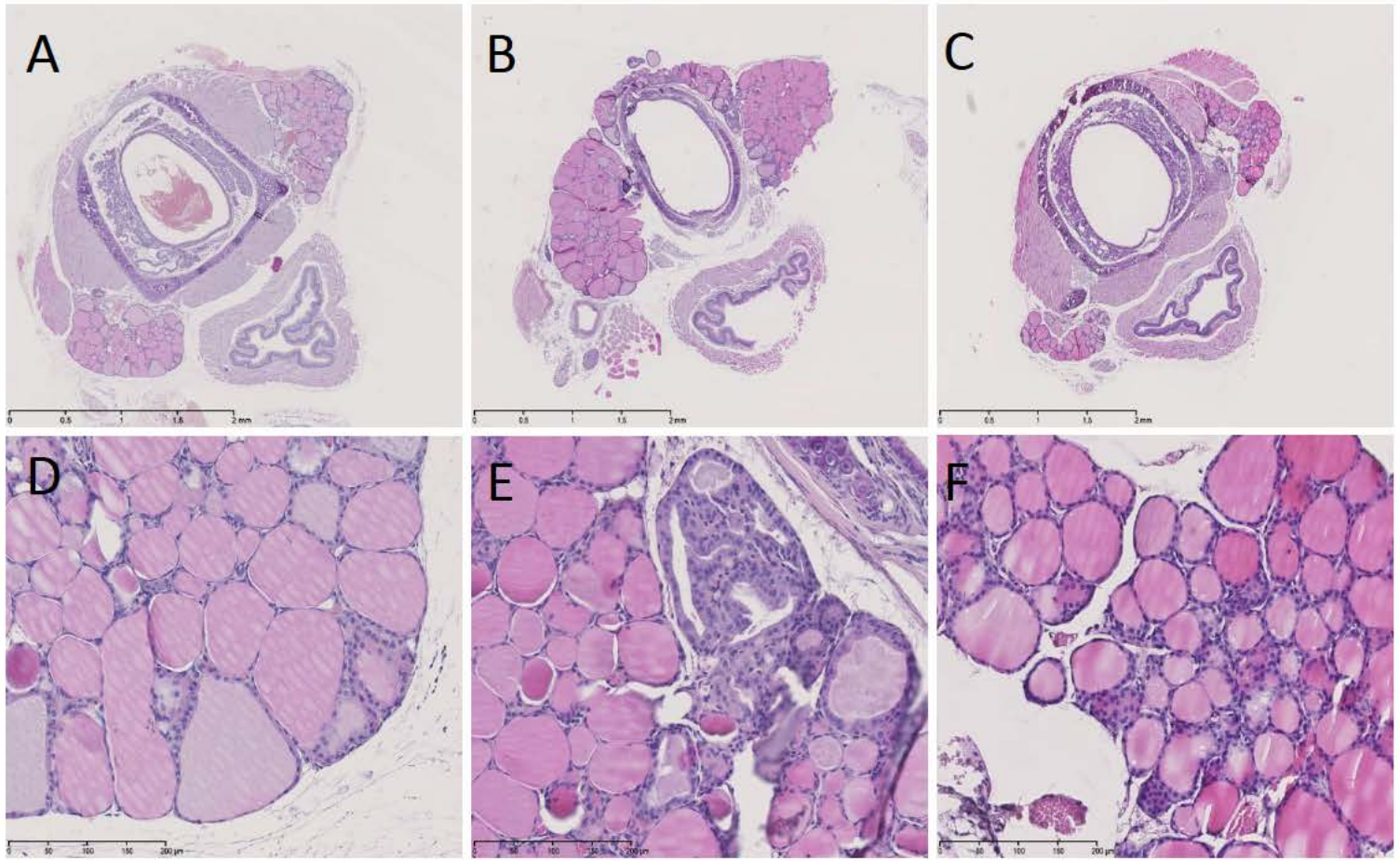

Supplementary Figure 7

16 months cohort

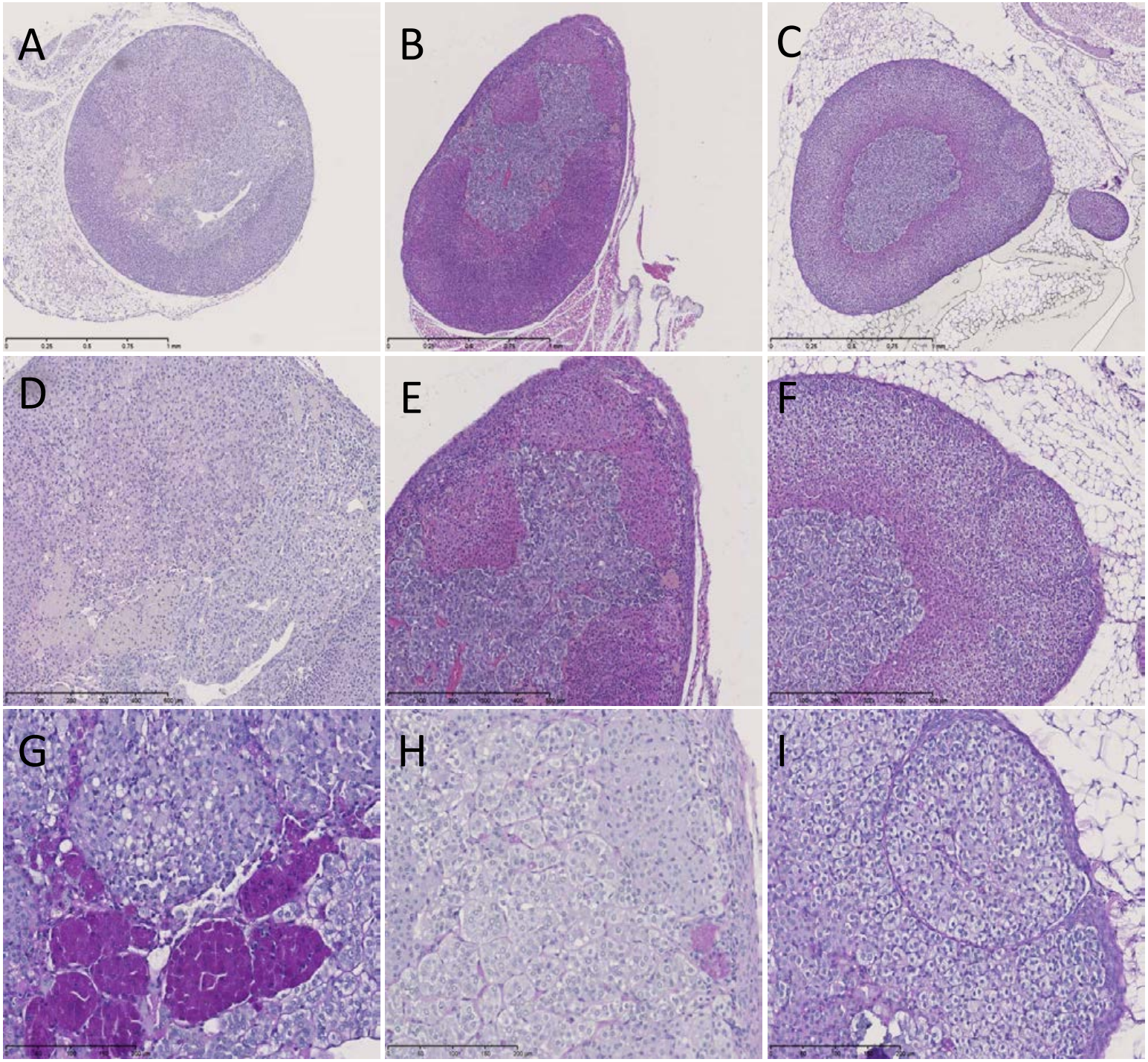

Supplementary Figure 8-I

34 months cohort

Old rapamycin

Old control

Young control

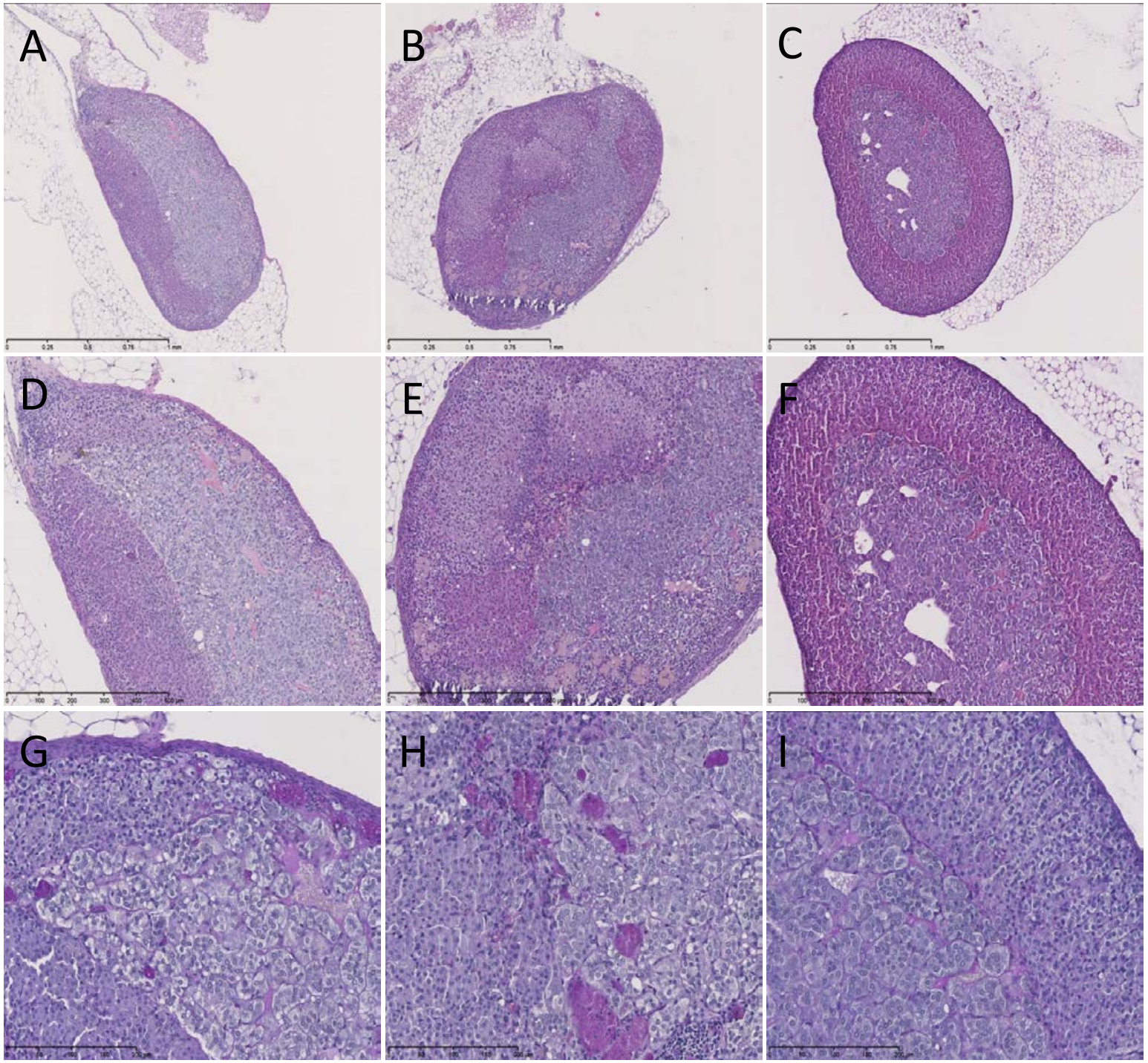

Supplementary Figure 8-II

25 months cohort

Old rapamycin

Old control

Young control

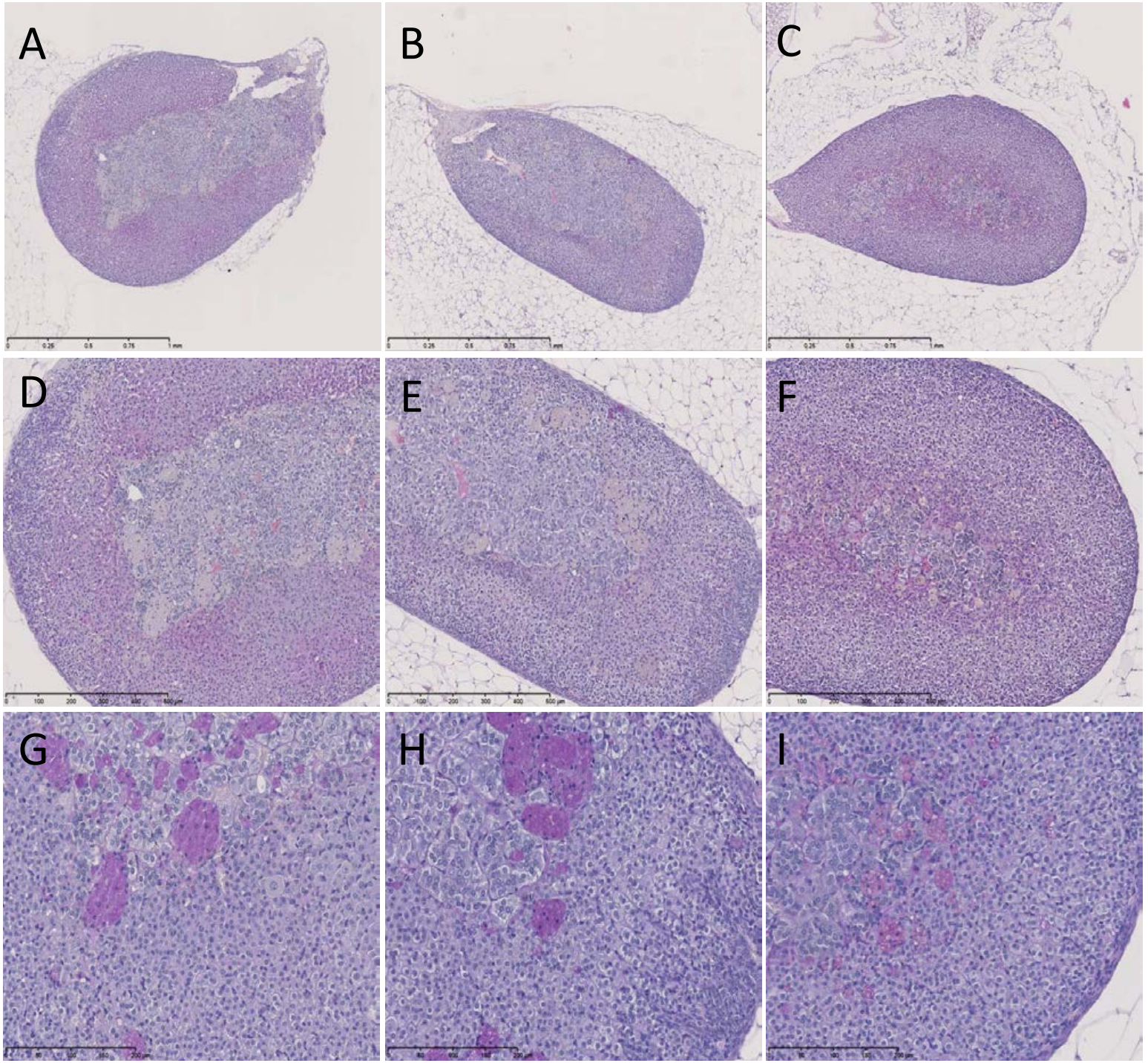

Supplementary Figure 8-III

16 months cohort

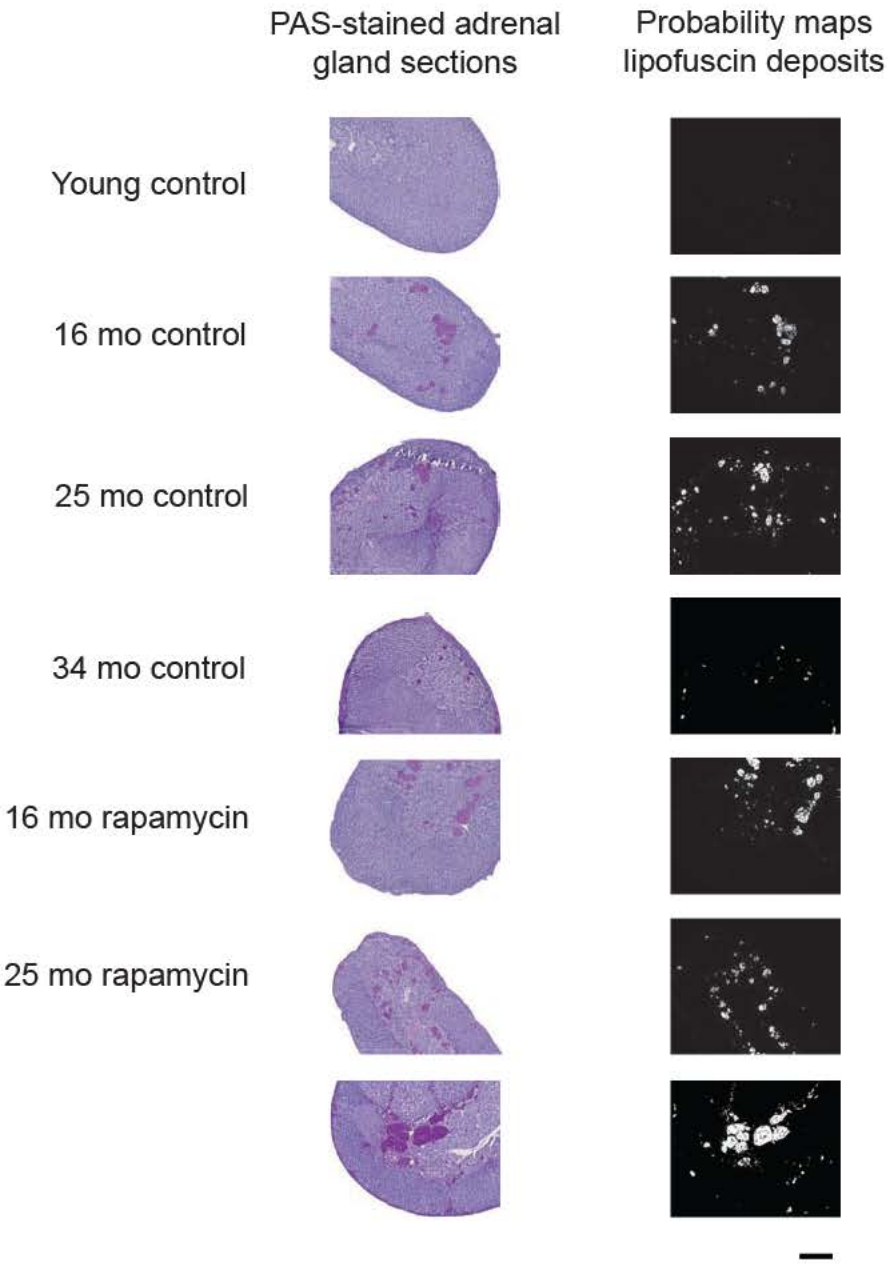

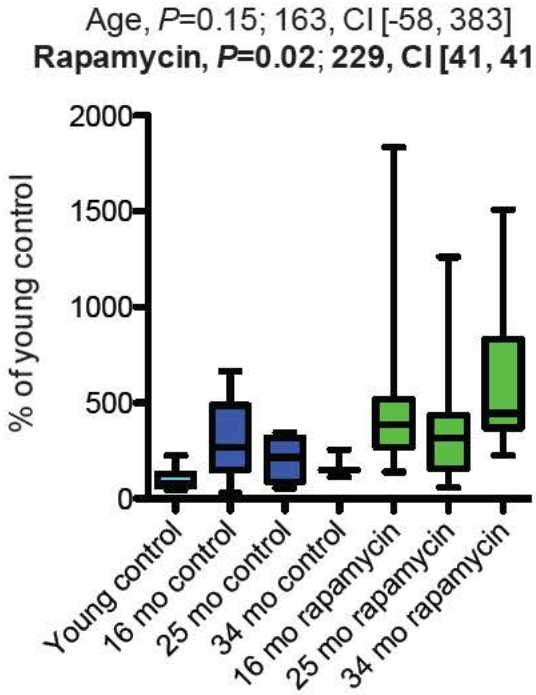

Supplementary Figure 9

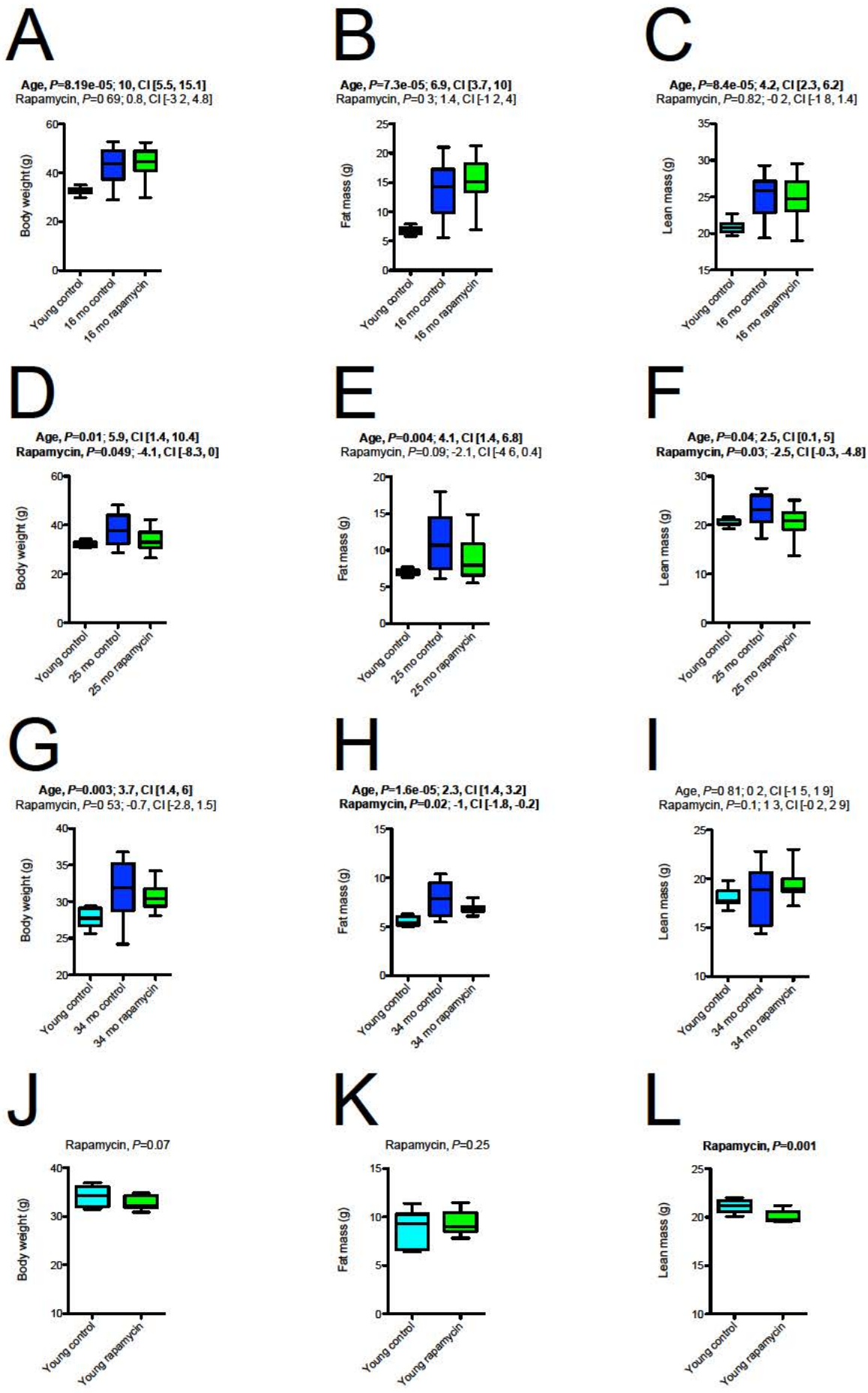

Supplementary Figure 10

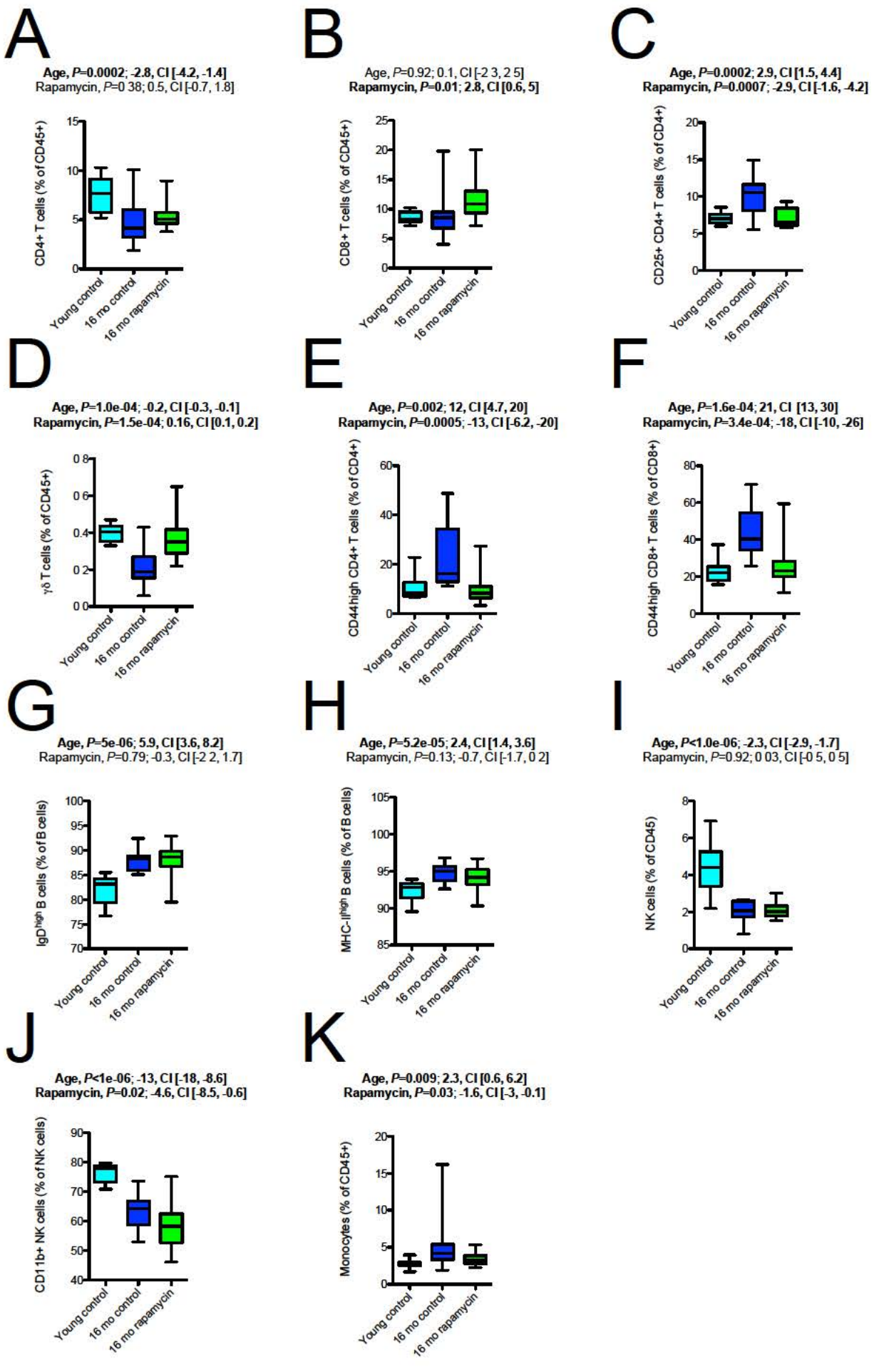

Supplementary Figure 11

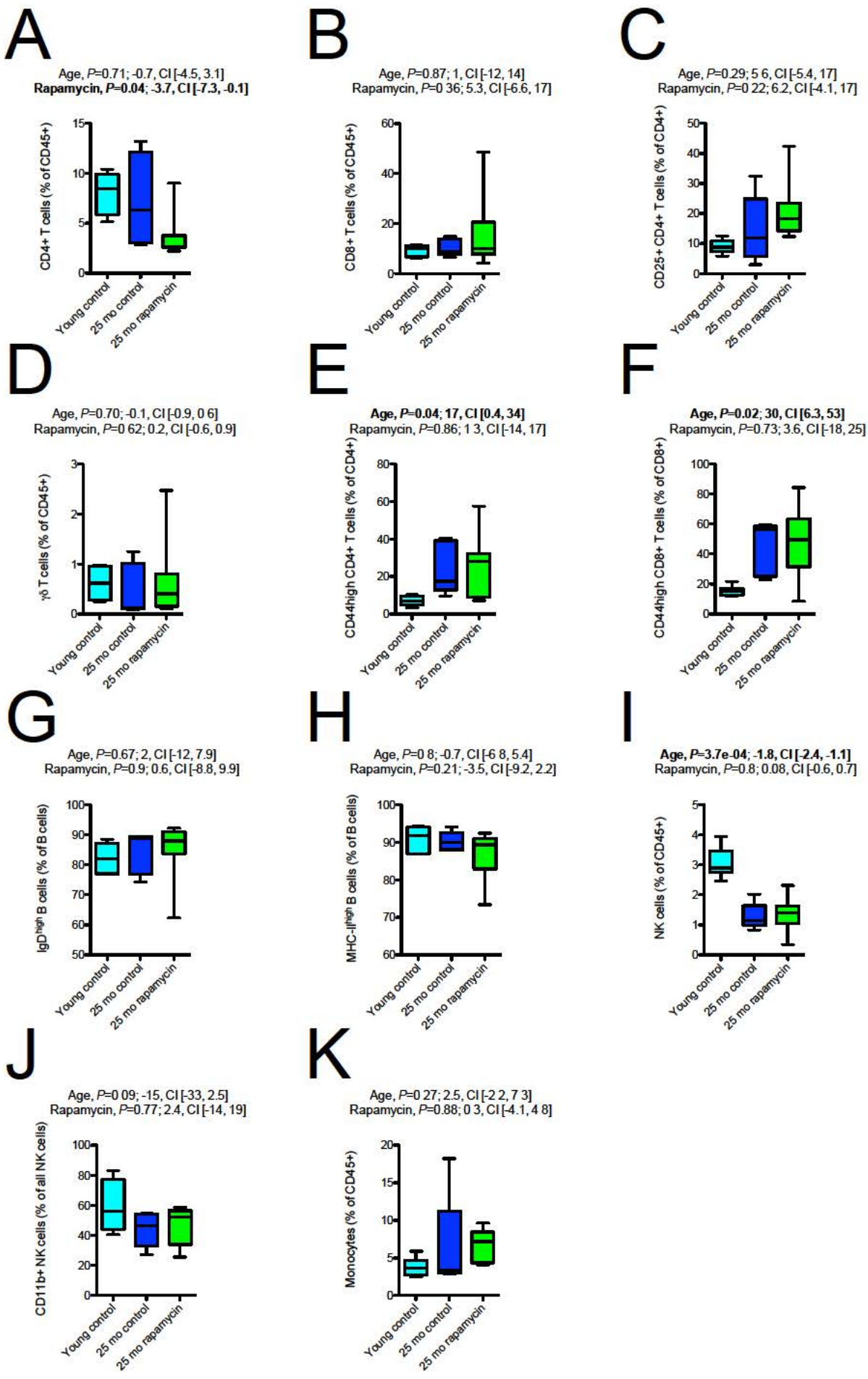

Supplementary Figure 12

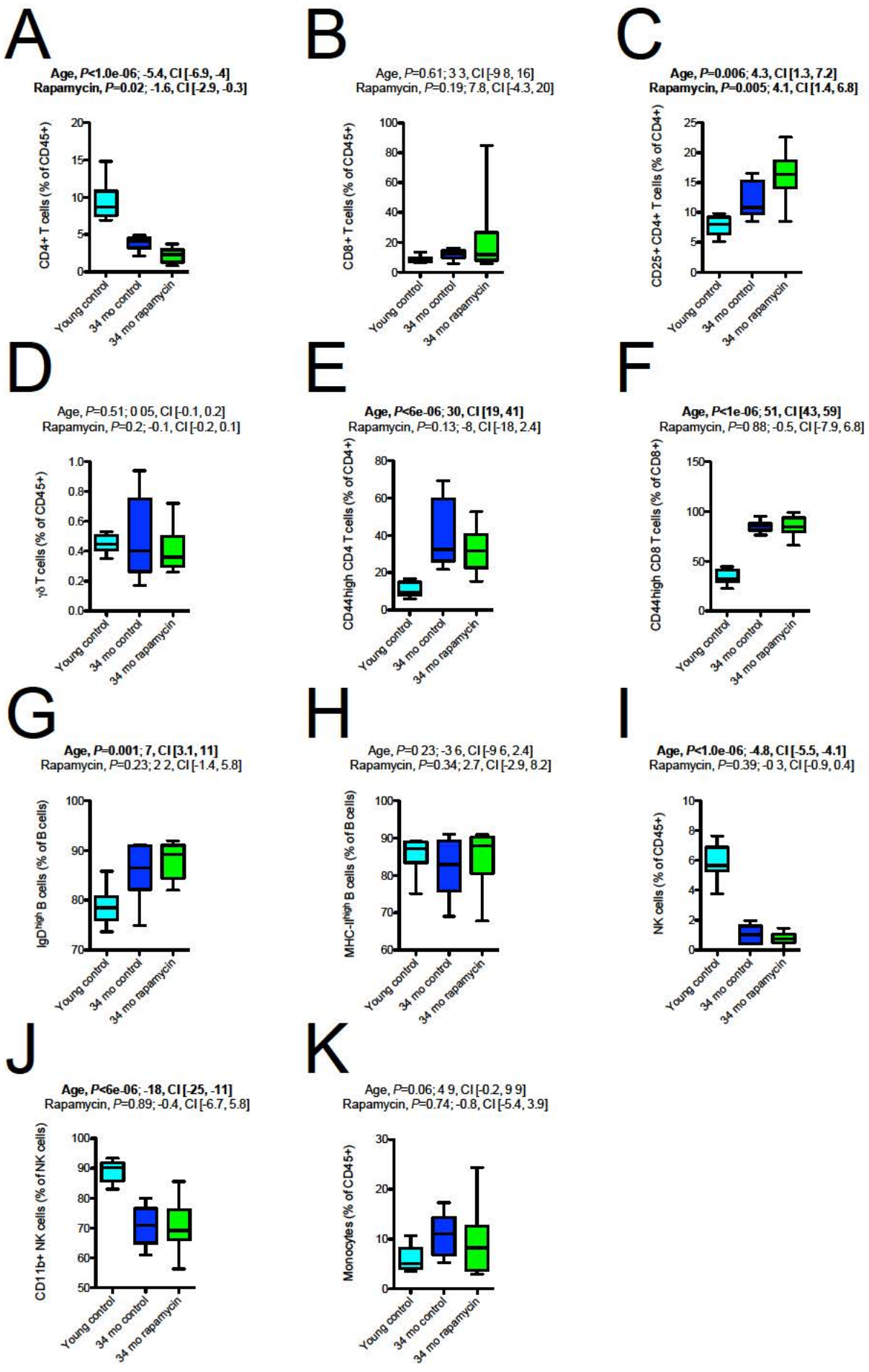

Supplementary Figure 13

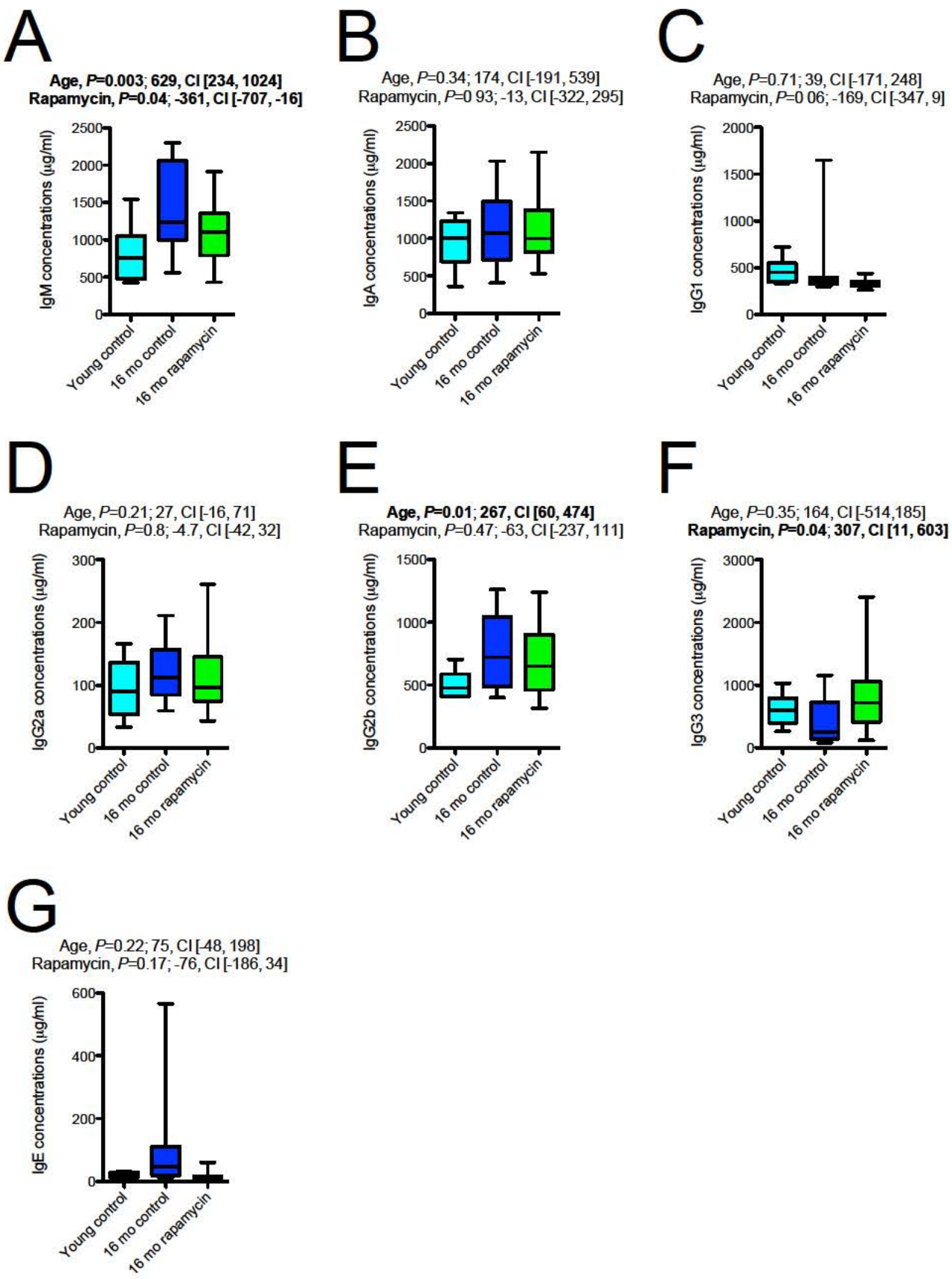

Supplementary Figure 14

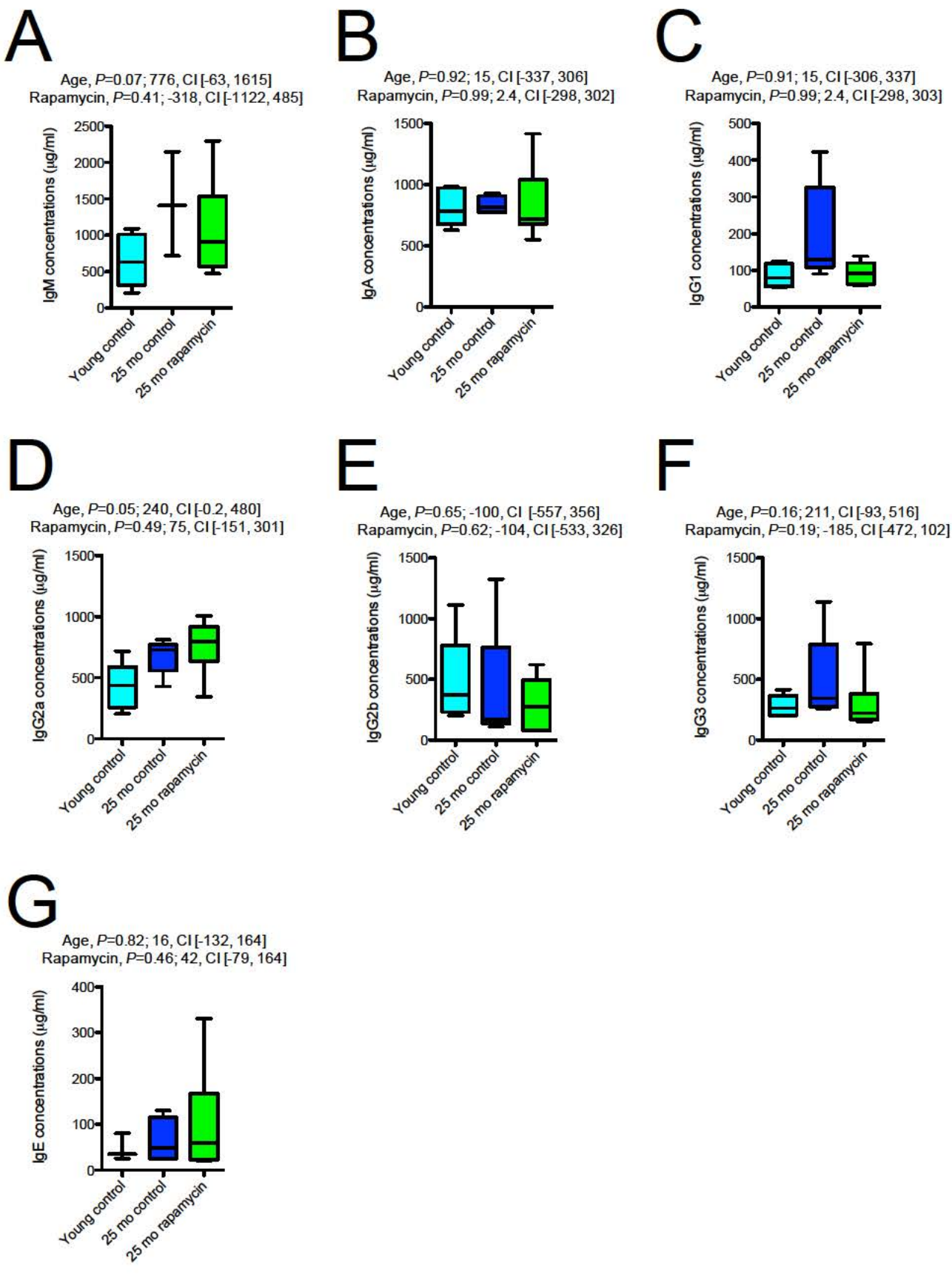

Supplementary Figure 15

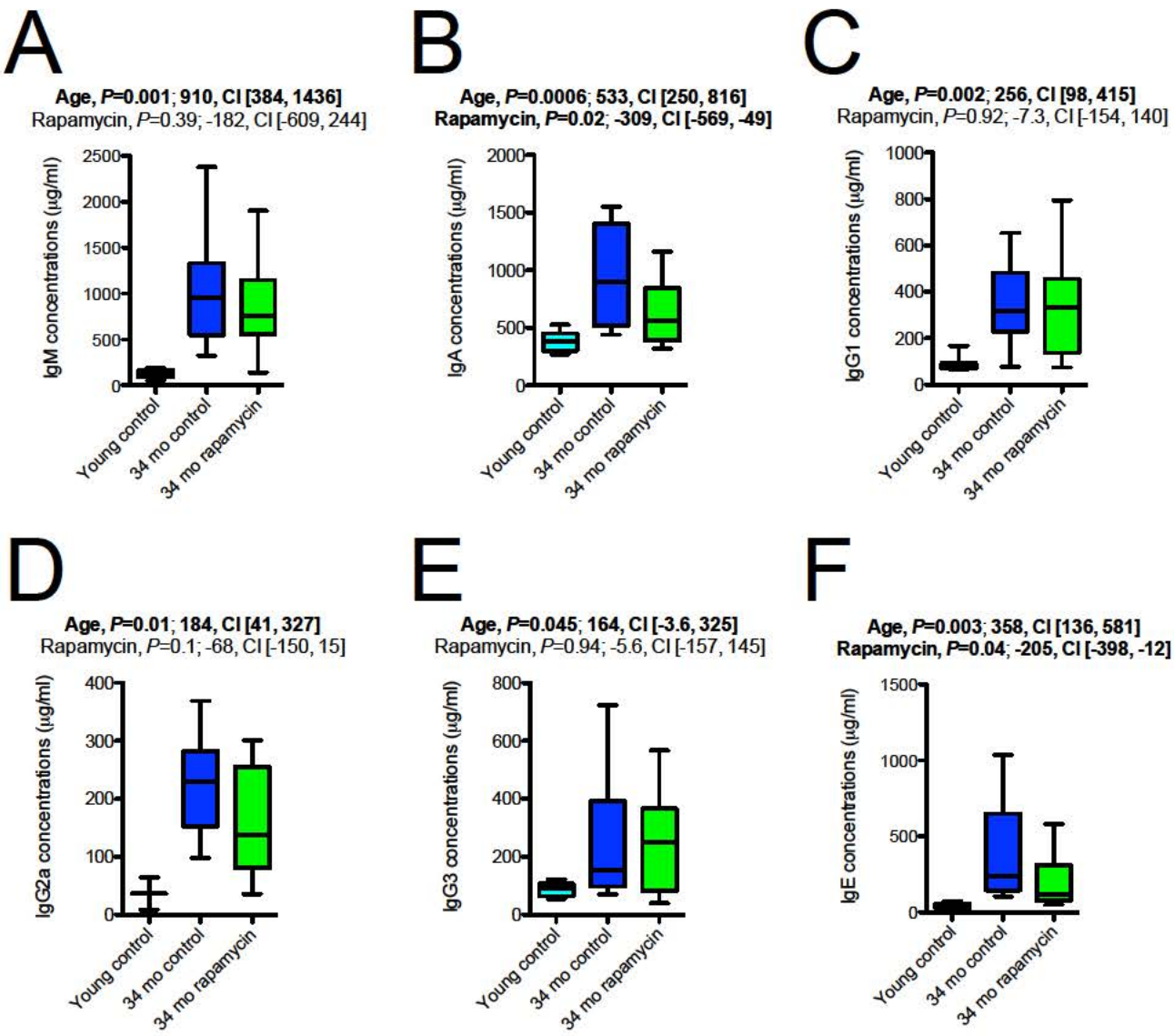

Supplementary Figure 16

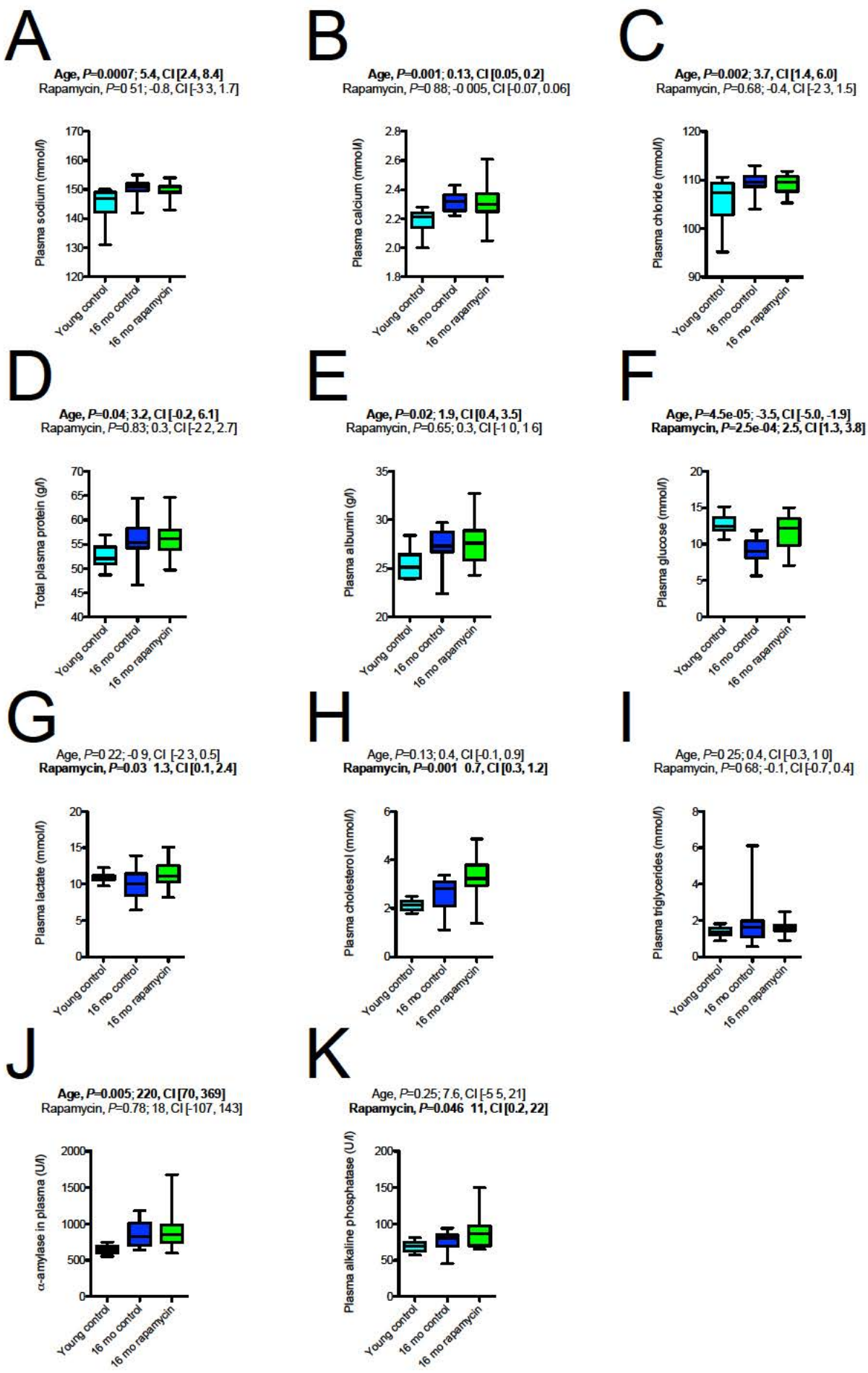

Supplementary Figure 17

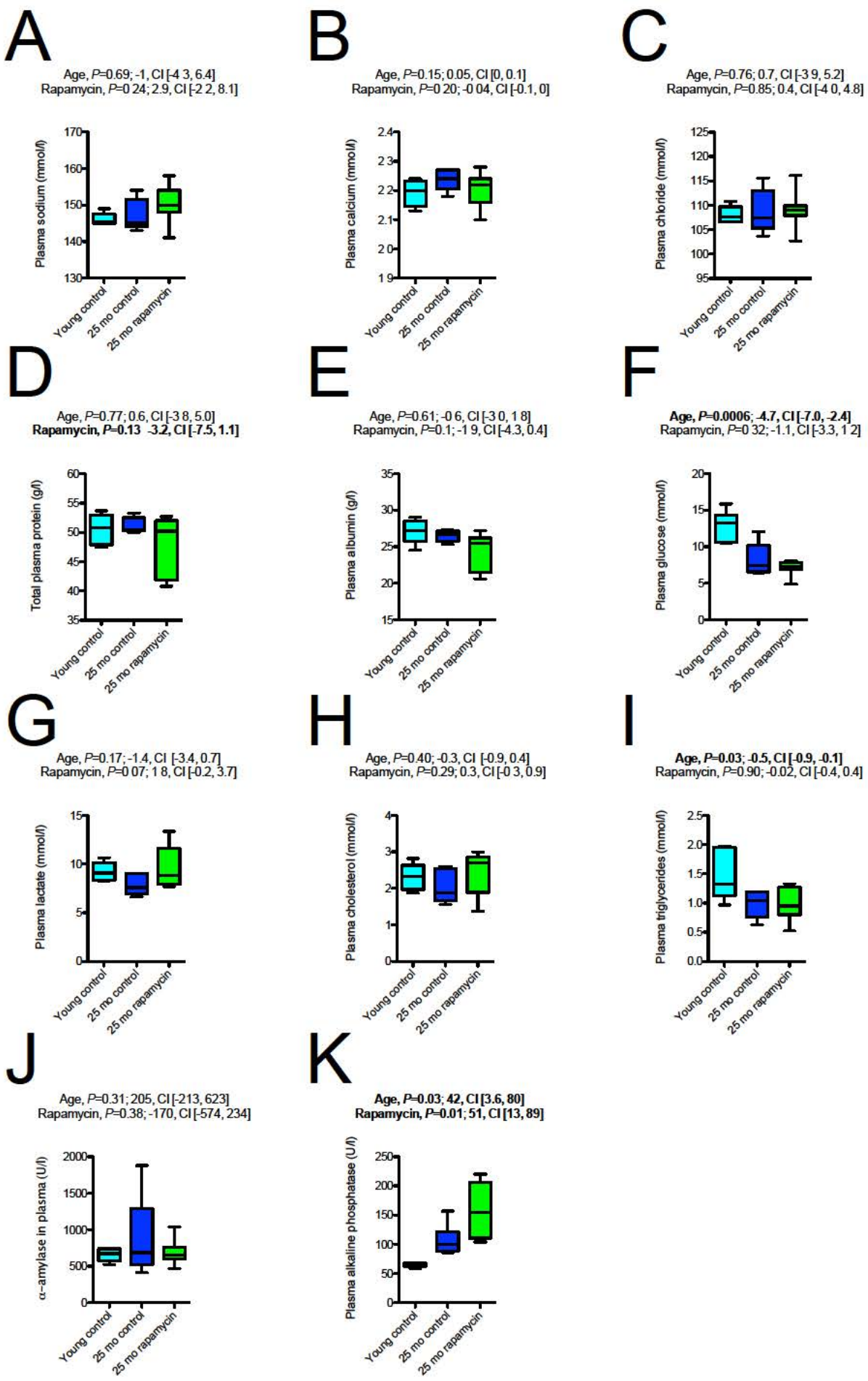

Supplementary Figure 18

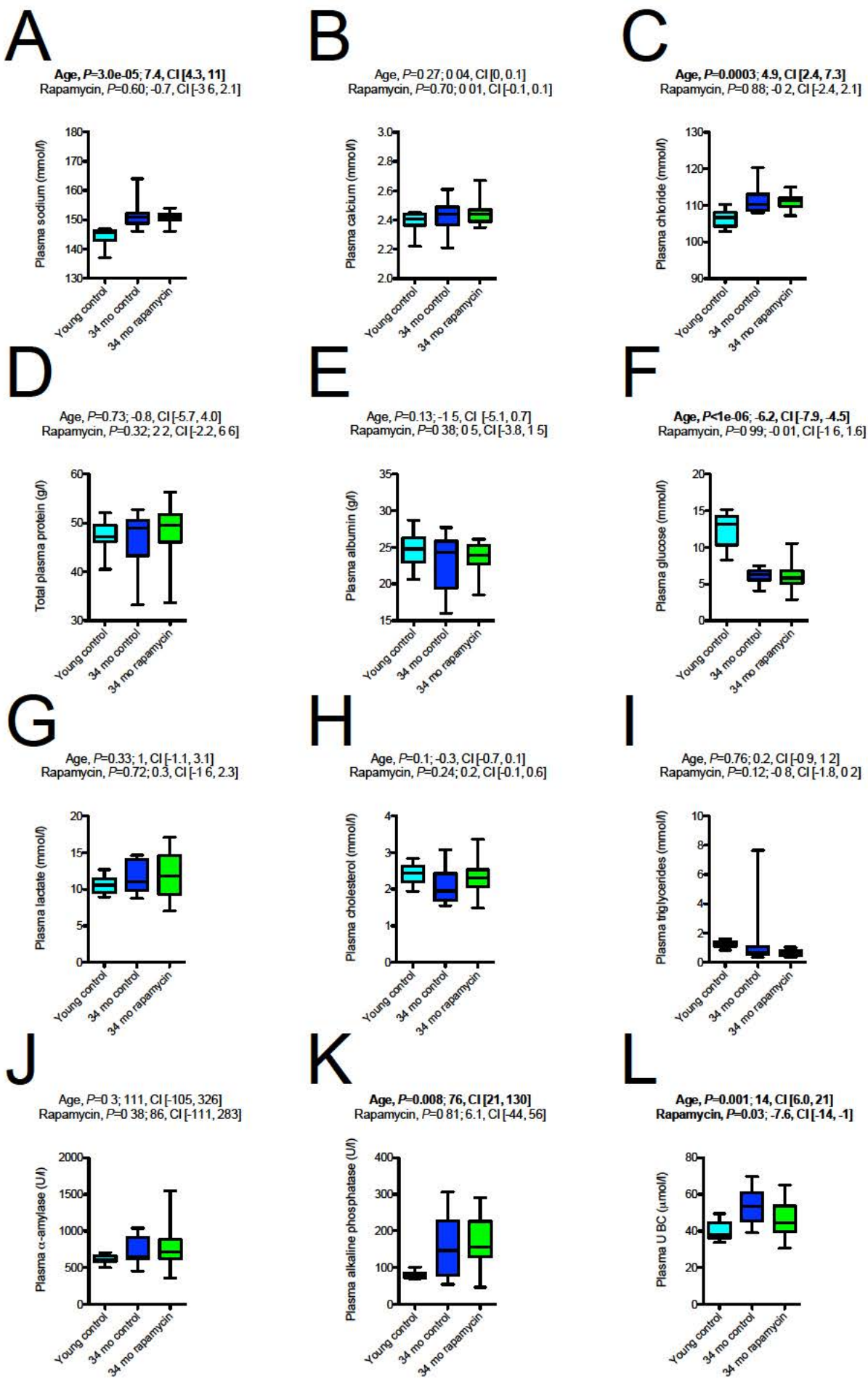

Supplementary Figure 19

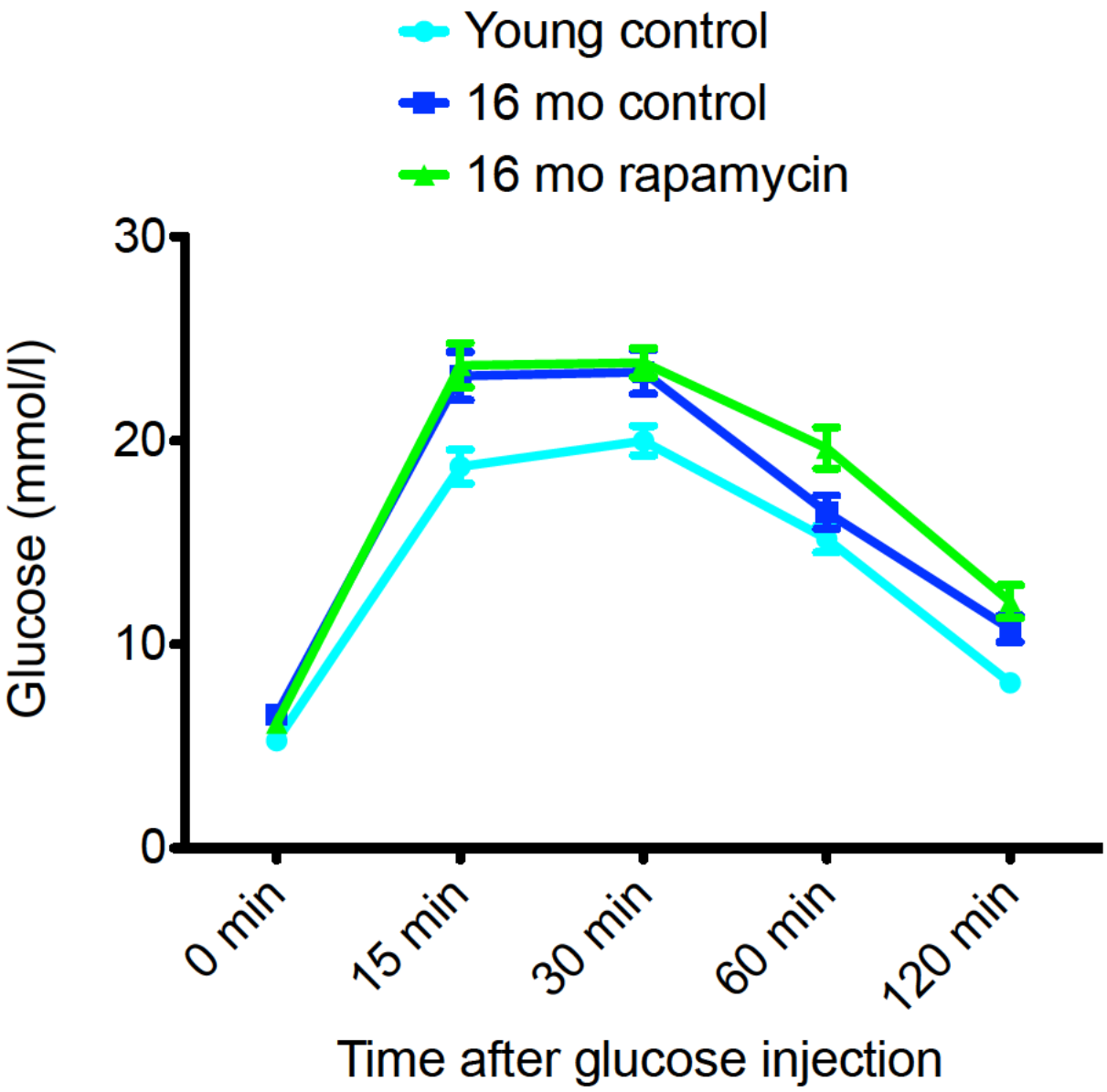

Supplementary Figure 20

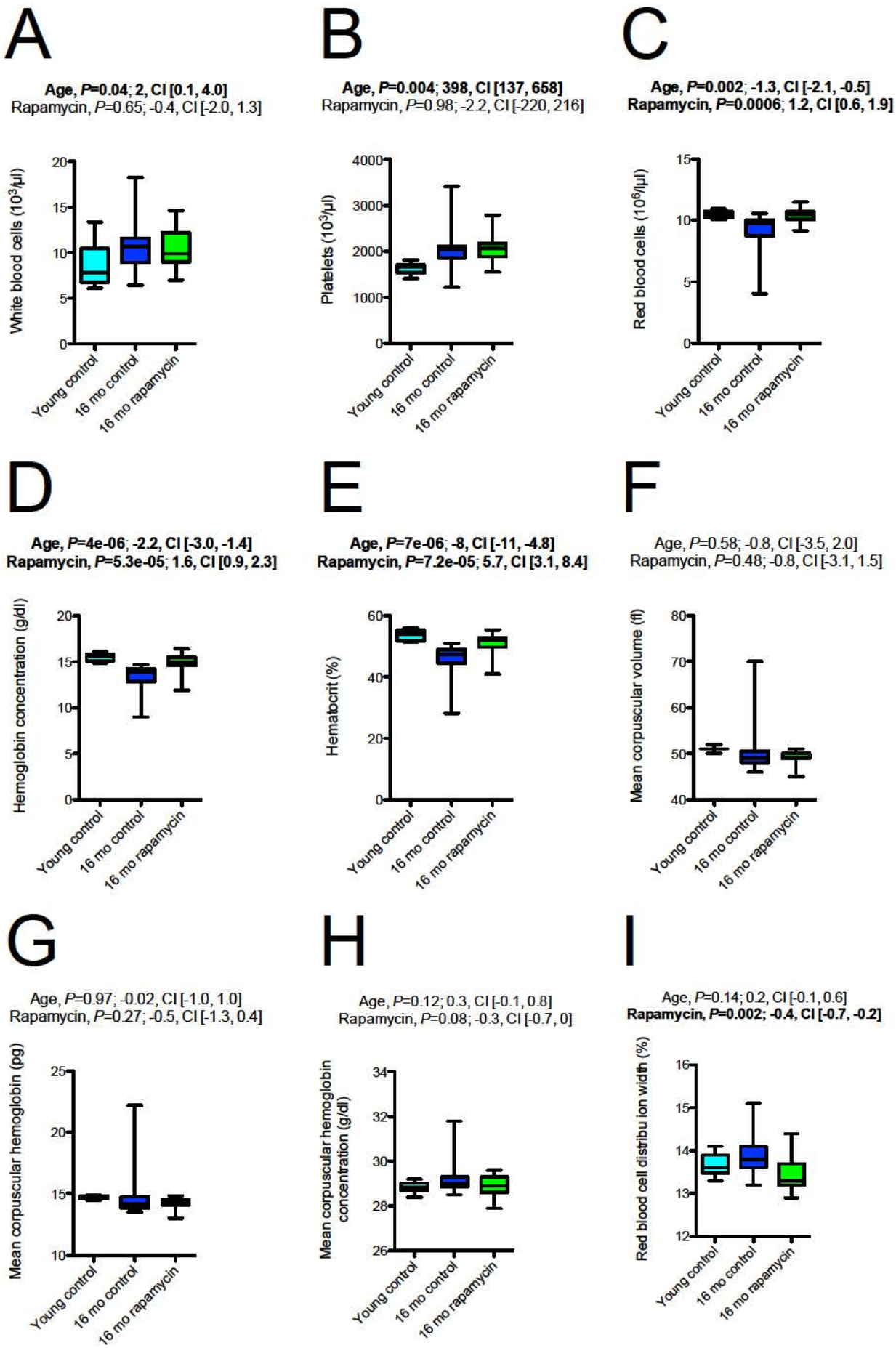

Supplementary Figure 21

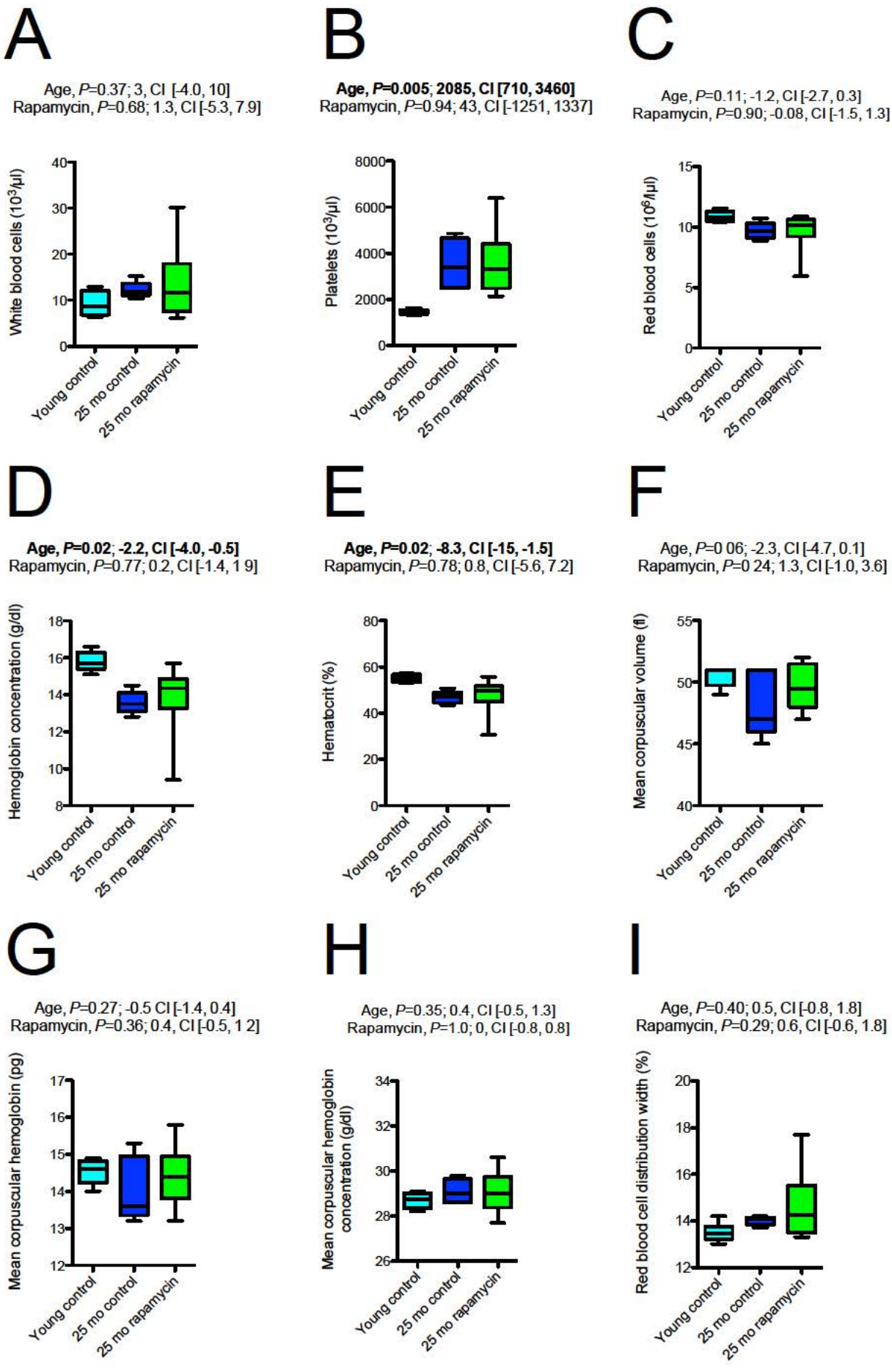

Supplementary Figure 22

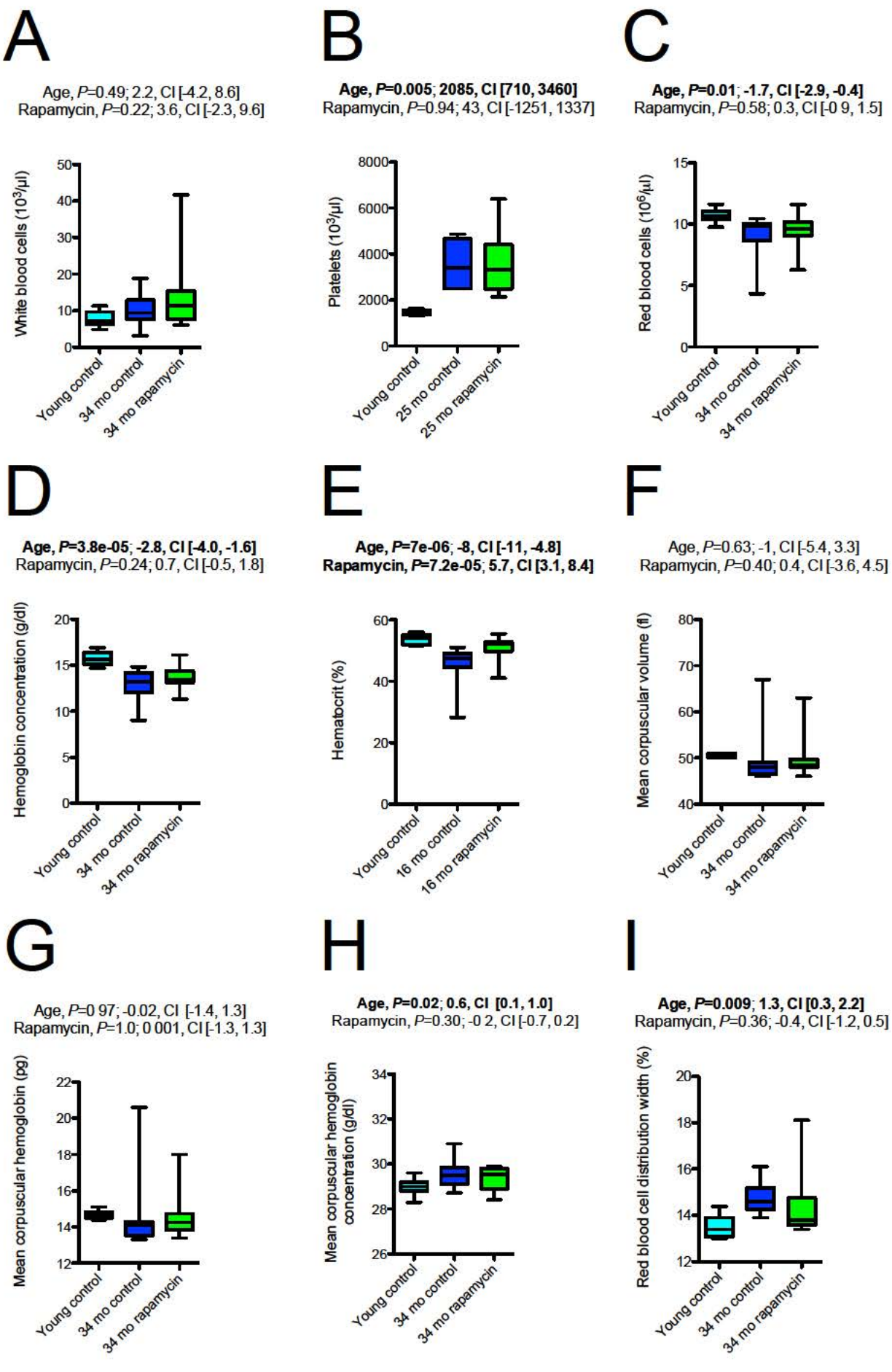

Supplementary Figure 23

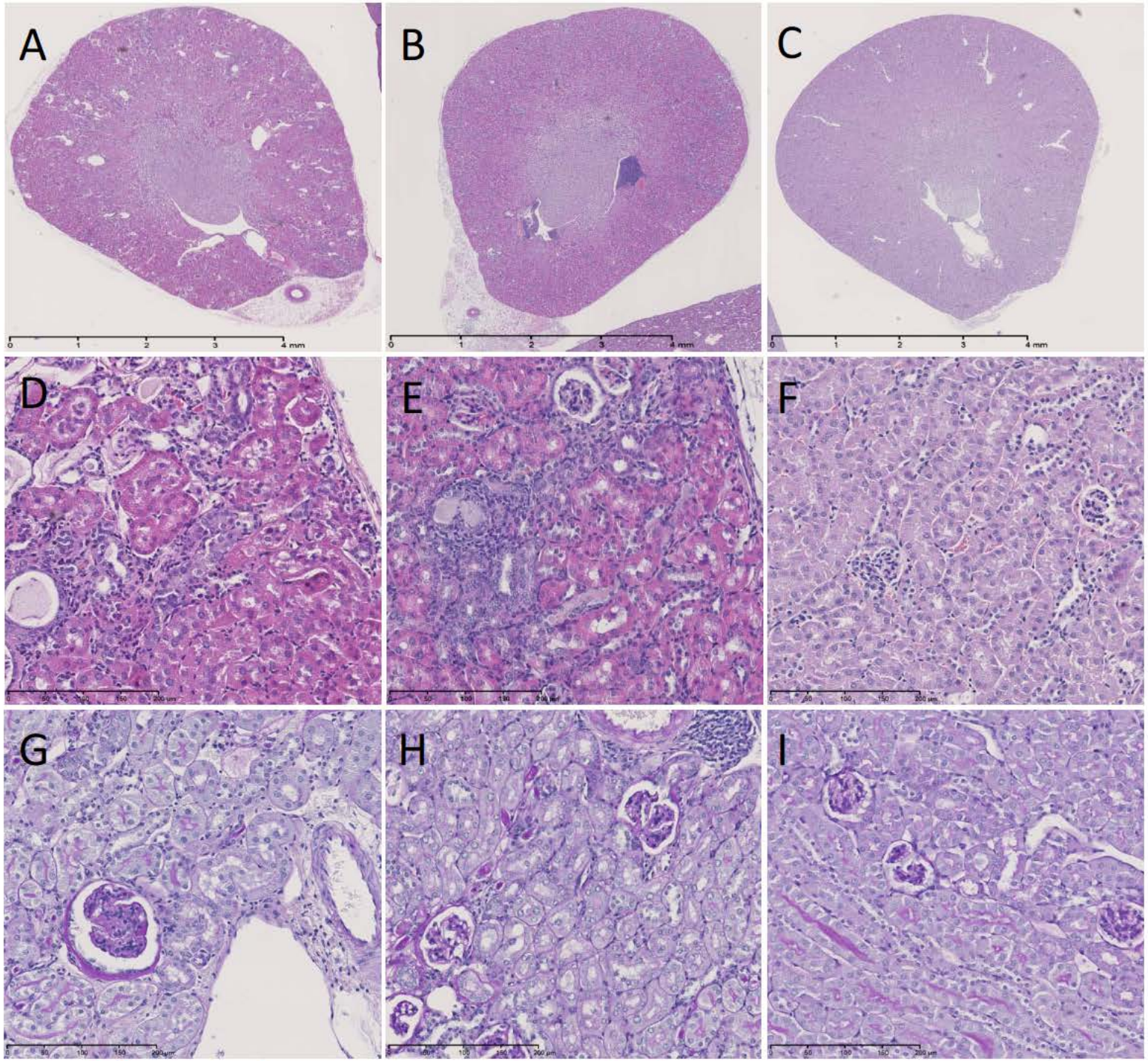

Supplementary Figure 24-I

34 months cohort

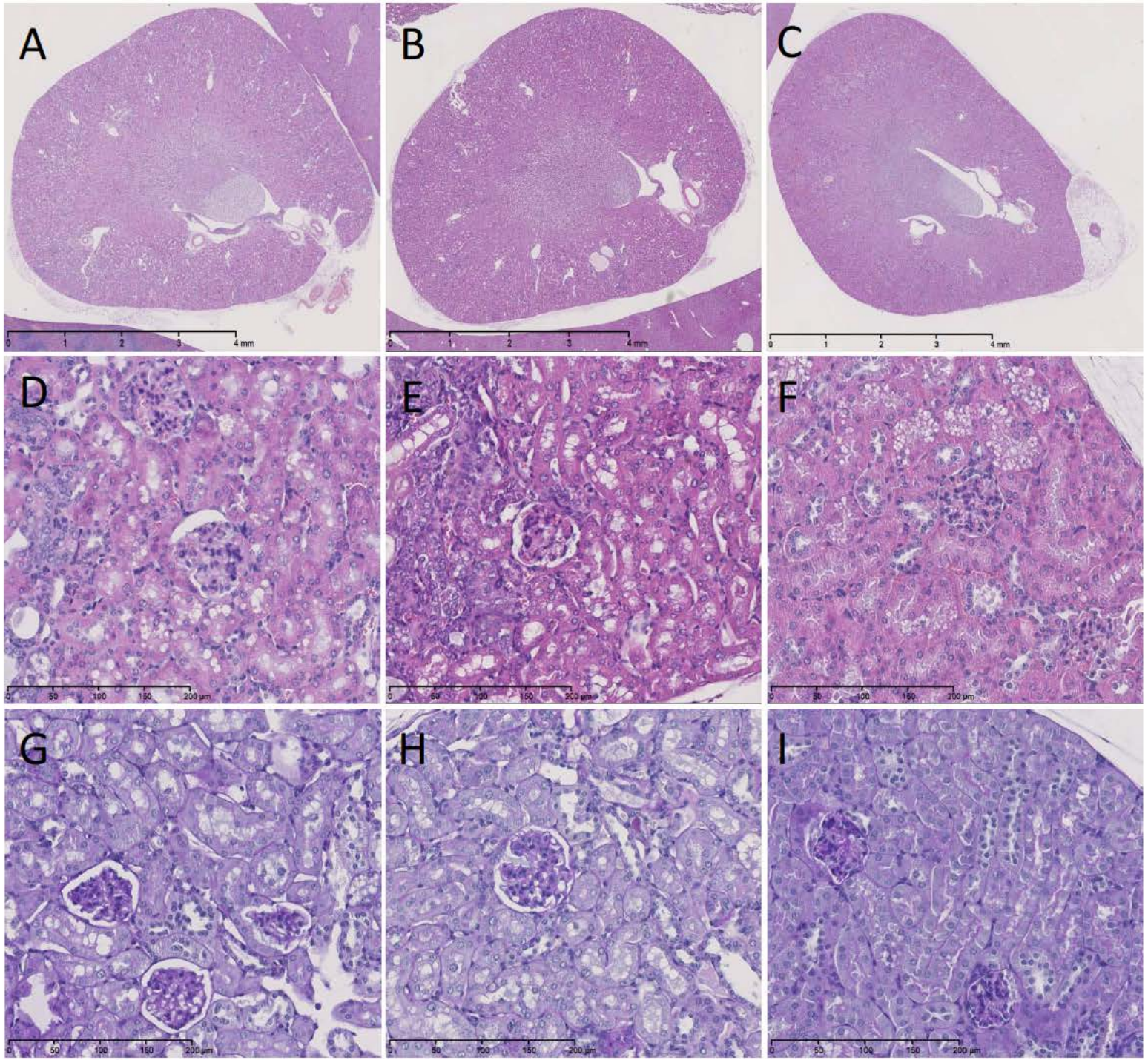

Supplementary Figure 24-II

25 months cohort

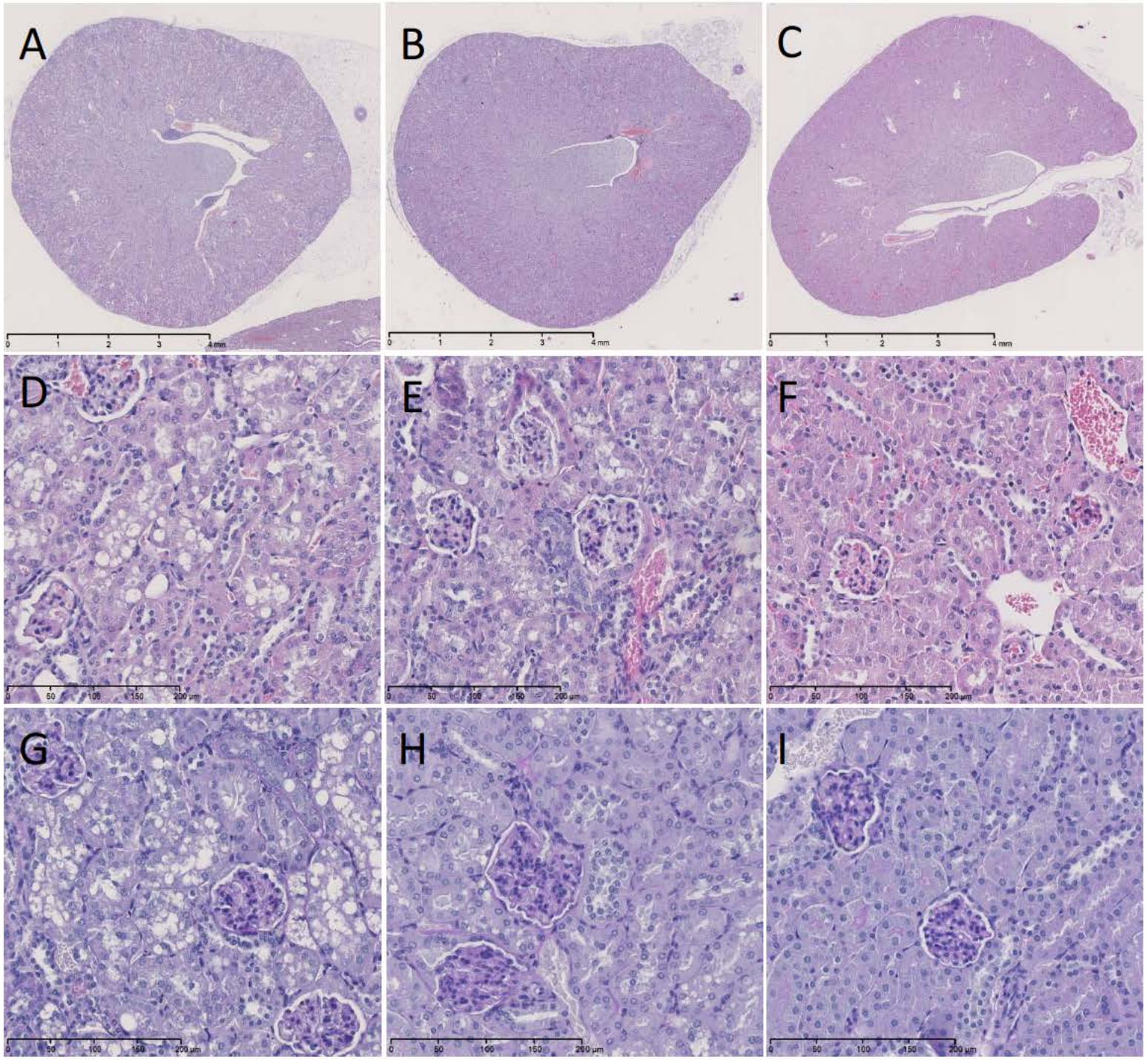

Supplementary Figure 24-III

16 months cohort

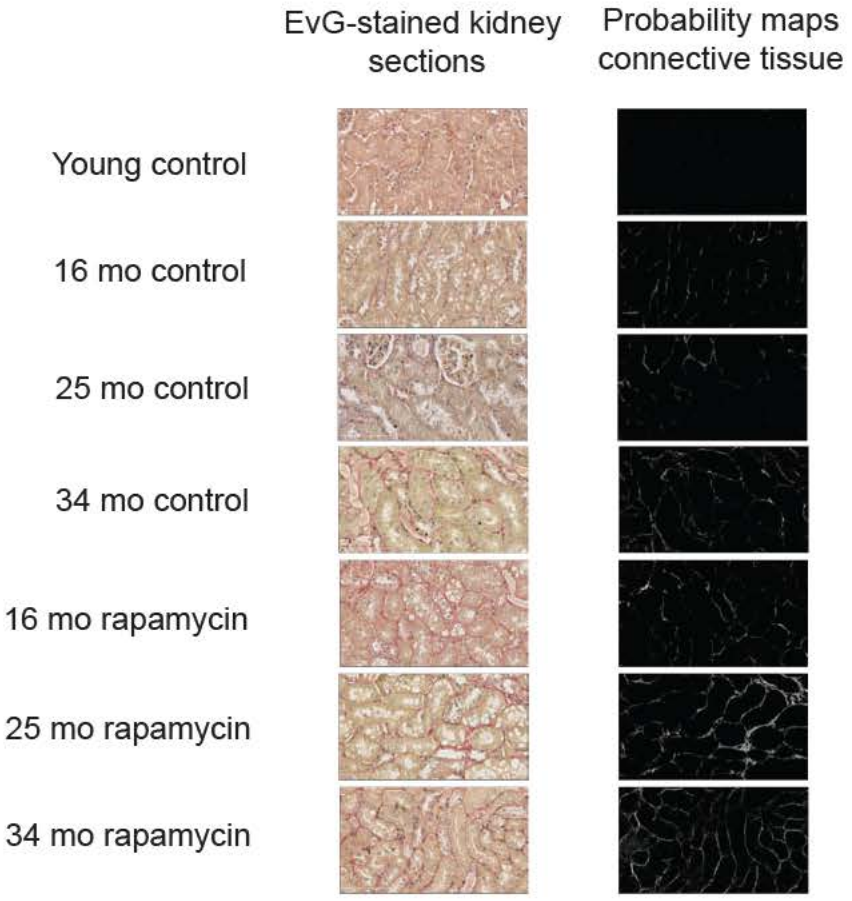

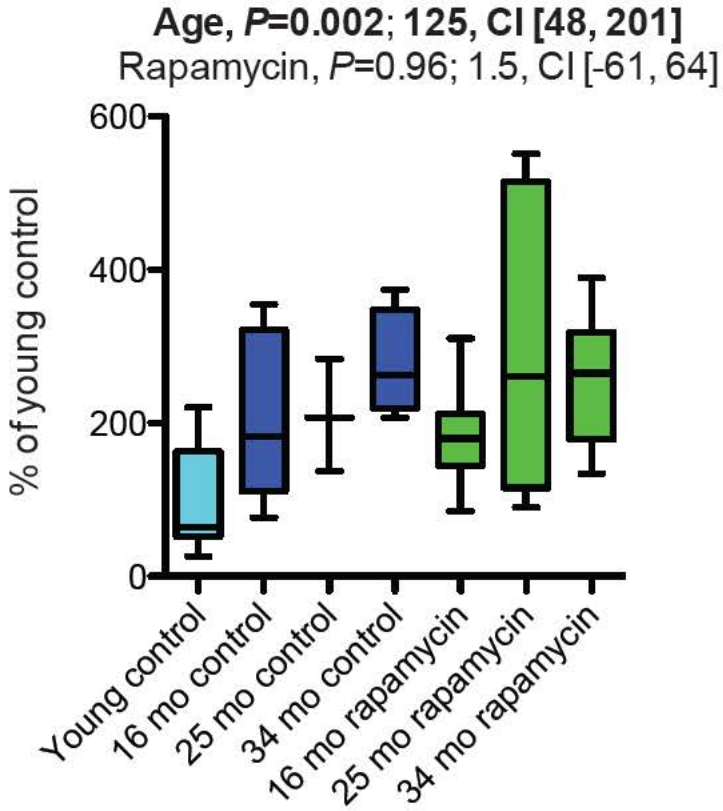

Supplementary Figure 25

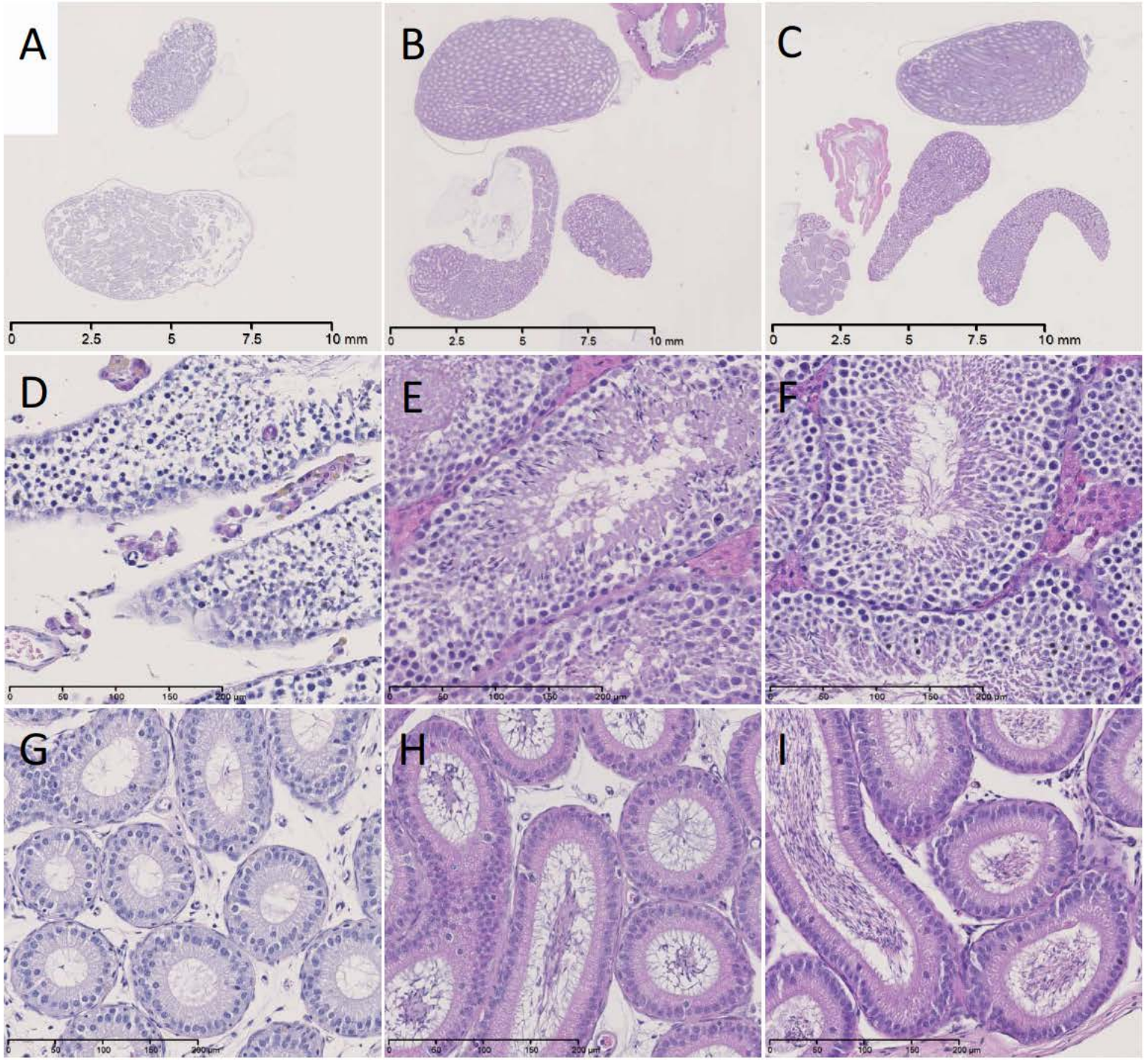

Supplementary Figure 26-I

34 months cohort

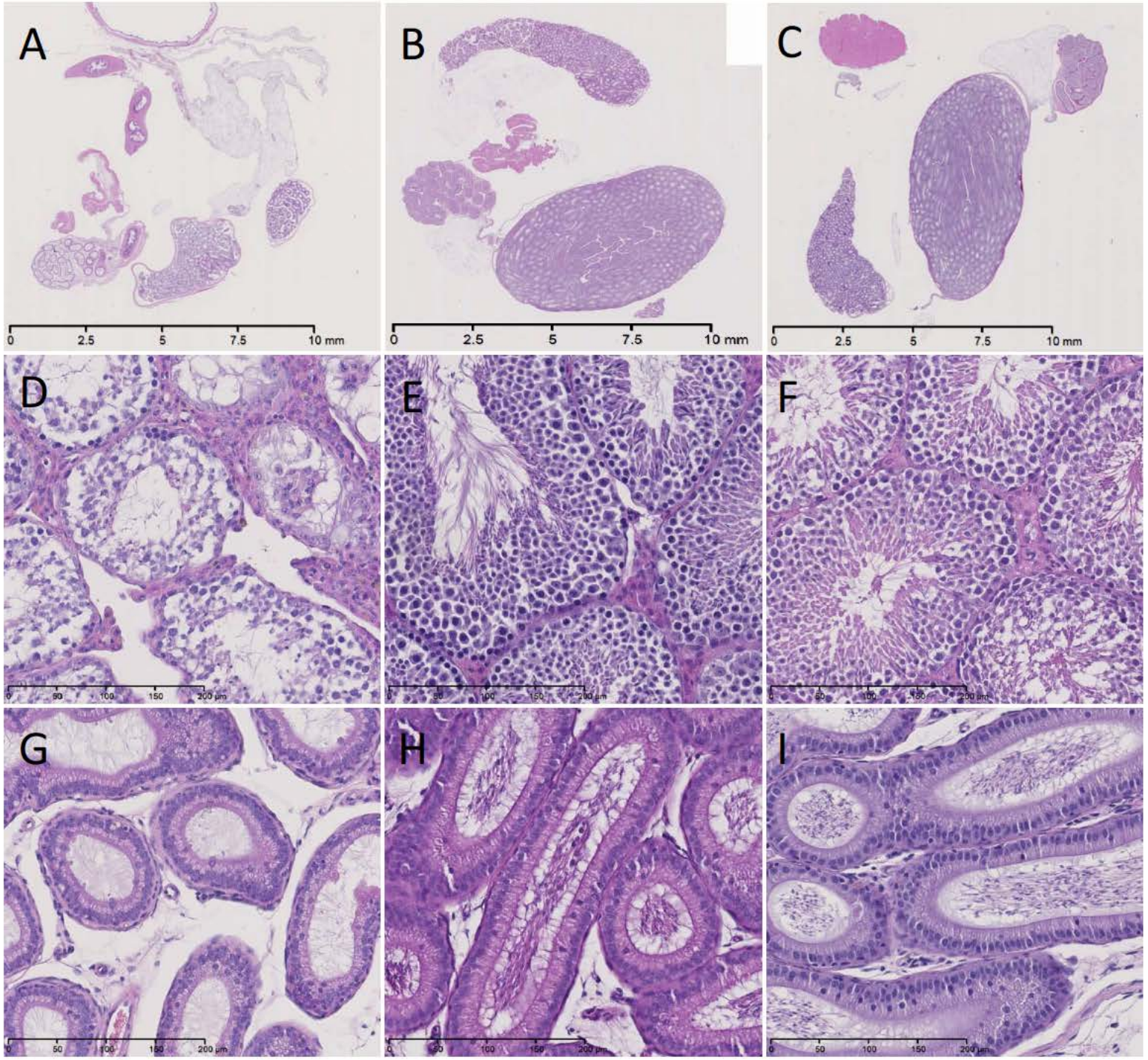

Supplementary Figure 26-II

25 months cohort

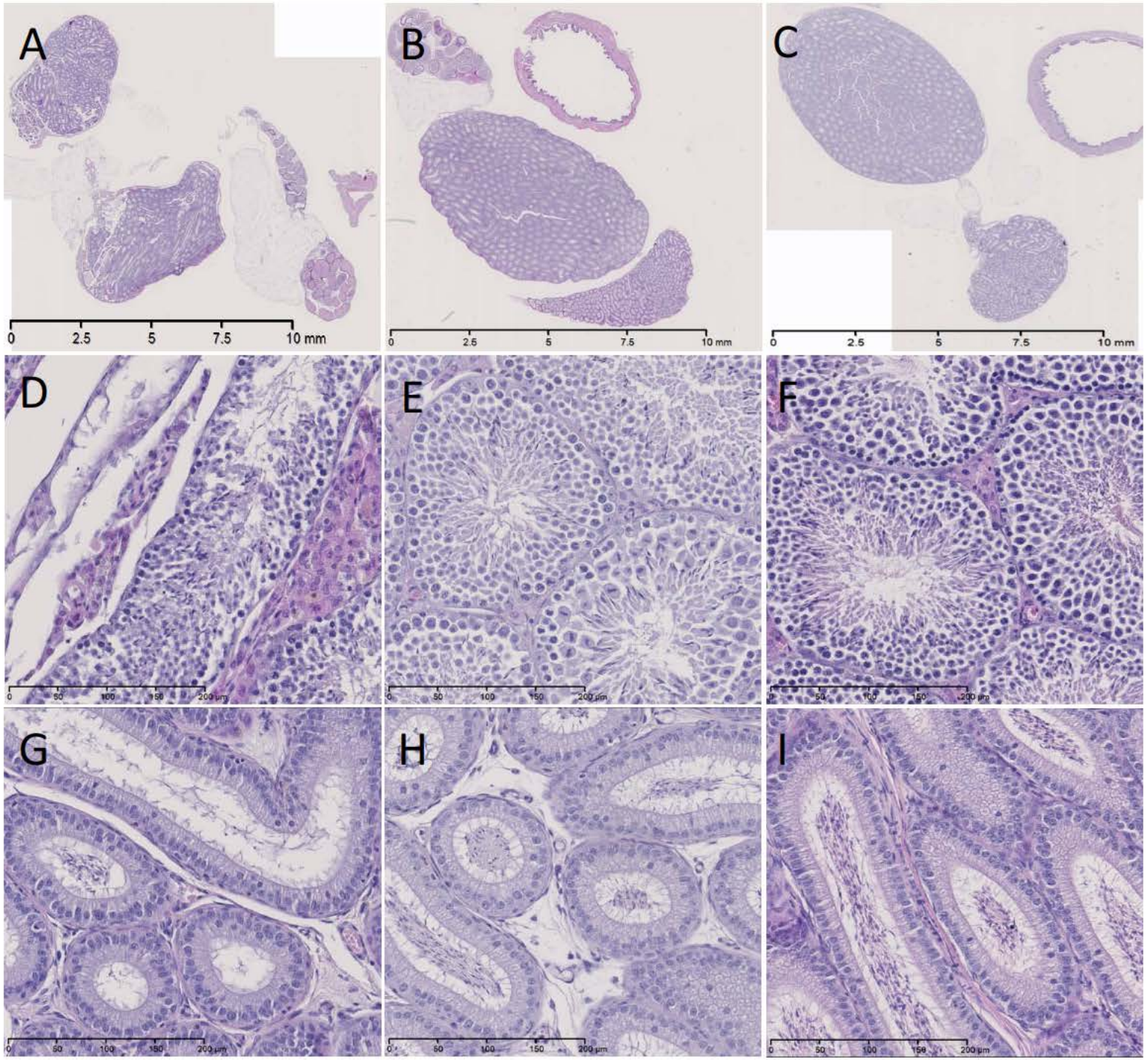

Supplementary Figure 26-III

16 months cohort

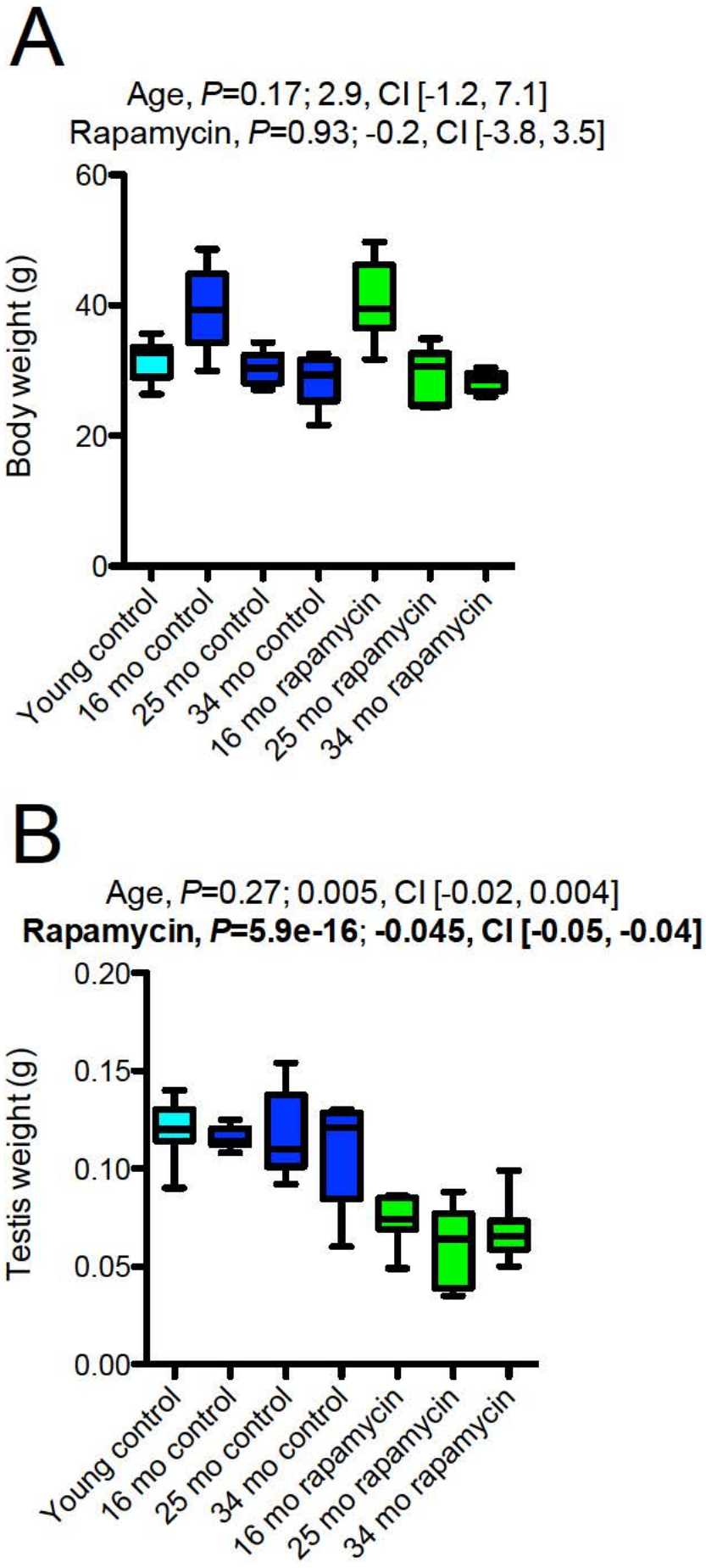

Supplementary Figure 27

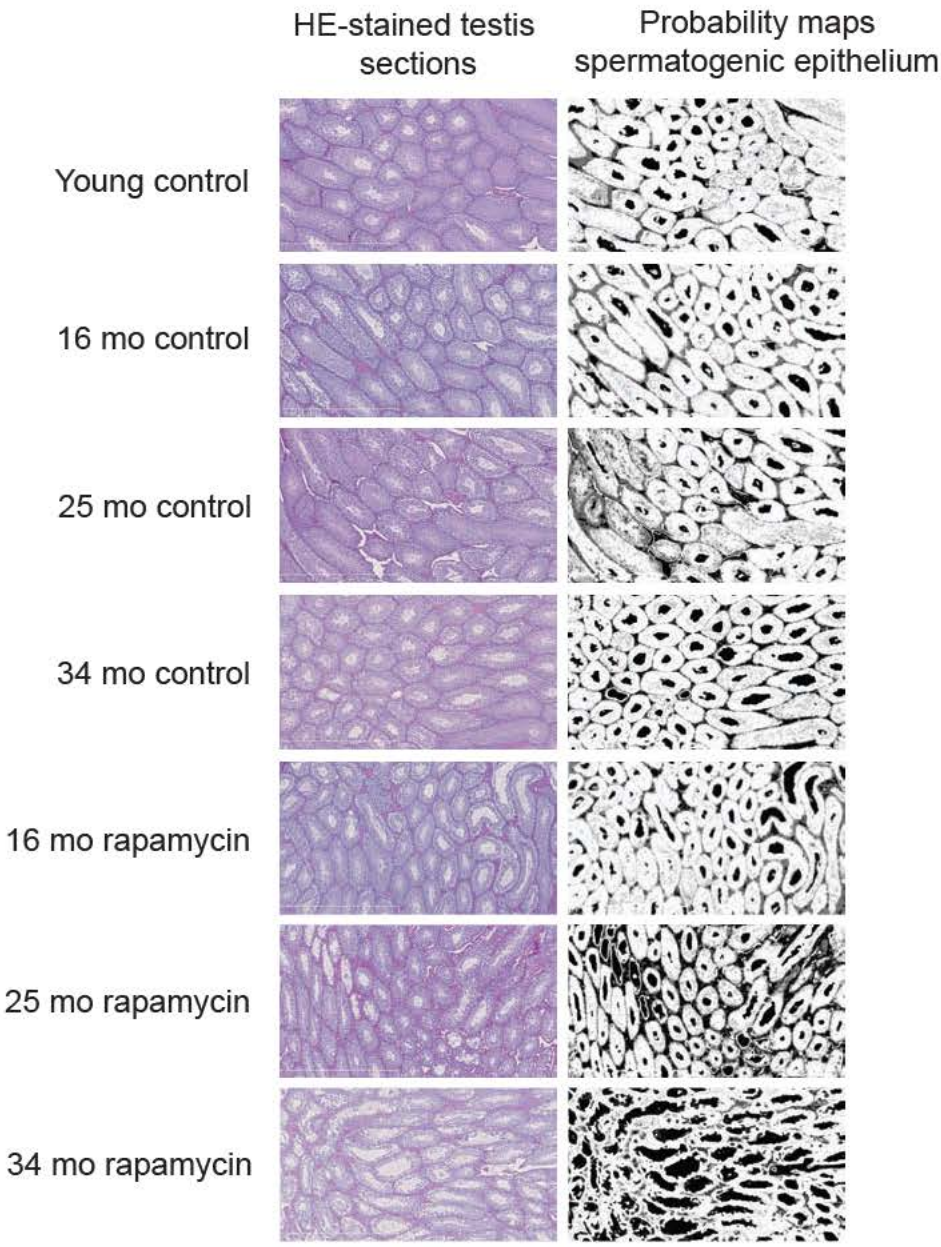

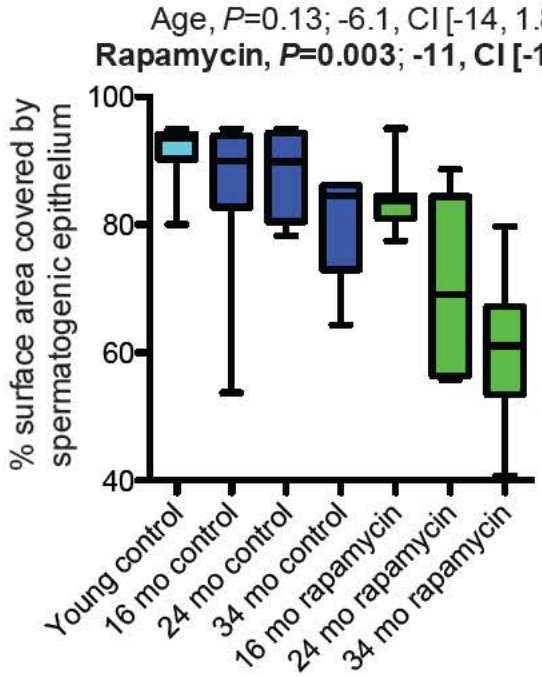

Supplementary Figure 28

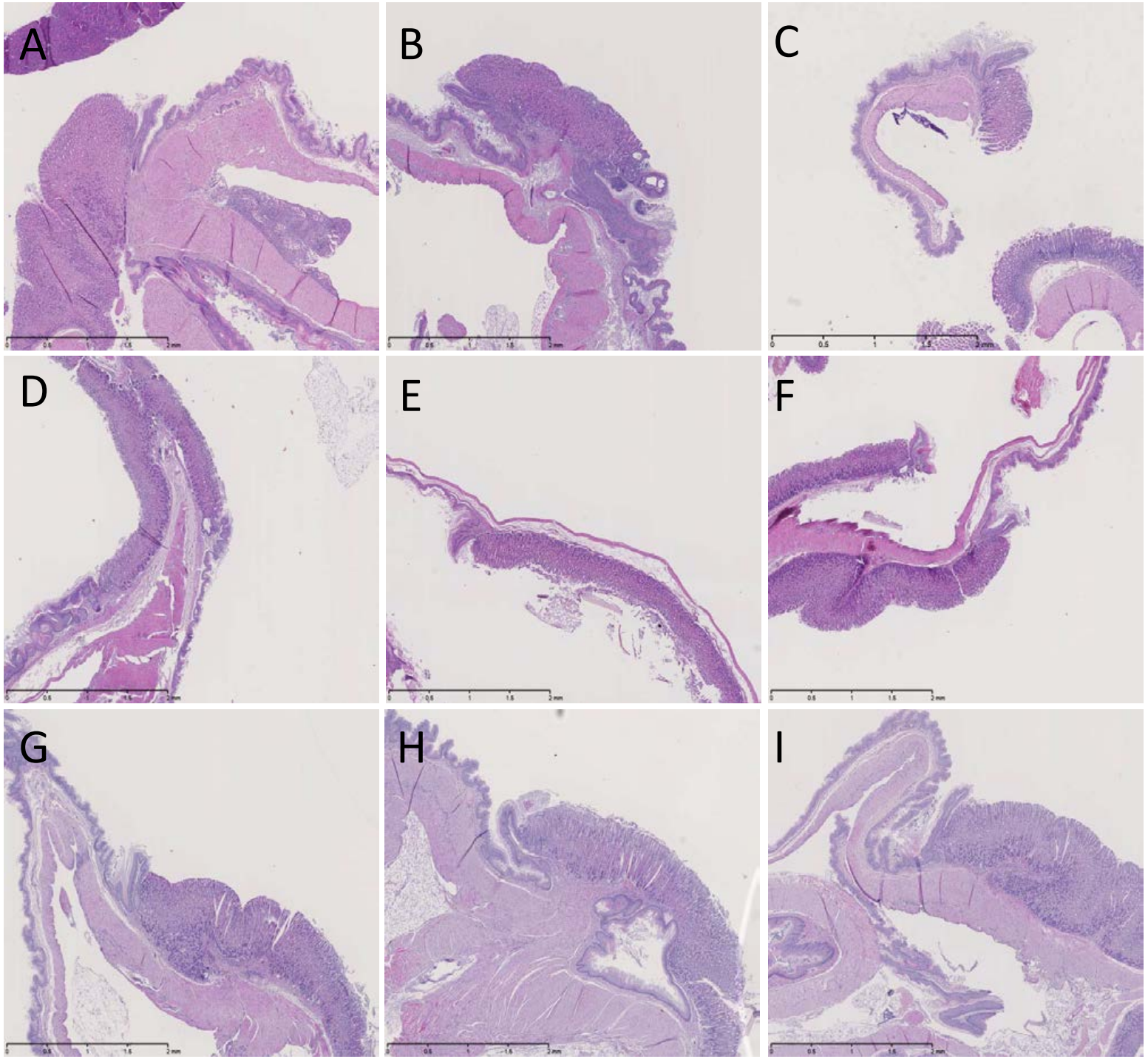

Supplementary Figure 29

34 months cohort

25 months cohort

16 months cohort

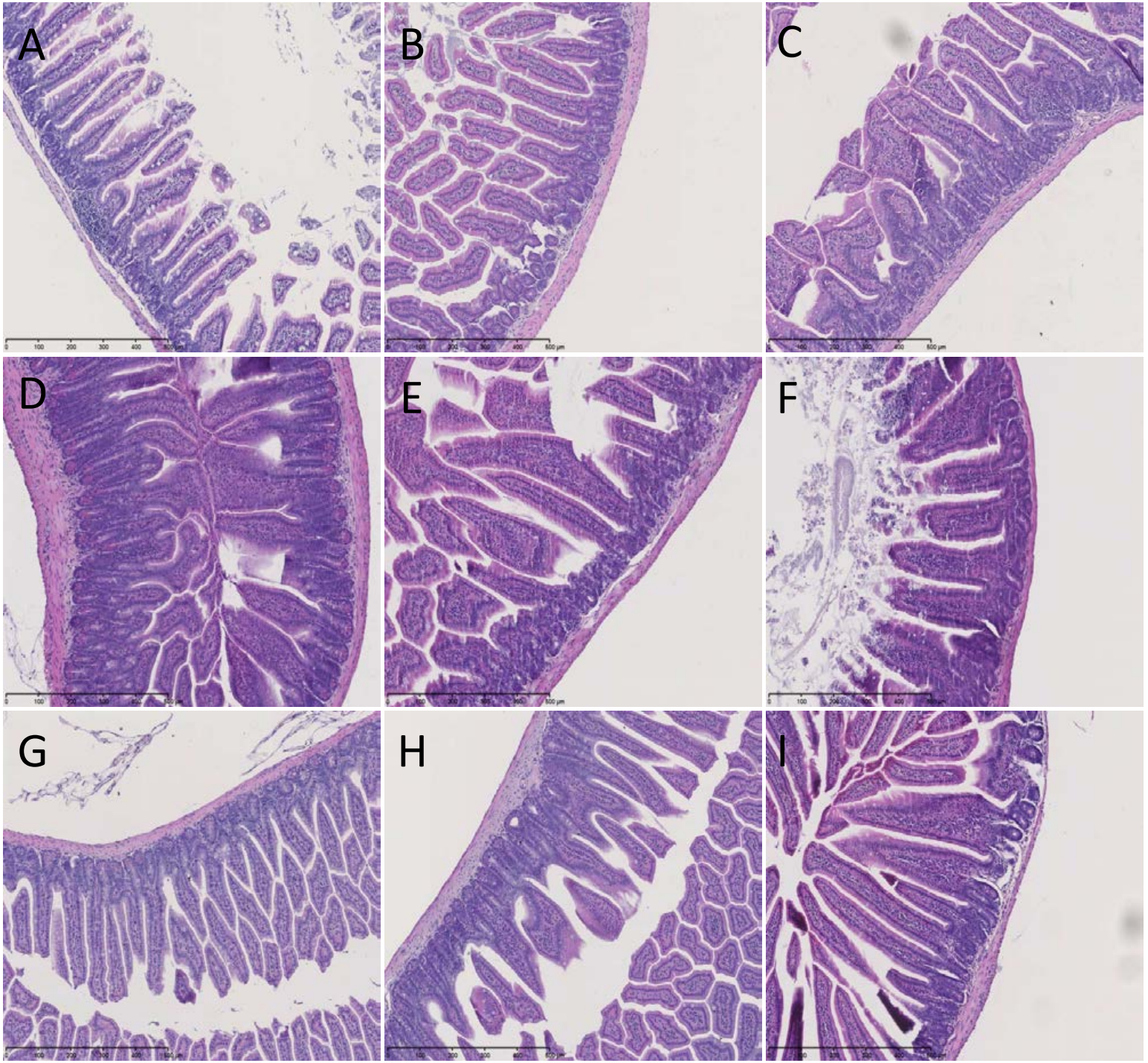

Supplementary Figure 30-I

34 months cohort

25 months cohort

16 months cohort

Old rapamycin

Old control

Young control

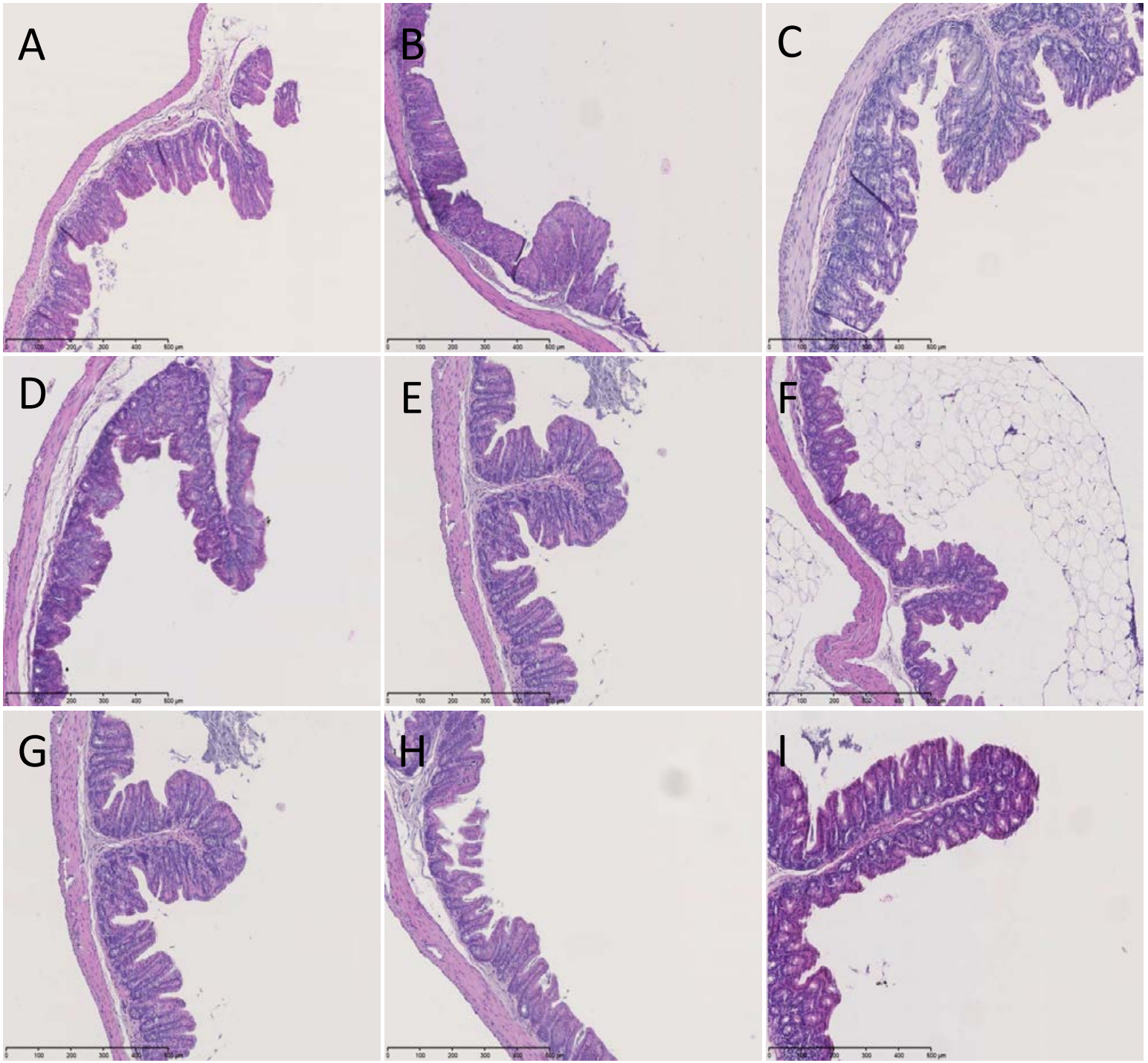

Supplementary Figure 30-II

34 months cohort

25 months cohort

16 months cohort

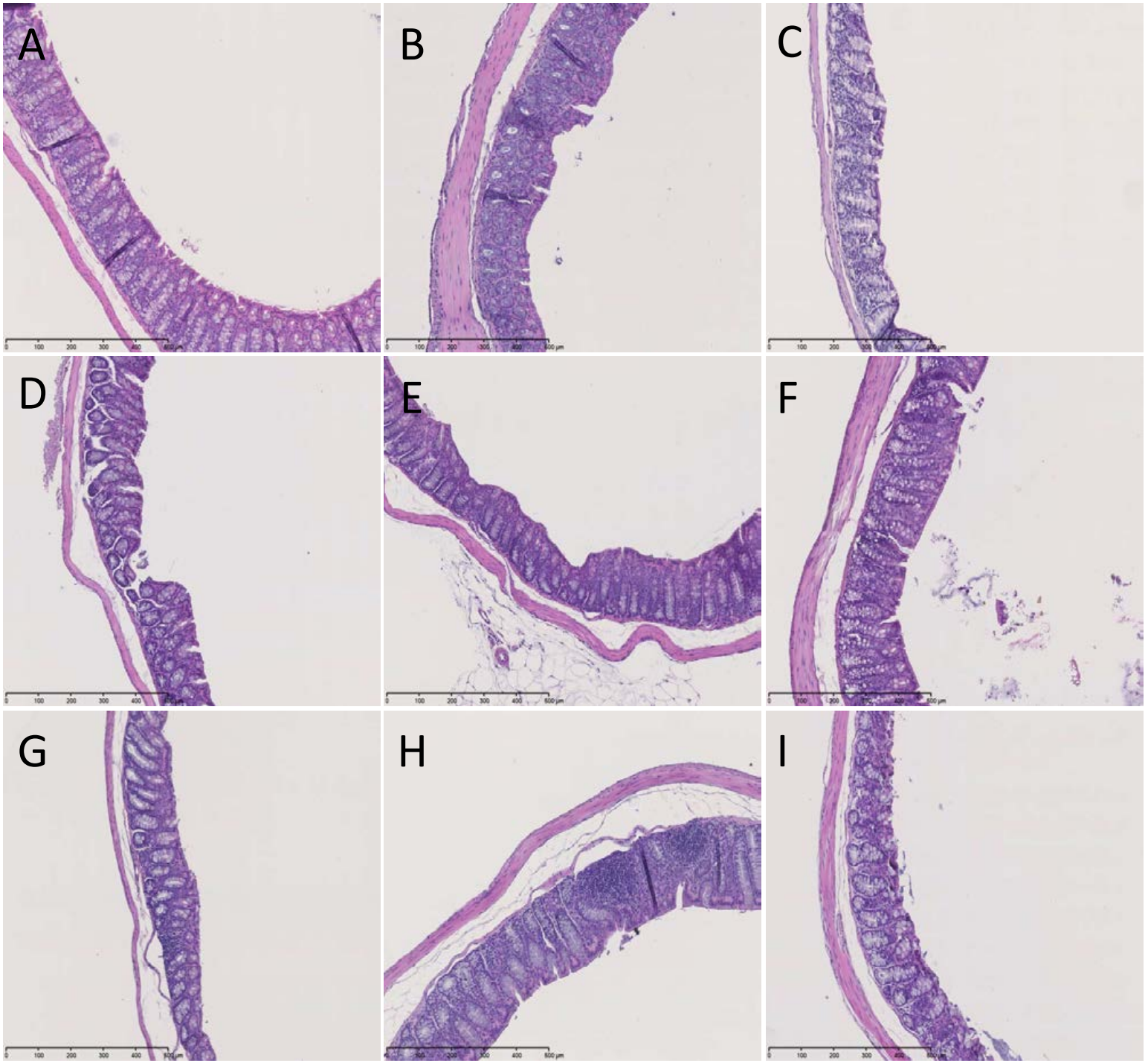

Supplementary Figure 30-III

34 months cohort

25 months cohort

16 months cohort

Old rapamycin

Old control

Young control

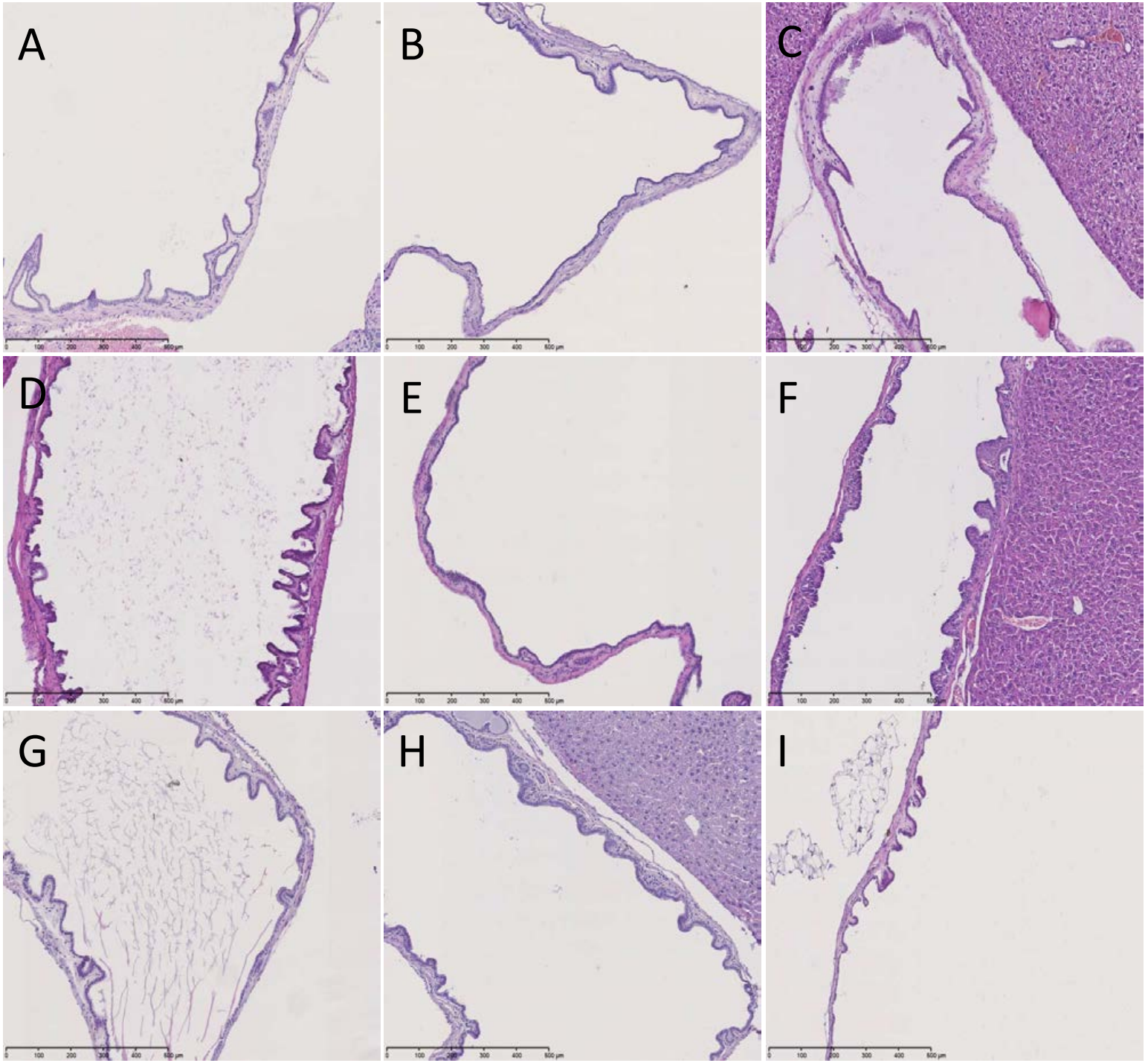

Supplementary Figure 31

34 months cohort

25 months cohort

16 months cohort

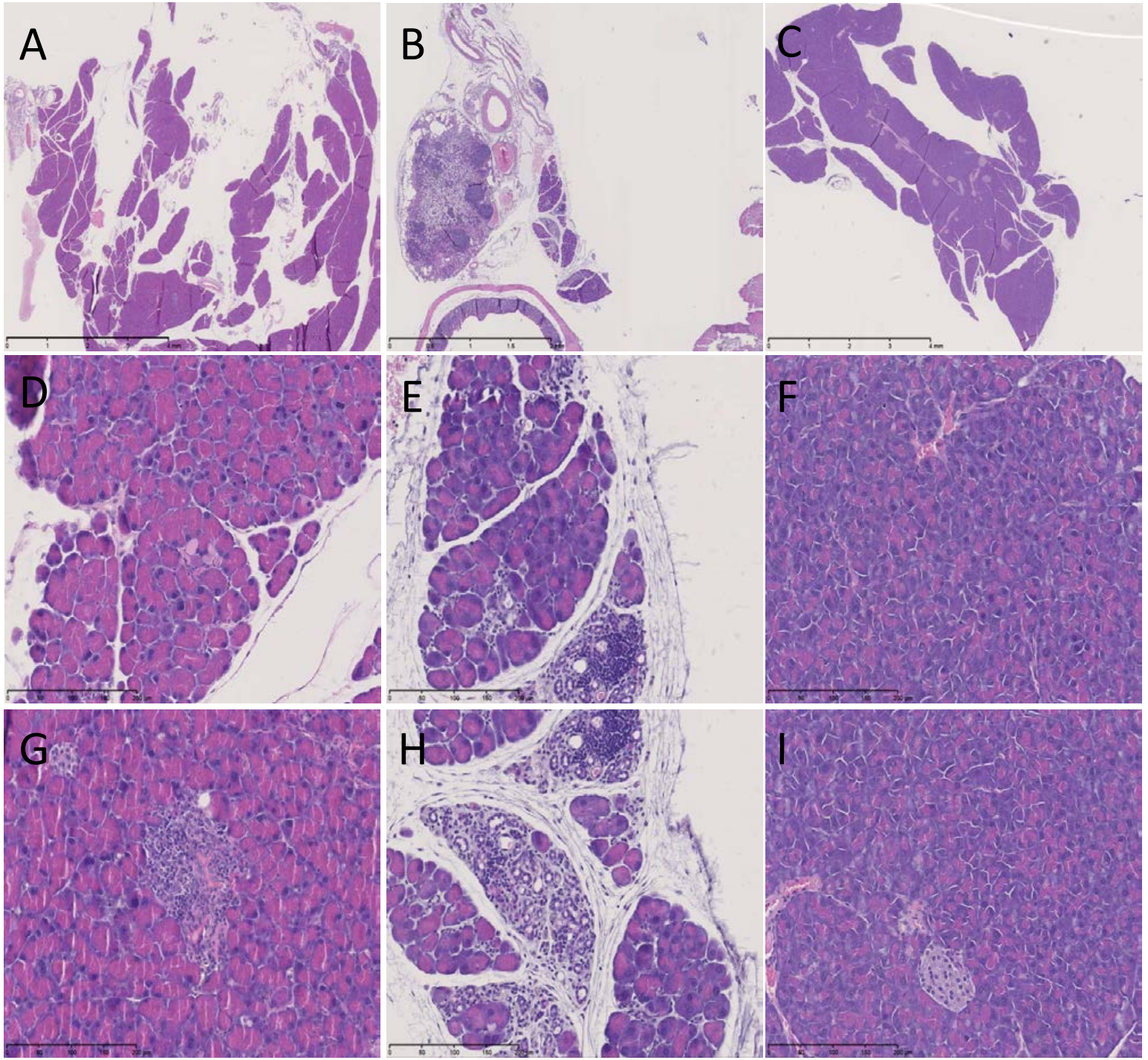

Supplementary Figure 32-I

34 months cohort

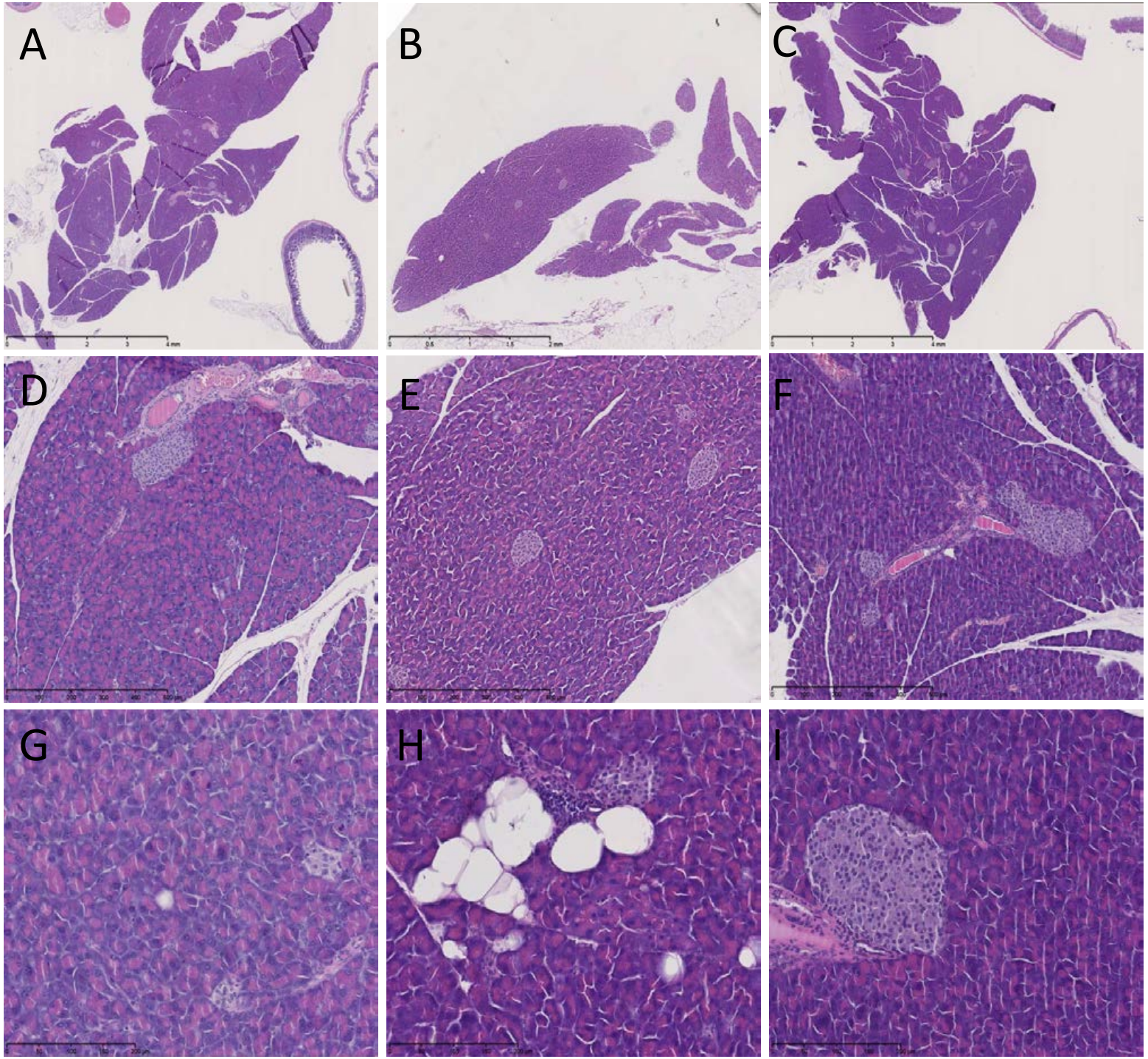

Supplementary Figure 32-II

25 months cohort

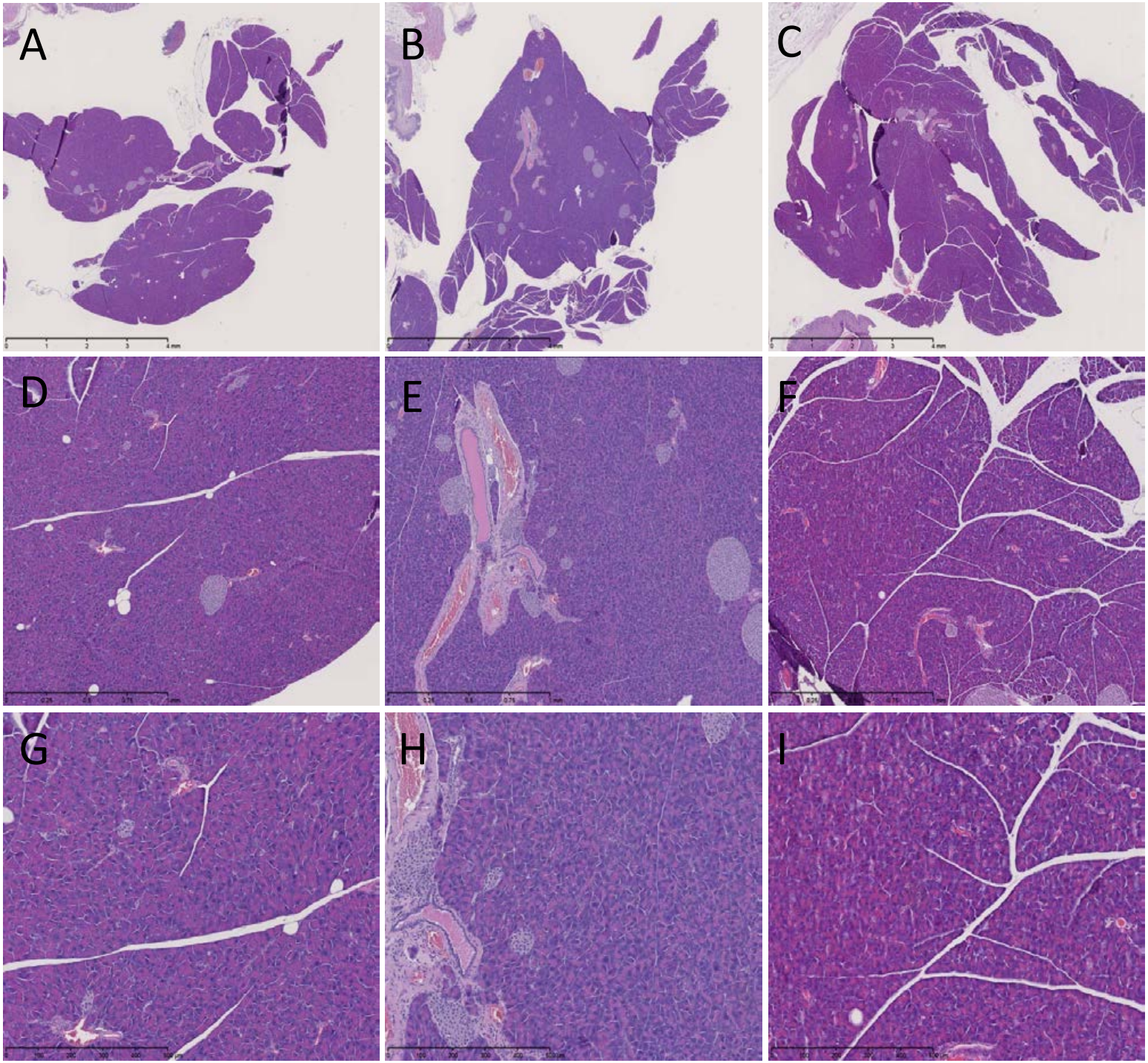

Supplementary Figure 32-III

16 months cohort

Old rapamycin

Old control

Young control

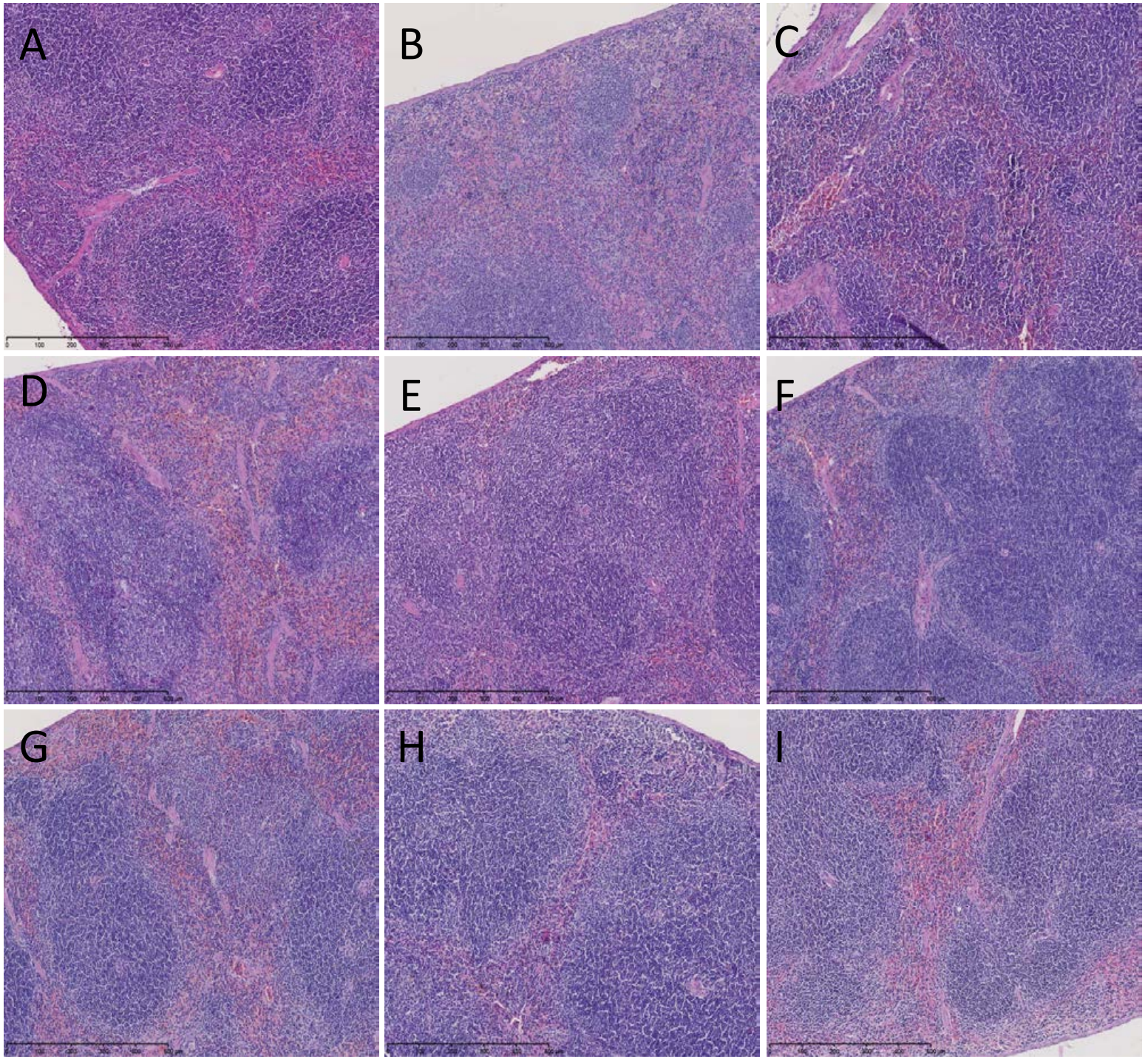

Supplementary Figure 33

34 months cohort

25 months cohort

16 months cohort

Old rapamycin

Old control

Young control

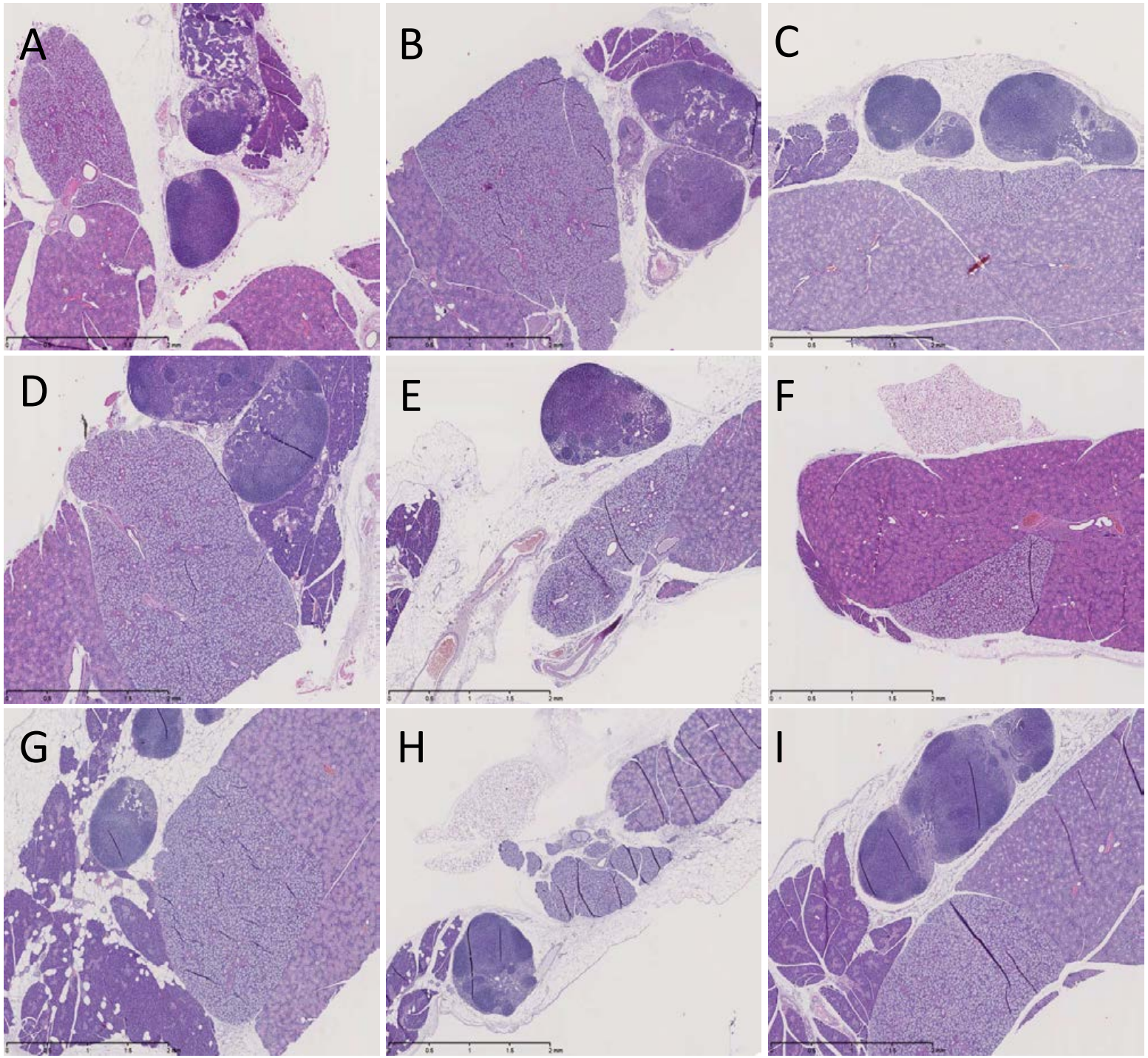

Supplementary Figure 34

34 months cohort

25 months cohort

16 months cohort

Old rapamycin

Old control

Young control

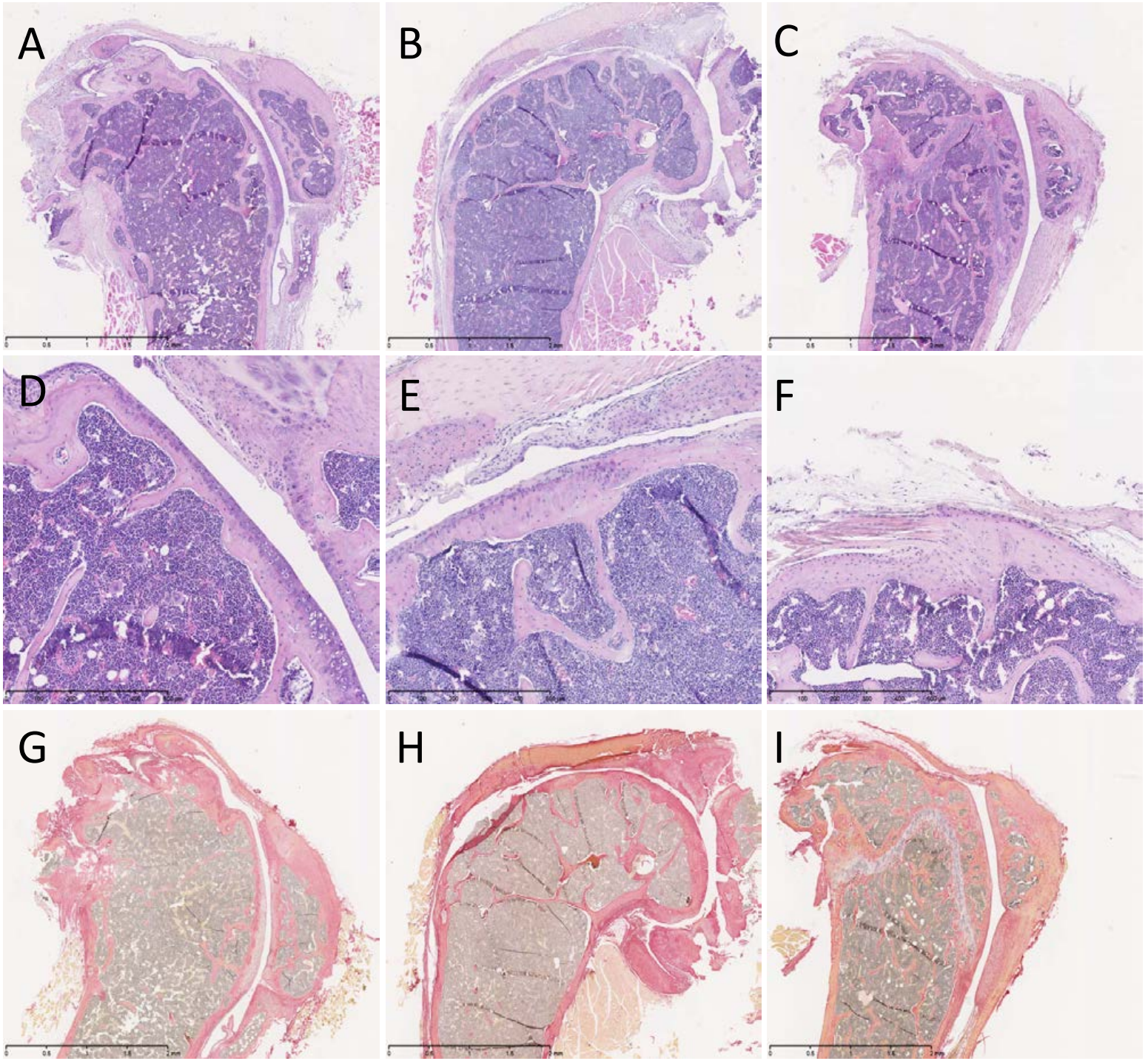

Supplementary Figure 35-I

34 months cohort

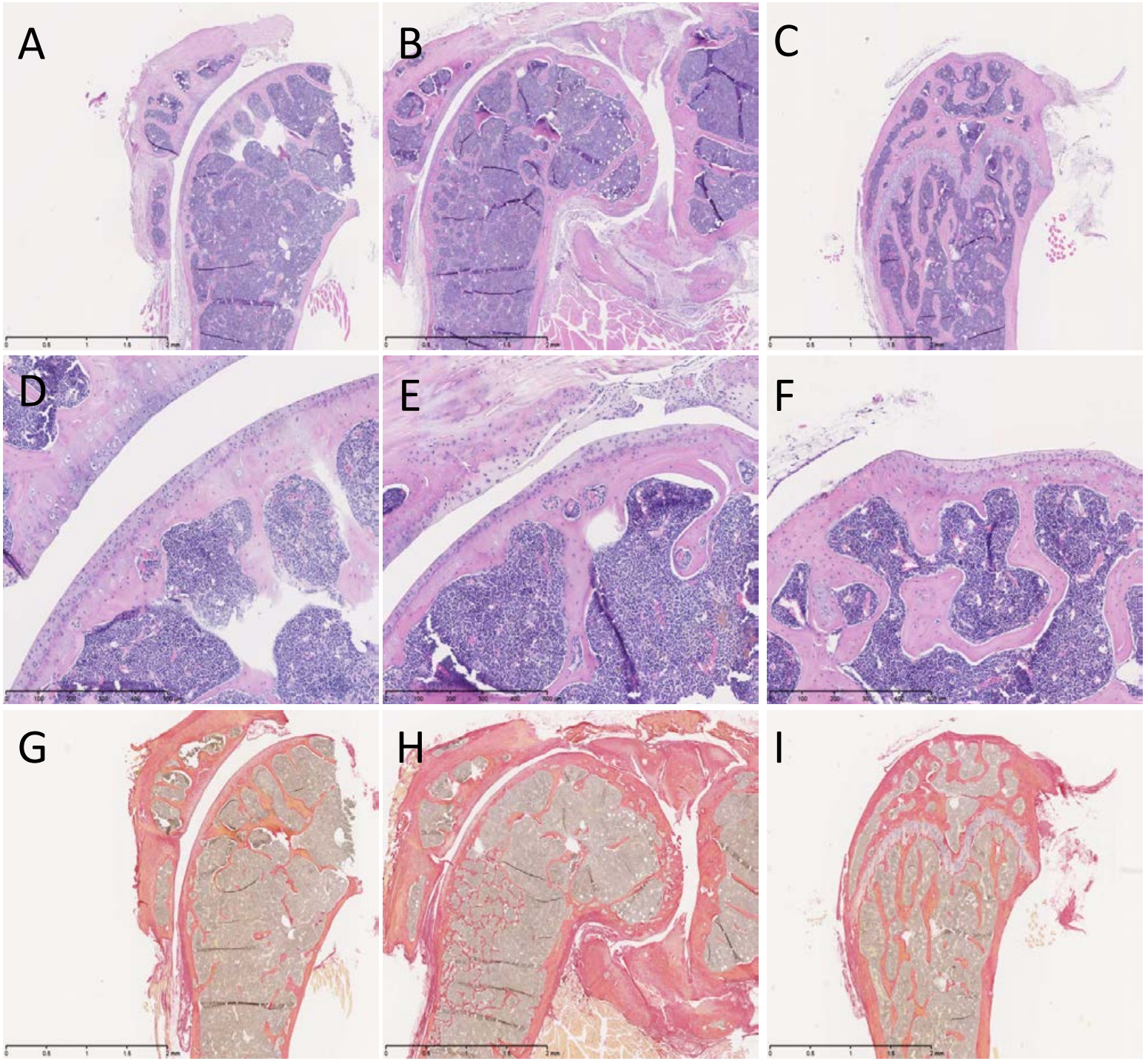

Supplementary Figure 35-II

25 months cohort

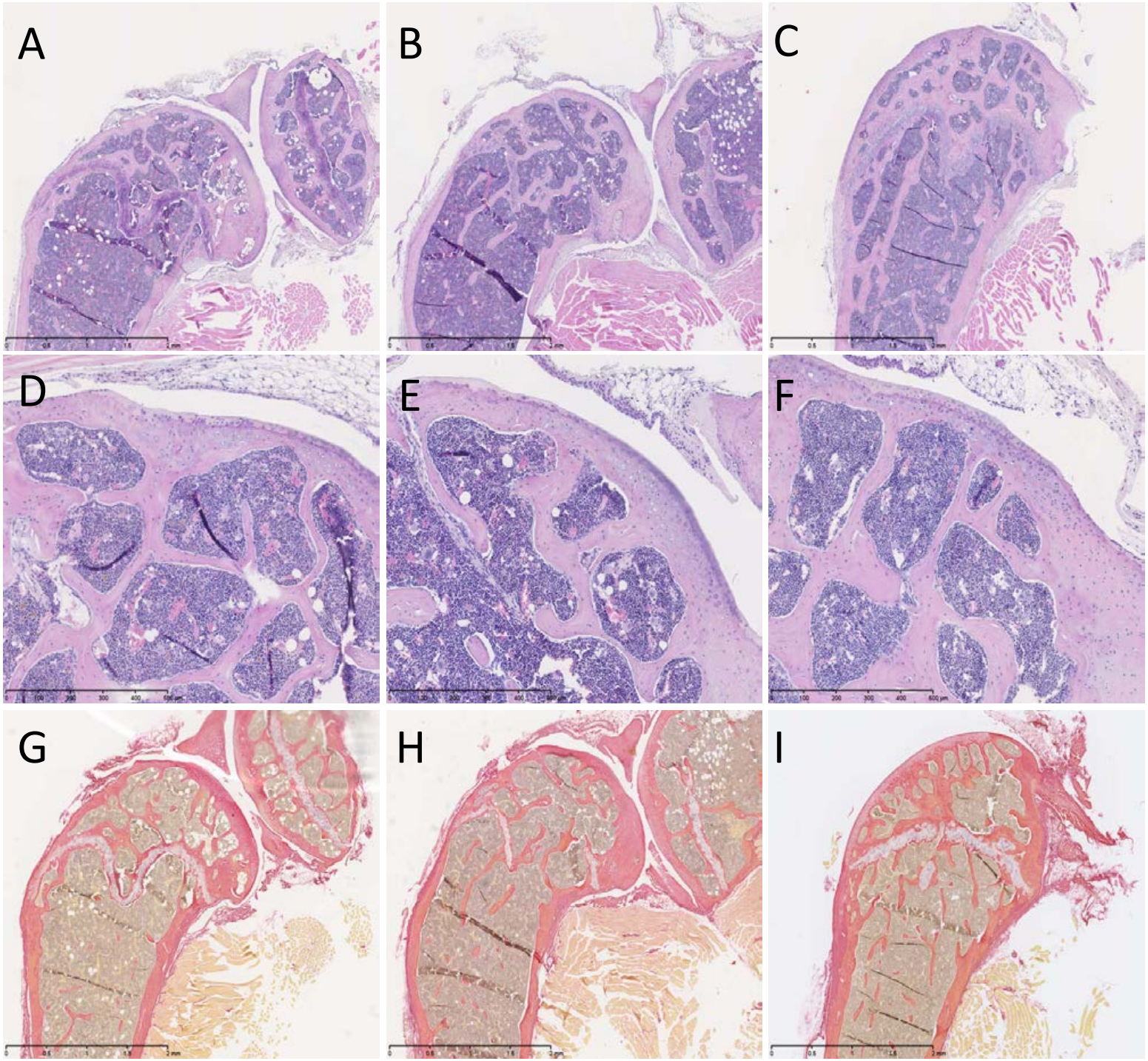

Supplementary Figure 35-III

16 months cohort

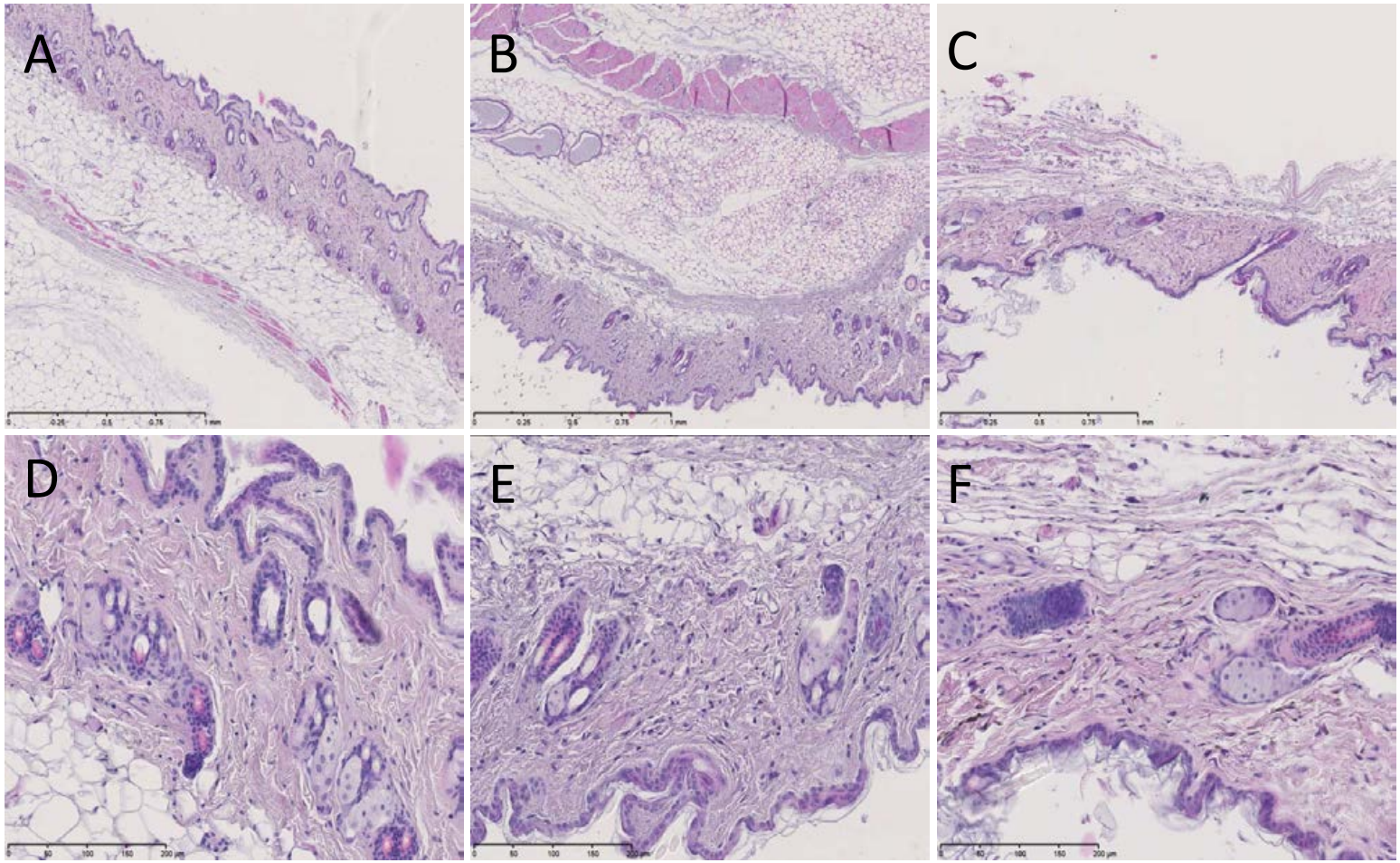

Supplementary Figure 36-I

34 months cohort

Old rapamycin

Old control

Young control

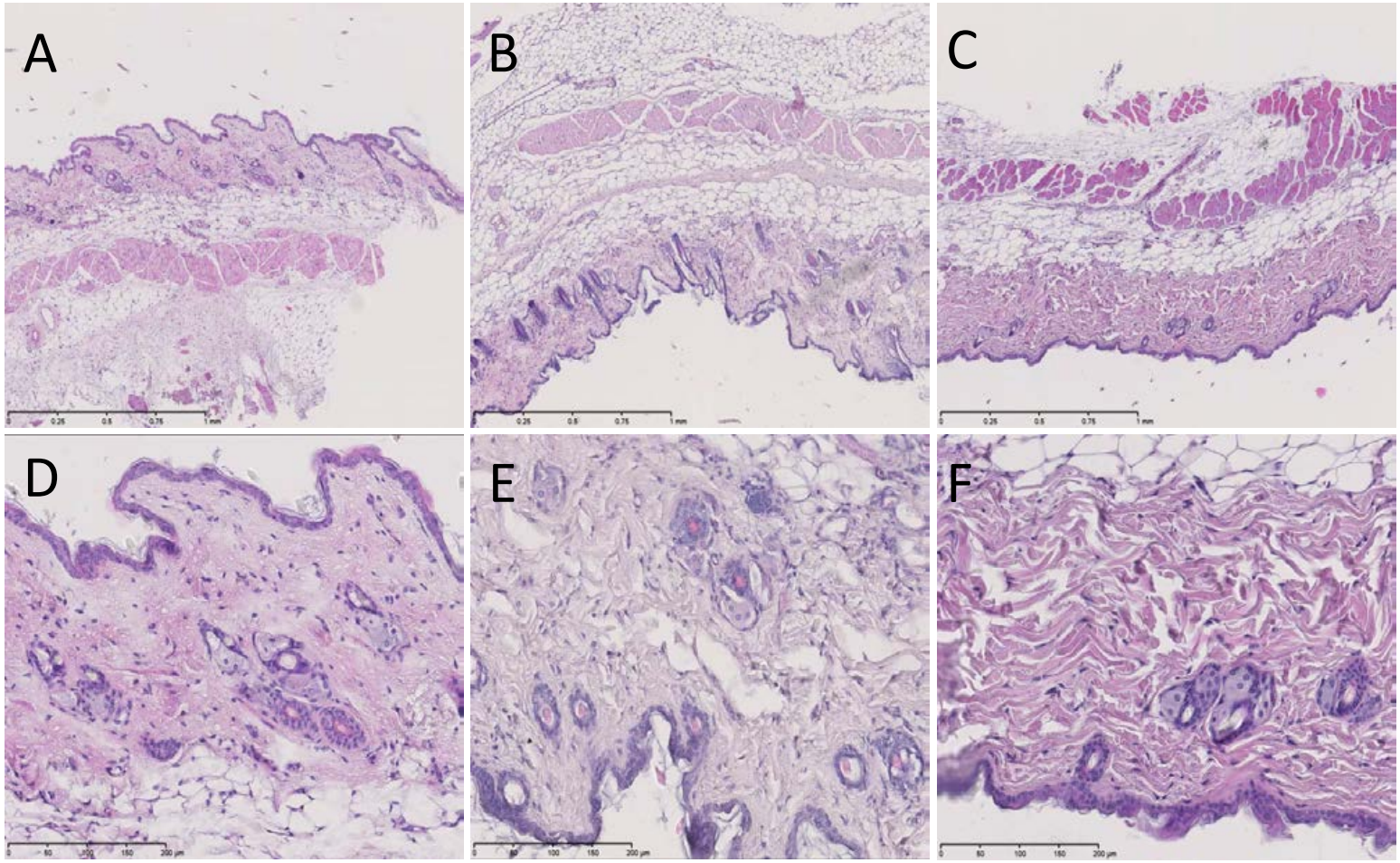

Supplementary Figure 36-II

25 months cohort

Old rapamycin

Old control

Young control

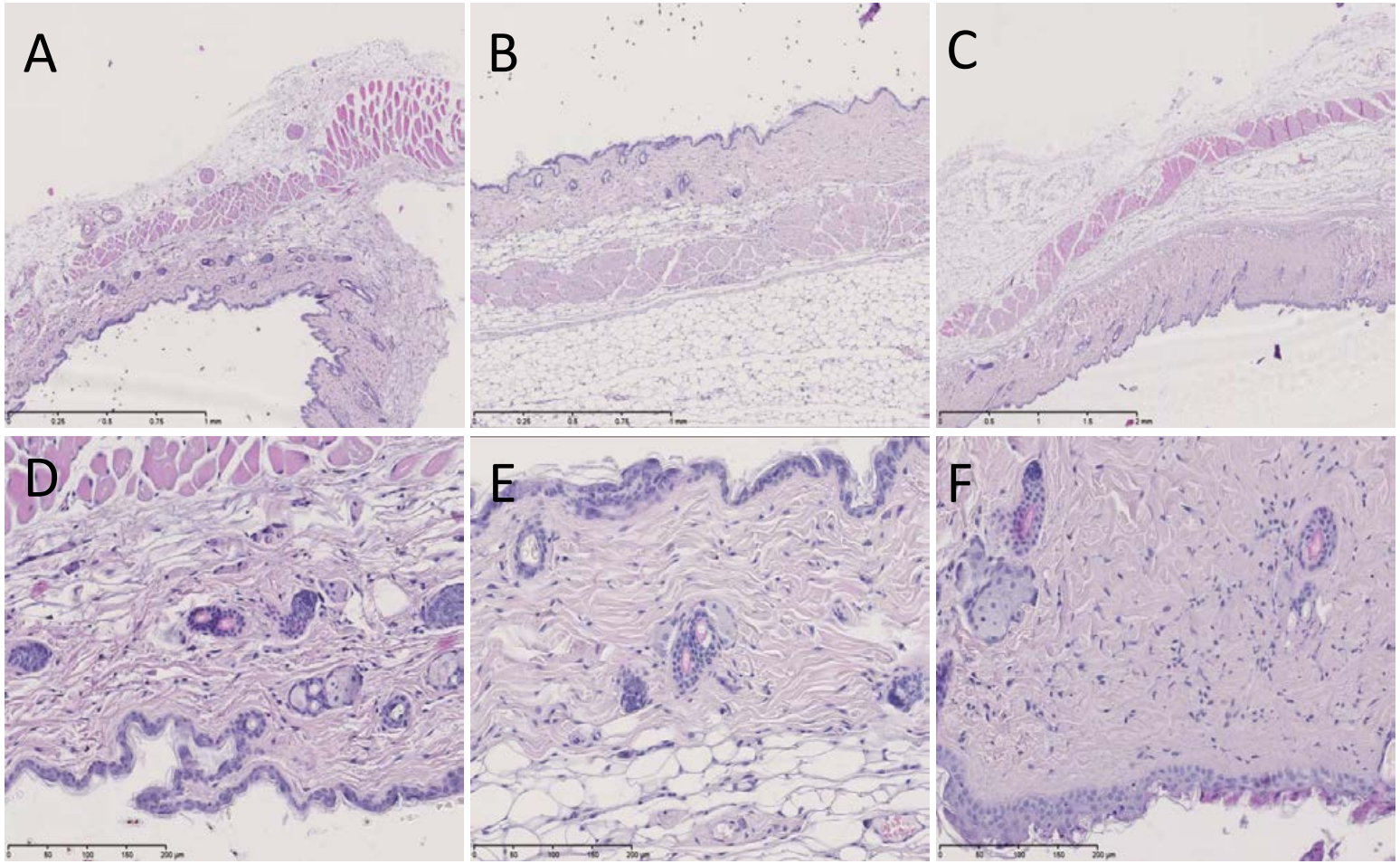

Supplementary Figure 36-III

16 months cohort

Old rapamycin

Old control

Young control

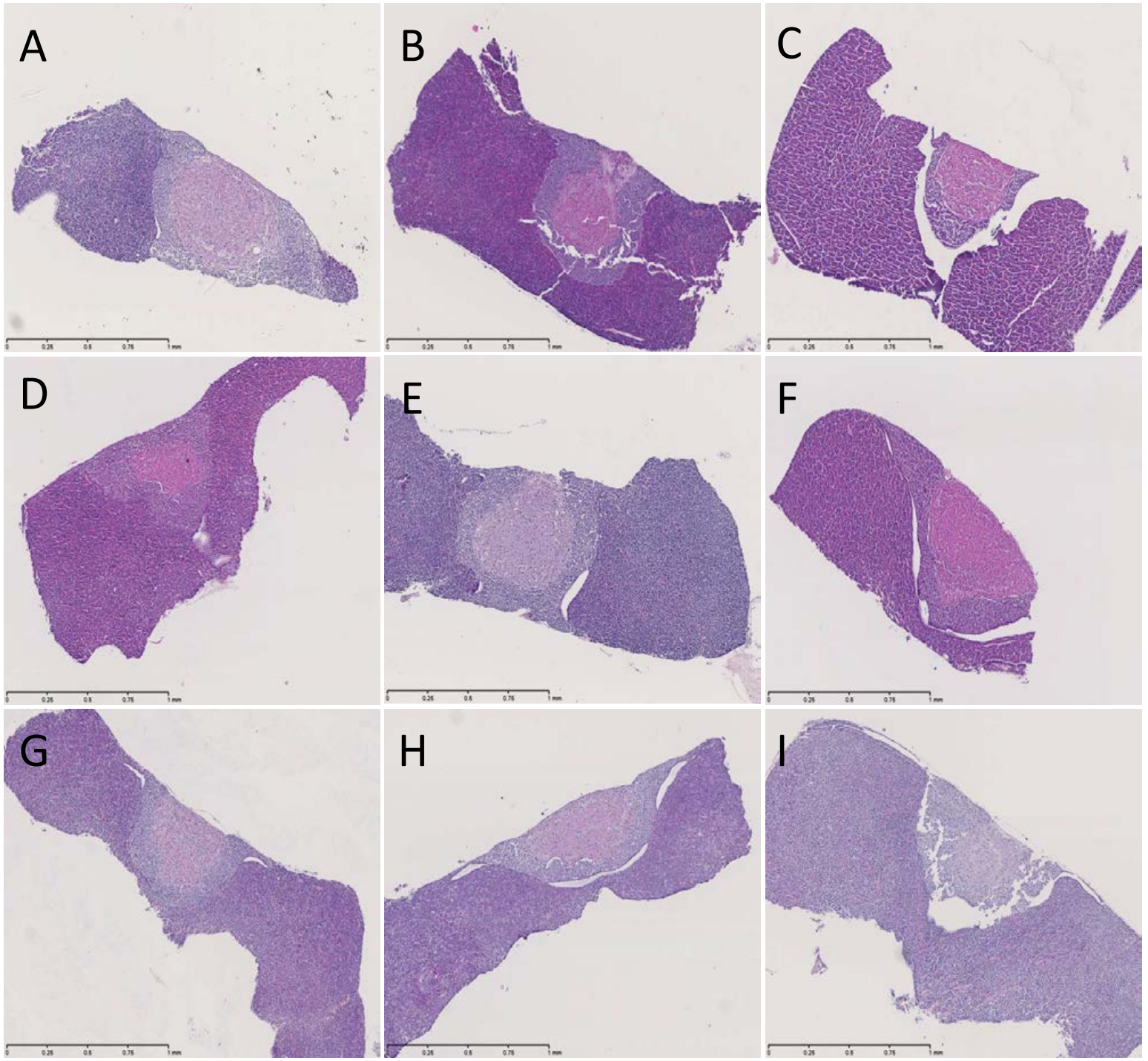

Supplementary Figure 37

34 months cohort

25 months cohort

16 months cohort

Old rapamycin

Old control

Young control

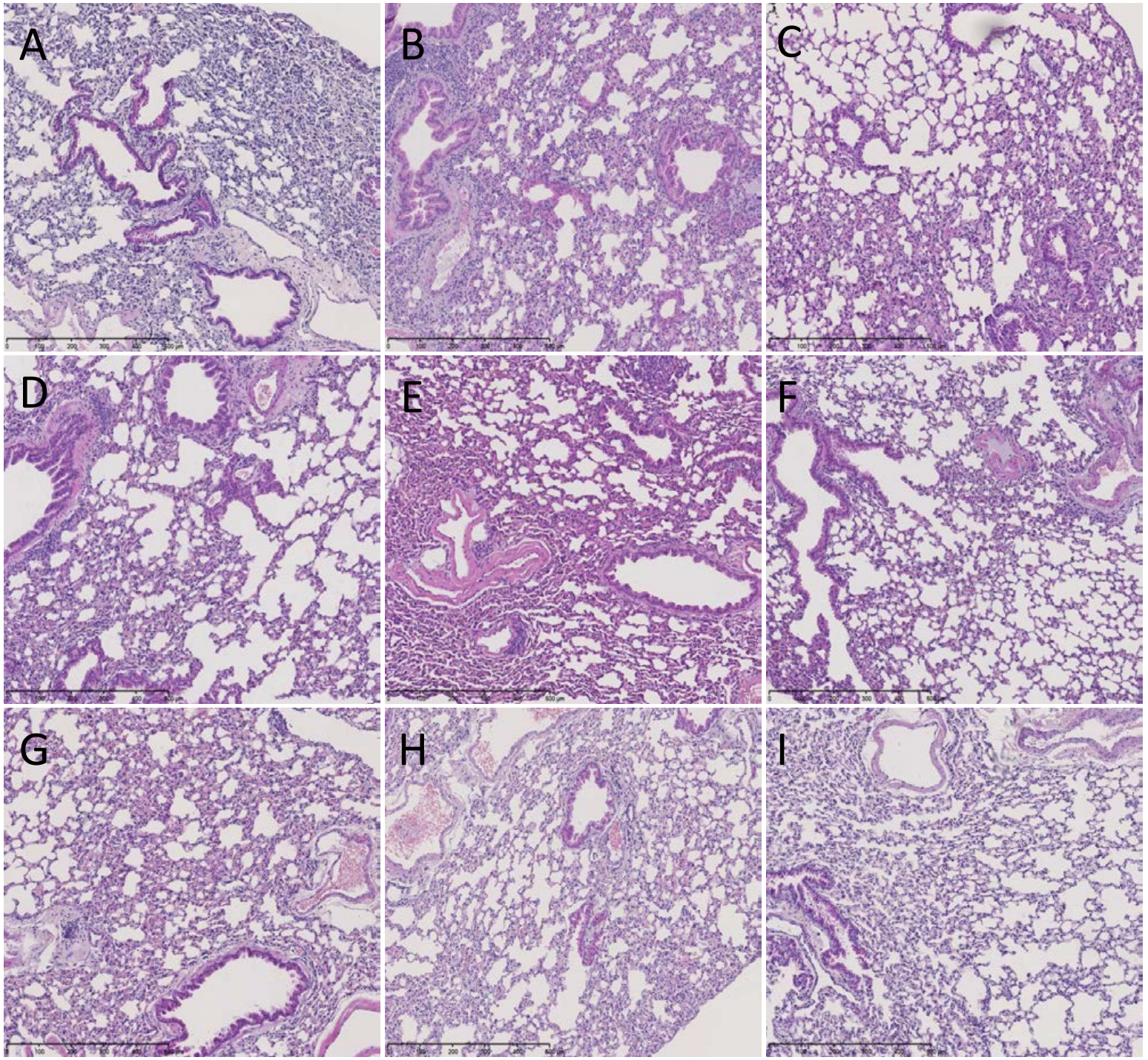

Supplementary Figure. 38-I

34 months cohort

25 months cohort

16 months cohort

Old rapamycin

Old control

Young control

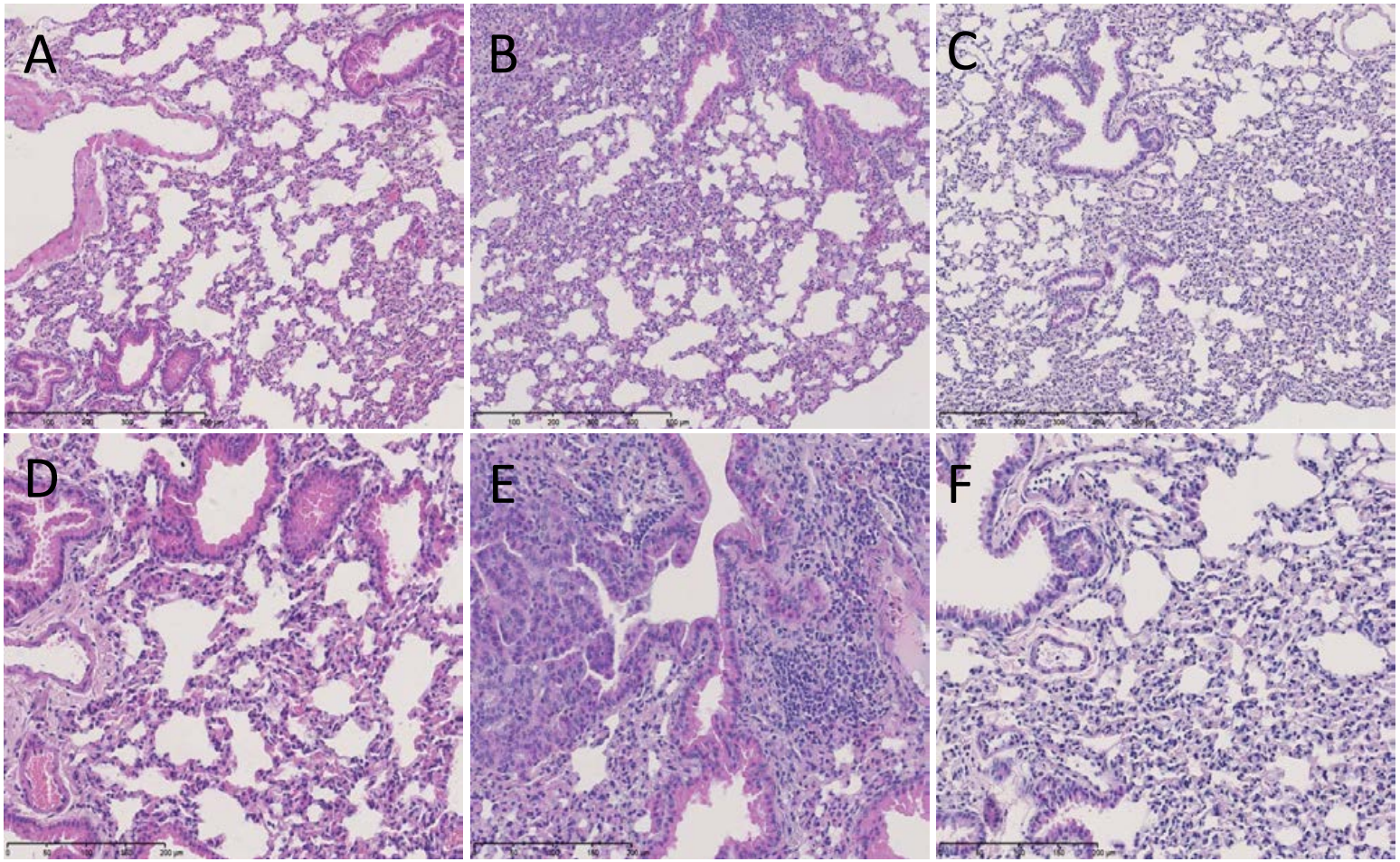

Supplementary Figure 38-II

34 months cohort

Old rapamycin

Old control

Young control

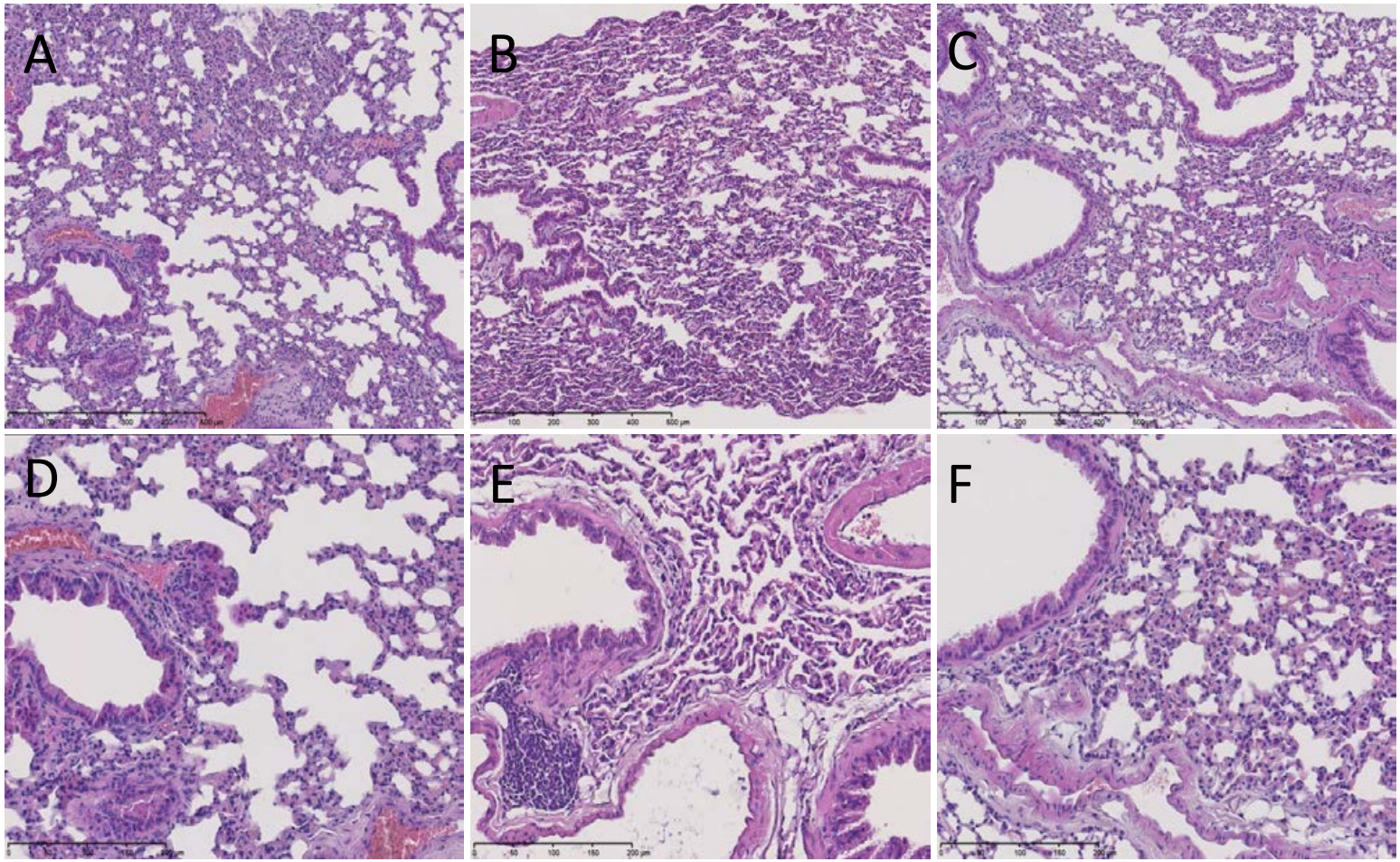

Supplementary Figure 38-III

25 months cohort

Old rapamycin

Old control

Young control

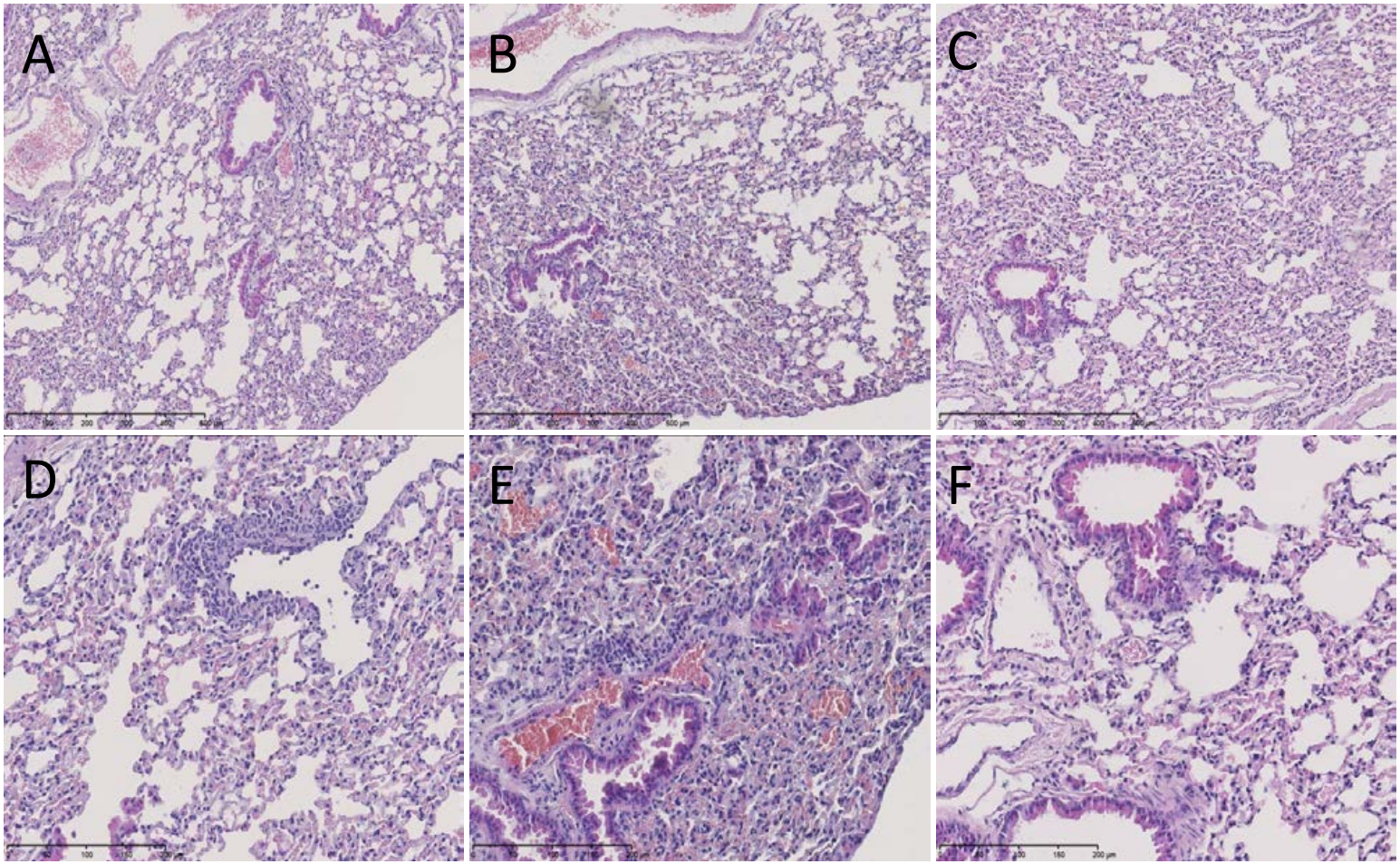

Supplementary Figure 38-IV

16 months cohort

Old rapamycin

Old control

Young control

A

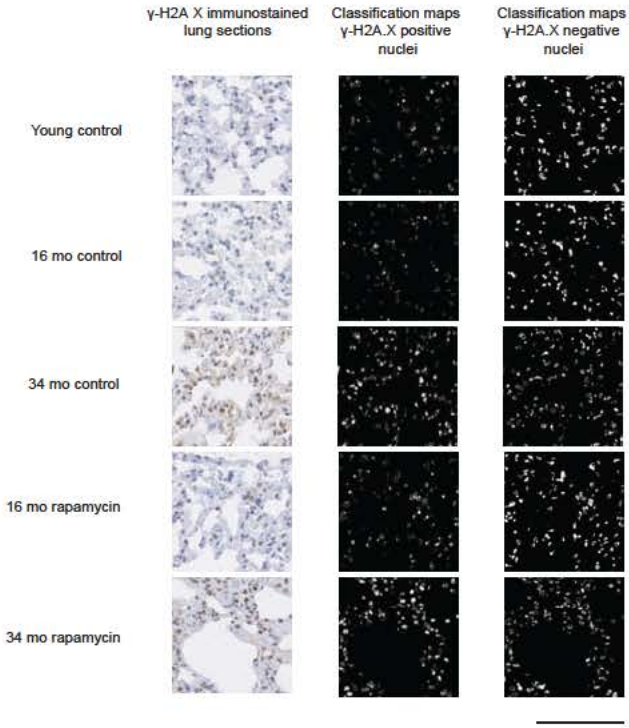

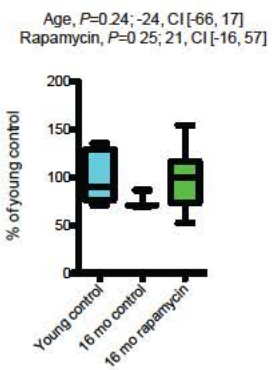

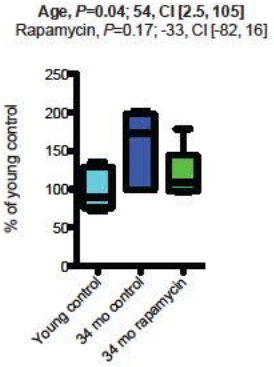

B

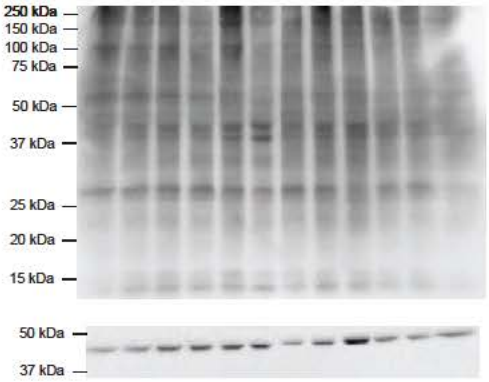

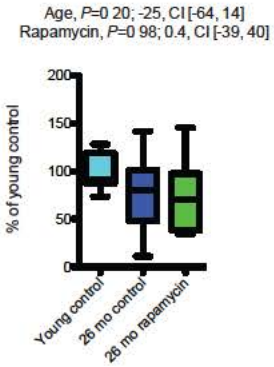

C

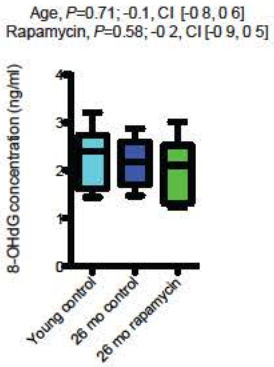

Supplementary Figure 39

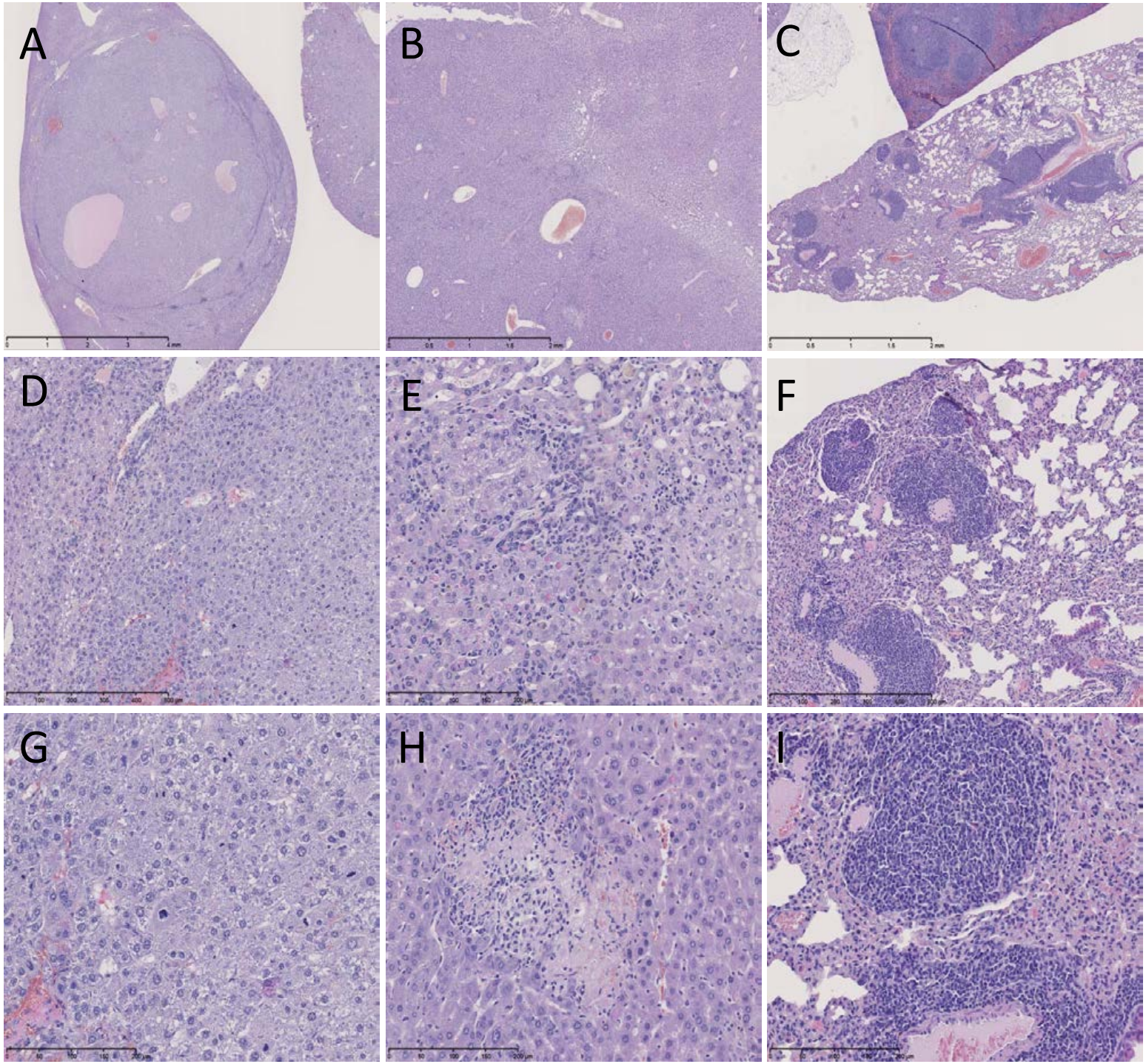

Supplementary Figure 40-I

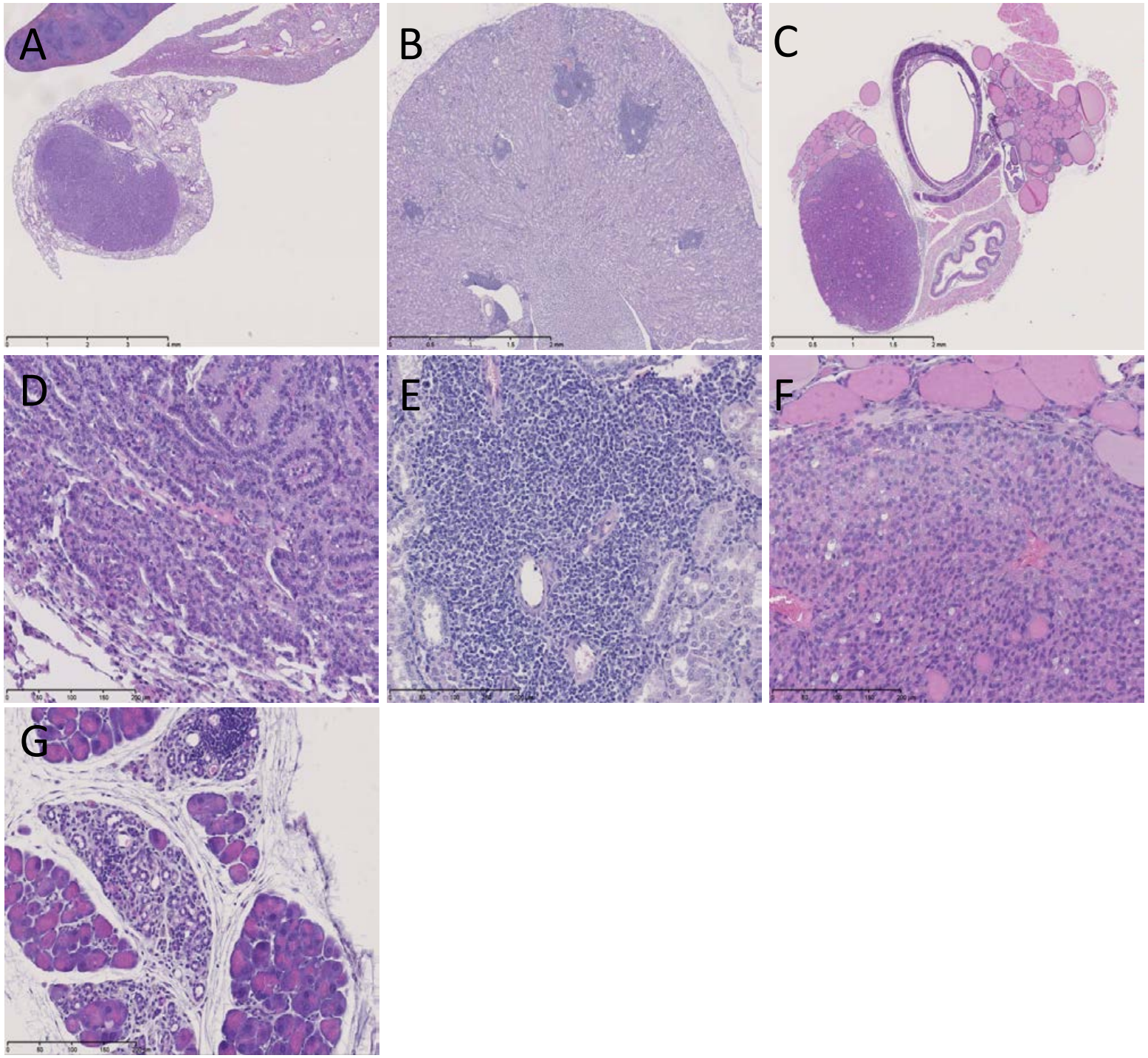

Supplementary Figure 40-II